POLITECNICO DI MILANO

Scuola di Ingegneria Industriale e dell'Informazione

Corso di Laurea Magistrale in
Ingegneria Chimica

Synthesis and characterisation of Pluronic hydrogels for biomedical applications

Relatore: Prof. Maurizio MASI

Co-relatore: Dr. Francesco CELLESI

Tesi di Laurea di:

Giulia CAMANA
Matr. 797471

Mirko TAVANO
Matr. 798943

Anno Accademico 2013 – 2014

Summary

List of Figures

List of Tables

Abstract

The aim of this thesis work was to develop new hydrogel materials based on Pluronic, an A-B-A block copolymer of poly(ethylene glycol) (PEG) and Poly(propylene glycol) (PPG), to control their final physico-chemical properties and explore their possible applications in nanomedicine.

In the last years the use of Pluronic F-127 as biomaterial has been widely investigated, due to its particular physico-chemical characteristics, which include thermoresponsiveness, easy chemical functionalization and relatively good biocompatibility. Previous works have demonstrated the applicability of Pluronic hydrogels in microencapsulation and tissue engineering. Pluronic F-127 was functionalized and then crosslinked both via a Michael-type addition reaction and via radical polymerization (i.e. photopolymerization). In this research project, novel polymeric precursors, namely Pluronic F-127 hexaacrylate (F-127 HA) and Pluronic F-127 thioacetate (F-127 TA), have been successfully sinthesized and easily crosslinked under physiological conditions, to form injectable thermoresponsive gels.

These functional Pluronics were characterized using standard chemical analysis (^{1}H-NMR and IR spectra), the crosslinking kinetics was studied using Dynamic Light Scattering and the physical properties of gels, formulated at different polymer concentrations, were also characterised, including swelling and diffusion properties.
Pluronic hydrogels obtained from Pluronic diacrylate (F-127 DA) crosslinked through a free radical polymerisation were also tested, in order to assess differences and similarities with Michael-type crosslinked gels.

In vitro cell tests were carried out using three different cell lines: fibroblasts, endothelial cells and podocytes, aiming to evaluate their different response in term of cellular

adhesion to the gels. In order to promote cell adhesion, Pluronic gels were functionalized with an RGD peptide or pre-treated with serum proteins. It was demonstrated that both gel formulations (i.e Michael-type crosslinked gels and free radical crosslinked gels) can provide good fibroblast adhesion, whereas adhesion was not confirmed for endothelial cells and podocytes, possibly because they may require more complex adhesion mechanisms and cell-matrix signalling.

The work was supported by the Fondazione CEN – Centro Europeo di Nanomedicina and it was carried out in Politecnico di Milano laboratories for what concerns Pluronic functionalization and hydrogel formulation, and in Fondazione IRCCS Ca' Granda Ospedale Maggiore Policlinico di Milano – Laboratorio di Nefrologia, for what concerns cytotoxicity and cell adhesion tests.

These experiments were carried out to obtain preliminary information on the biological responses of kidney glomerular cells in presence of soft biomaterials, which may find future applications in cell-culture models of kidney pathologies.

Abstract

Scopo di questo lavoro è lo sviluppo di una libreria di hydrogel a base di Pluronic, un copolimero a blocchi del tipo A-B-A composto da glicole polietilenico (PEG) e polipropilenglicole (PPG), di studiarne le proprietà chimico-fisiche finali e valutare le possibili applicazioni in nanomedicina.

Negli anni la ricerca si è ampiamente interrogata sulla possibilità di utilizzare il Pluronic F-127 come biomateriale, considerate le sue caratteristiche fisico-chimiche come la termosensitività, la facile funzionalizzazione e la buona biocompatibilità.

Recenti studi hanno dimostrato la possibilità di utilizzare efficacemente il Pluronic F-127 nell'ambito della microencapsulazione e dell' ingegneria tissutale

Nel nostro lavoro il Pluronic F-127 è stato funzionalizzato e quindi reticolato sia tramite addizione di Michael, sia tramite polimerizzazione radicalica (fotopolimerizzazione). La funzionalizzazione ha permesso la sintesi di nuovi precursori polimerici, chiamati Pluronic F-127 esacrilato (F-127 HA) e Pluronic F-127 tioacetato (F-127 TA), in grado di reticolare in condizioni assimilabili a quelle fisiologiche e adatti quindi per applicazioni di tipo biomedicali.

Entrambi i nuovi precursori polimerici sono stati caratterizzati tramite spettroscopia NMR e IR, mentre il tempo di gelazione è stato valutato tramite Dynamic Light Scattering. Nel contempo si sono studiate le proprietà fisiche del gel finale, che includono la determinazione dell'indice di swelling e le proprietà di diffusione.

Un secondo gel, a base di Pluronic diacrilato (F-127 DA) è stato ottenuto tramite polimerizzazione radicalica e ugualmente caratterizzato con lo scopo di valutare somiglianze e differenze rispetto al gel realizzato tramite addizione di Michael.
Infine entrambi i gel sono stati testati in vitro utilizzando tre differenti linee cellulari: fibroblasti, cellule endoteliali e podociti, al fine di valutare la differente risposta biologica e le proprietà adesive. In particolare per favorirne l'adesività, i gel sono stati sia funzionalizzati con un peptide, l'RGD, ampiamente utilizzato in queste applicazioni, sia trattati con medium cellulare.
Entrambe le metodologie si sono rivelate efficaci nell'adesione di cellule semplici come i fibroblasti, cosa non confermata nel caso delle più complesse cellule endoteliali e dei podociti.

Il presente lavoro è stato supportato finanziariamente dalla Fondazione CEN – Centro Europeo di Nanomedicina ed è stato svolto presso i laboratori del Politecnico di Milano per la parte più propriamente chimica (sintesi e formulazione del gel). I test cellulari in vitro sono stati invece condotti nei laboratori della Fondazione IRCCS Ca' Granda Ospedale Maggiore Policlinico di Milano – Laboratorio di Nefrologia.

I risultati ottenuti hanno consentito una valutazione preliminare sulla risposta biologica delle cellule costituenti il glomerulo renale alla presenza di biomateriali sintetici, e riguardo la possibilità di produrne un modello 3D utile nello studio delle patologie ad esso associate.

Fondazione CEN CentroEuropeo Nanomedicina

FONDAZIONE IRCCS CA' GRANDA
OSPEDALE MAGGIORE POLICLINICO
Regione Lombardia

List of Abbreviations

Å	Angstrom (10^{-10} meter)
AIBN	2,2'-Azobis(2-methylpropionitrile)
APS	Ammonium Persulfate
cmc	Critical micellar concentration
cgc	Critical gel concentration
FT-IR	Fourier Transform Infrared Spectroscopy
D_2O	Deuterium Oxide
DCM	Dichloromethane
DLS	Dynamic Light Scattering
DMEM	Dulbecco's modified eagle's medium
DMF	DiMethyl Formamide
DMSO	DiMethyl SulfOxide
meq	Milliequivalent
EDTA	EthyleneDiamineTetraacetic Acid
FBS	Fetal Bovine Serum
FDA	Food and Drug Administration
F-127	Pluronic
F-127 DA	Pluronic F-127 Diacrylate
F-127 ALL	Pluronic F-127 Allyl ether
F-127 TA	Pluronic F-127 Thioacetate
F-127 HA	Pluronic F-127 Hexaacrylate
F-127 ALD	Pluronic F-127 Aldheyde
F-127 TA-HA	Hydrogel based on F-127 thioacetate and F-127 Hexaacrylate
GPC	Gel Permeation Chromatography
Hz	Hertz
IR	Infrared

kPa	KiloPascal (10^3 Pascal)
LCST	Lower critical Solution Temperature
m	Meter
mL	Millilitre (10^{-3} liter)
mmol	Millimole (10^{-3} mole)
MW	Molecular Weight
nm	Nanometer (10^{-9} meter)
NMR	Nuclear Magnetic Resonance
NPs	Nanoparticles
PBS	Phosphate Buffered Saline
PDI	Poly Dispersity Index
PEG	Poly(ethylene glycol)
PPG	Poly(propylene glycol)
RGD	Synthetic peptide, sequence GRGDSPC
rpm	Revolution Per Minute
T701	Tetronic
T701 ACR	Tetronic 701 Acrylate
TCEP	Tris(2-carboxyethyl)phosphine hydrochloride
TEA	Triethylamine
TEMED	Tetramethylethyldiamine
Tetra ACR	Pentaerythritol tetraacrylate
T_g	Glass Transition Temperature
THF	Tetrahydrofuran
UCST	Upper Critical Solution Temperature
UV	Ultraviolet
μm	Micrometri (10^{-6} m)

1 Tissue Engineering

Tissue engineering is a multidisciplinary field involving chemistry, physics, medicine, biology, materials science and engineering. The major goal in tissue engineering is the solution of medical problems such as tissue loss and organs failure with their replacement. To accomplish this main objective, tissue engineering researchers must understand the complicated relationships in normal and pathological tissues to develop biological substitutes to maintain or improve tissue functions. In fact, in order to replace or repair damaged tissues with viable ones it is necessary to create a complex environment, which promotes the natural capacity of cells to integrate, differentiate and proliferate [1].

A major activity in tissue engineering is the design of biomaterials scaffolds with specific physical, mechanical and biological properties. Scaffolds might be defined as an artificial structure capable of being the substrate for cellular growth, proliferation and support for new tissue formation. Normally, in vivo tissue engineering implies the formation and implantation of three-dimensional scaffolds seeded with appropriate living cells, which secrete their own extracellular matrix (ECM).

In this context, it is clear that biomaterials and fabrication technologies play a key role in tissue engineering. Materials used for the applications must present biocompatible surfaces and favourable mechanical properties, to promote specific interactions with cells, thus they represent a key point for the success of tissue engineering practice. This success is usually achieved by adding bioactive molecules which are able to stimulate the intercellular communication and attachment of cells to a scaffold [2].

Continue innovations in technologies related to tissue engineering have led to great advances in this field in the last years. The rapid metamorphosis of tissue engineering

has occurred primarily through creative collaboration between engineers, surgeons, physicists, biologists, and scientists.

1.1 Historical evolution

To date, organ and tissue transplantation remains one of the most important, while complex, option in order to restore or enhance life expectancy. All reports for the requests of organ transplantation demonstrate that there are more patients than available organs and considering also the steady increase in life expectancy, this difference seems to increase, emphasizing the shortage of organ donors. In addition, diseases, infections and rejection of the tissue by the host, often complicate transplantation. In order to overcome problems associated with transplantation, in the last few decades tissue engineering has grown as a new inter- and multi-disciplinary scientific field [3].

Tissue engineering strives to achieve the same goals as those of clinical practice, with an emphasis on tissue and cell-based therapy. It is when the attention of medical treatment focused more on the regeneration of living tissues in vitro or ex vivo, using biotechnology approaches, that reconstructive surgery came to be called tissue engineering [4].

Tissue engineering is a recent discipline and still evolving. Because of this it is in continue evolution and also the term tissue engineering has changed connotation during the years. In the 1980's, the term tissue engineering was loosely applied to the use of prosthetic devices and the surgical manipulation of tissues [5]. The first recorded use of the term Tissue Engineering, as it is used today, so relied on the generation of new biocompatible tissue similar to the living ones, was in a published article entitled, "Functional Organ Replacement: The New Technology of Tissue Engineering" in "Surgical Technology International" in 1991[5].

When tissue and organs are damaged by infection, disease or injury, the first priority has always been the development of methods to save life and restore tissue/organ functions. Artificial or prosthetic materials to replace limbs, teeth, and other tissues resulted in the partial restoration of lost function. In the sixteenth century, Tagliacozzi of Bologna, Italy, reported in his work, "De Custorum Chirurigia per Insitionem," a description of a nose replacement that he constructed from a forearm flap [6]. With the advent of modern concepts of sterility and anesthesia, the success in the reconstructive surgery activity increased and the quality of life has been improved. The idea of improving on nature by using manmade materials was favoured by the discovery and availability of the new synthetics during World War II. Thermoplastic synthetic polymers such as nylon, Dracon, polyurethane, polypropylene, and many others, not originally designed for uses in the human body, were used by doctors and scientists for rebuilding damaged, diseased, aged, or genetically deficient body parts [6].

A pediatric orthopedic surgeon at the Children's Hospital, W. T. Green, M.D., tried in the early 1970's to generate new cartilage using chondrocytes seeded onto spicules of bone and implanted in nude mice. Although unsuccessful, he correctly concluded that with innovative biocompatible materials it would be possible to generate new tissues by seeding viable cells onto appropriately configured scaffolds. Several years later, Drs. Burke and Yannas of the Massachusetts General Hospital and M.I.T. collaborated to generate a tissue-engineered skin substitute using a collagen matrix to support the growth of dermal fibroblasts [5]. Dr. Howard Green later transferred sheets of keratinacytes onto burn patients. All of these examples represent seeds of the new discipline now known as Tissue Engineering [5].

The key point in the birth of this emerging field was in the mid-1980's when Dr. Joseph Vacanti of the Children's Hospital approached Dr. Robert Langer of MIT with an idea to design appropriate scaffolds for cell delivery as opposed to seeding cells onto available naturally occurring scaffolds having physical and chemical properties that could not be manipulated, thus resulting in unpredictable outcomes [5]. Dr. Vacanti realized extensive studies to generate functional tissue equivalents utilizing a branching

network of synthetic biocompatible/biodegradable polymers, configured as scaffolds seeded with viable cells. Although the most cited manuscript describing this new discipline may be the article published in Science by Langer and Vacanti, the original article describing the new technology was published five years earlier (in 1988) in Archives in Surgery [5].

In the mid-to late-1990's starting from Boston we see the creation of many Tissue Engineering Societies in Europe and Asia, and all over the world scientists took their first steps in studies on stem cells and bioactive scaffolds. In 1994 there was felt the necessity to organize a society and to create a journal dedicated to scientific interactions and the communication of high quality scientific presentations and publications**.** The Tissue Engineering Society (TES) founded by Drs. Charles A. and Joseph P. Vacanti in Boston in 1994, was officially incorporated in the state of Massachusetts on January 8, 1996 [5]. Over the next decade, in conjunction with the Asian and European Societies, TES would evolve and reorganize to become TERMIS, the Tissue Engineering and Regenerative Medicine International Society, by 2005. The society was to be an international society that would "continually encourage and promote the exchange of information in the field of Tissue Engineering through education, research and the dissemination of information useful to the individual and beneficial to mankind" [5]. After the formation of the Society a journal was created with the aim of exchange scientific information and to publish new ideas. The journal "Tissue Engineering" was founded in 1994 by Drs. Charles A. and Joseph P. Vacanti and Antonios Mikos of Rice University. Its Editorial Board was composed of an international balance of physicians and scientists. The name "Tissue Engineering" accurately reflects the scope of this specialized, multidisciplinary field [5].

In 1991, at the Children's Hospital in Boston, a young patient with Polands Syndrome, a congenital malformation of the rib-cage and absence of a sternum, became the first human to receive a tissue-engineered implant composed of a synthetic polymer scaffold implant seeded with autologous chondrocytes, intended to replace his absent sternum [5]. The procedure was performed by 3 of the original 8 members of the founding

governing board of the Tissue Engineering Society, Dr. J. Upton and Drs. J. and C. Vacanti. In 1998 a similar approached was utilized to replace an avulsed distal phalanx at UMass Medical Center by Drs. J. Shuffelberger and C. Vacanti. Dr. Toshiharu Shin'oka of the Department of Cardiovascular Surgery in Tokyo Women's Medical University, applied this discipline, on a larger scale, to humans, utilizing tissue-engineered pulmonary arteries in surgery. These examples supported the tremendous potential in generating new replacement parts for humans [5].

In spite of scientific progress, there are few examples of tissue engineering applications in humans. This could be due to the difficulties associated with "scale up" and cell death associated with implantation. In fact, large numbers of cells are needed to generate also relatively small volumes of tissue. To ultimately be effective in humans, it will be necessary to generate large volumes, starting with very few cells. To be effective, cells should be easily procured, expanded in vitro, survive at the initial implantation, and then be accepted as self from the human body. Another great limit to the complete application and diffusion of tissue engineering in human diseases is the difficulty to reproduce and generate a correct vascularization. Any tissue artificially designed must present as a central component a perfusing blood supplier, without which, the engineered tissue cannot rightly integrate and survive [7]. Effective strategies for inducing vascularization in engineered tissues include delivery of growth factors such as vascular endothelial growth factors (VEGF) and basic fibroblasts growth factors (bFGF) as recombinant proteins or gene vectors. Another possibility is to use progenitor cells such as endothelial progenitor cells (EPC) and mesenchymal stem cells (MSC). Moreover, vessel conduits or endothelium-lined channels directly fabricated into an implant could be a strategy or combination of these exposed therapies.

There is a considerable debate concerning different cell sources. A great success in the future would be the possibility of removing organ-specific cells from patients with certain diseases, genetically manipulate them *in vitro*, and return them to the patient: this could allow the development of a "mosaic tissue" or tissue consisting of the patient's own cells reducing recognition problems and as consequence lots of complications after implantation augmenting the probability of success [5].

1.2 Key aspects in tissue engineering

To realize the main goal of replicate tissues in vitro, complete knowledge of how normal tissues are built in vivo and how they developed themselves is the overwhelming challenge. To meet this objective, tissue engineering relies upon three essential points in the organ regeneration process [8]:

- The biomaterial or the scaffold.
- The cells seeded on the surface or embedded in the biomaterial.
- The environmental conditions.

As mentioned before, the most promising approach is to grow cells on scaffolds that acts as a temporary substrate for them during the regeneration, allowing the formation of a three dimensional stable structure. The main characteristics that have to be taken into account in the development of the scaffold are the pore size and shape, the porosity, the surface area, the interconnectivity between pores and mechanical properties. These parameters are important because they influence cell seeding, migration, growth, mass transport and tissue formation [9]. It is fundamental to develop and validate computational models of the scaffold to predict degradation rate and any other characteristics of the newly generated tissue in vitro and then in vivo. The biocompatibility of the material, which constitutes the scaffold, is a priority. In fact, the substrate materials must not cause inflammatory response or present cytotoxicity. The scaffolds must be easily sterilisable in both the surface and the bulk to prevent infection [9].

Regarding the use of cells in tissue engineering, two different strategies have been proposed: cellular and acellular tissue engineering strategies. In the first case, the cells are seeded on or encapsulated within the scaffold before its implantation. Cells embedded within the scaffold after the implantation merge, and encourage new tissue to

infiltrate, while the scaffold material itself is gradually degraded in vivo [4]. Once the material is fully reabsorbed, only the newly generated functional tissue remains. In the acellular approach, an unseeded scaffold is directly implanted into the damaged region to allow cell infiltration and possibly new blood vessels formation, associated with the deposition of macromolecule networks which constitute the new extracellular matrix (ECM). A combination of both cellular and acellular strategies can also be employed, whereby scaffolds are first cellularized, then de-cellularized by enzyme treatment, resulting in a scaffold "shell". This approach has the advantage of minimizing host tissue rejection of foreign cells [4].

The natural environmental conditions are obtained by adding to the scaffold natural biological signals, i.e. molecules that promote cell signalling and interactions, and cell adhesion.

1.3 Materials and production

Depending on the type of tissue to be engineered, such as cartilage, bone or soft tissue, biomaterials are fabricated into scaffolds with different properties to meet specific tissue requirements. Scaffolds have to be designed specifically in terms of size, shape but the clinical success of the construct is largely dependent on the quality of the starting materials, directly relied to its composition [10].
Since a biomaterial is designed to be used in contact with living tissues and cells it is necessary that it does not cause any harmful effects to host tissues and organs. Furthermore, every material and every scaffold need a high level of specification: in fact, a material used satisfactory in orthopedic surgery, may be inappropriate for cardiovascular applications for example [4].

Materials used in tissue engineering applications could be divided in three main categories:

- Naturally derived materials.
- Synthetic materials.
- Hybrid materials: a combination of the two categories mentioned before, to take advantages from both types of materials.

1.3.1 Natural and naturally derived materials

Natural and naturally-derived materials include polysaccharides, proteins and their derivatives. The advantages of natural materials are that they may exhibit low toxicity and low chronic inflammatory response, moreover they may possess biological activities such as cell recruiting and the promotion of neovasculature formation. They can be combined in composites with other natural material or synthetic ones, to generate a hybrid material and can be degraded by natural enzymes. A major disadvantage related to a natural material is their poor mechanical strength and difficulties in their manipulation due to a complex structure, complexities in purification methods and also immunogenicity, pathogen transmission, cost and availability [11,12].

A commonly used natural material is collagen. It exhibits good cell and tissue compatibility as it forms the major protein of the extracellular matrix (ECM). Collagen is a fibrous protein with a long, stiff, triple-stranded helical structure. It exists in different forms in various tissues, in fact it is classified in "Types", for example Type I is present in skin and bone, Type II in cartilage, Type III is predominant in the wall of blood vessels and Type IV from human placenta and differently from most collagens, it occurs only in basement membranes (BMs) [13]. The type IV collagen is the major component of basement membranes [14]; it has a globular head from one side and an additional tail in the other. The heads bind strongly to one another, head to head, furthermore four collagen molecules associate together with their tails forming a complex X-shaped [14].

Thanks to this type of interactions collagen type IV forms an extended network that promotes cells adhesion. Collagen scaffolds for tissue engineering application could present highly porous structure that favours cells penetration through them [15].

Hyaluronic acid (HA) is a non-sulfated, unbranched, linear glycosaminoglycan with repeating units of the disaccharide, β-1,4-D glucuronic acid- β-1,3-N-acetyl-D-glucosamine. It mediates cellular signalling, wound repair, morphogenesis, matrix organization, cell proliferation, and cell differentiation and promotes angiogenesis. Hyaluronic acid is a promising material for tissue regeneration due to its viscous properties, ability to retain water, biocompatibility and biodegradability. Thermosensitive and photopolymerizable injectable HA hydrogels have been developed and have shown potential for tissue engineering [16].

Chitosan is a cationic polysaccharide, hydrophilic, biocompatible and non-toxic extensively used for therapeutic applications such as tissue engineering and drug delivery. Chitosan is obtained as partially deacetylated derivative of chitin (1,4 β-linked N-acetyl-D-glucosamine) from the shells of crabs and shrimps [16].

Alginate, derived from brown algae, is a negatively charged polysaccharide composed of β-D-mannuronic acid and α-L-guluronic acid. It is considered as a biocompatible and non-immunogenic polymer. Upon addition of multivalent cations, alginate solution rapidly forms an ionotropic gel. An ionotropic gel has, in contrast to conventional gels, additional electrostatic associations through the cation species. This rapid gelation property makes it suitable for cardiac tissue regeneration [16].

Fibrin naturally formed during the wound healing process, it is also produced from fibrinogen and thrombin. It has been extensively employed as a tissue sealant and for the delivery of growth factors specific for tissue repair. Fibrin could acquire desired physical properties by modulation of the fibrinogen/ thrombin composition during the development of the tissue engineered scaffold [16].

Matrigel is a basement membrane protein mixture secreted by a mouse sarcoma. Its chemical composition has not been completely identified; some of the known constituents are collagen Type IV, laminin, entactin, heparan sulfate proteoglycan and growth factors. Its heterogeneous bioactive composition has a positive influence on cell adhesion, differentiation, and proliferation and promotes angiogenesis [16].

Decellularized extracellular matrices are biological scaffolds derived from various tissues and organs that have received significant attention for tissue regeneration. The use of decellularized tissue as scaffold has the advantage of being the best mimic of the architecture of the natural ECM having the right mechanical properties and by-passing the need to engineer all these characteristics in an artificial scaffold [8,16].

1.3.2 Synthetic materials

Synthetic materials have the advantage that could be designed with specific characteristics for a particular application. They can be made biocompatible and biodegradable, moreover they can replace natural materials thanks to their predictable, tuneable and reproducible mechanical, chemical and physical properties.

1.3.2.1 Polymers

Poly(ethylene glycol) (PEG) is a synthetic polymer used for the preparation of injectable hydrogels. It is biocompatible and suitable for the controlled release of growth factors. PEG chains show the interesting characteristic of being protein repellent: the high flexibility and the large exclusion volume of PEG strands in water avoid the adsorption of other macromolecules such as proteins, guaranteeing a prolonged residence in body and a reduction of protein immunogenicity [17]. Scaffolds incorporated with PEG chains can be subjected to further modification using bioactive peptides to stimulate cellular behaviours such as adhesion to proteins [16]. A variety of block copolymers

based on PEG with poly(propylene glycol) (PPG), known as Pluronics or Poloxamers (see Chapter 3), can be also utilized in tissue engineering applications taking advantage of PEG biocompatibility.

Aliphatic biocompatible polyesters polymers including poly(glycolic acid) (PGA), poly(lactic acid) (PLA) and their copolymer poly(lactic acid-co-glycolic acid) (PLGA) are used in sutures and meshes as they are approved by the FDA (Food and Drug Administration). These polymers degrade in a controlled manner, through hydrolysis of the ester bonds, with degradation products, non-toxic, eventually eliminated from the body in the form of low molecular weight compounds; their degradation rates can be tailored to satisfy the requirements from several weeks to several years by altering chemical composition, crystallinity, molecular weight and distribution [1].

PGA is widely used as polymer for scaffolds, due to its relatively hydrophilic nature, it degrades rapidly in aqueous solutions or in vivo environment, and loses mechanical integrity between two and four weeks. The extra methyl group in the PLA repeating unit makes it more hydrophobic respect to PGA, reduces the molecular affinity to water, and leads to a slower hydrolysis rate.

PLA is degraded by hydrolytic de-esterification into lactic acid. The morphology and crystallinity strongly influence PLA rate of biodegradation and mechanical properties, therefore PLA scaffold degrades slowly in vitro and in vivo, maintaining mechanical integrity until several months. The copolymers of these two synthetic polymers are diffused thanks to their intermediate degradation rates, obtained changing various lactic and glycolic acid ratios used to synthesize PLGA [1].

Poly(ε-caprolactone) (PCL) degrades at a significantly slower rate than PLA, PGA, and PLGA. The slow degradation makes PCL less attractive for some biomedical applications, but more attractive for long-term implants and controlled release applications. PCL, due to their good mechanical properties represents a candidate polymer for bone tissue engineering [1].

Another interesting synthetic polymer that forms gels is polyvinyl alcohol (PVA), a unique material as it exhibits semi-crystallinity even in its atactic form that lacks stereo-

regularity. PVA is a hydrophilic polymer obtained by polymerization of vinyl alcohol formed through the partial hydrolysis of vinyl acetate [16].

Poly(2-hydroxyethyl methacrylate) (pHEMA) is polymerized from the 2-hydroxyethyl methacrylate monomers by free radical precipitation polymerization. pHEMA hydrogels have been used as matrix material. The resultant hydrogel is relatively biologically inert, and it shows high resistance to protein adsorption and thereby prevents cell adhesion [18].

Poly(N-isopropylacrylamide) (PNIPAM) and its copolymers, such as PNIPAM with hydroxyethylmethacrylate, poly(trimethylene carbonate), acrylic acid, polycaprolactone, dextran, and dimethyl-γ-butyrolactone acrylate have been reported as effective strategy for cardiac regeneration [16].

Poly(glycerol sebacate) (PGS) is an elastomeric polymer with robust mechanical properties, biodegradability, and in vitro and in vivo biocompatibility [19].

Non-absorbable polymers such as polytetrafluoroethylene (PTFE) have been used in vascular grafts [20,16].

1.3.2.2 Ceramics and glasses

A wide range of inorganic/non-metallic materials are used in particular in tissue engineering bone. Bioactive glasses that cover network structures based on silica (O-Si-O) with ions such as calcium, sodium and phosphorus. There are two categories of bioactive glass: melt derived and sol-gel derived. The first one is produced by the melting and mixing of oxide components in a furnace. Sol-gel derived glass is obtained by the mixing of alkoxide components in solution in a fume hood. The silica network is then generated by hydrolysis of the alkoxides followed by condensation. polymerization [12].

The choice of the material, natural or synthetic one depends on the application and in particular on the desired cellular interactions.

1.3.3 Fabrication techniques

The development of novel biomaterials with different fabrication techniques is critical for the success of tissue engineering. Scaffolds can be manufactured in many forms and with different techniques to obtain the required characteristic for specific applications. 3D nanocomposite scaffolds based on biodegradable polymers have been developed by using different nanostructures and processing methods such as solvent casting and particulate leaching, gas foaming, emulsion freeze-drying, electrospinning, rapid prototyping and thermally induced phase separation. For example, solvent casting particulate leaching is an easy technique that has been widely used to fabricate biocomposite scaffolds: it involves the dissolution of the polymer in an organic solvent, mixing with porogen particles, and casting solution into a 3D mould. Gas foaming process can be used to fabricate highly porous polymers foams without the use of organic solvents. In these case nanofiber scaffolds or tubular ones can be obtained. Other types of scaffold fabricated for tissue engineering include hydrogels, microsphere-based scaffold and sponges [16]. In particular, hydrogels (seen further description in Chapter 3) are suitable for tissue engineering applications because their formation can occur in situ thus they can be injected directly at the desired location, by a minimally invasive procedure and they can show different shapes, also irregular, to fill tissue defects [21].

1.4 Cells

It is clear that an efficient reconstruction and replacement of damaged tissue or organs can be achieved only if living cells find the best environment to migrate, proliferate and differentiate. In this context, it is necessary to understand cells behaviour in both normal and healing conditions. Cells create or recreate functional structures using pre-programmed information and signalling. The specific knowledge of these natural

processes is fundamental to design precisely substitute of living tissues, to exploit all the possibilities of regenerative medicine [8].
There are different types of cells that could be used in tissue engineering applications, depending on the tissue or organ which has to be repaired or replaced.

1.4.1 Differentiated native cells from the organ of interest

Native targeted progenitor cells are found in every organ of the body. These cells are tissue-specific unipotent cells, being derived from most organs. They are already programmed to become the cell type needed when implanted in the tissue of interest, requiring no in vitro differentiation. They can also be obtained from the specific organ to be regenerated, expanded and used in the same patient thus avoiding any possible rejection problems. The only limitation regards with cell expansion from a diseased organ, since there may be not enough progenitor cells in that organ to be isolated. They are considered as reservoirs for new cell formation, being programmed to give rise to normal tissue, regardless of whether they reside in a normal or diseased environment [8].

1.4.2 Embryonic stem (ES) cells

Pluripotent human stem cells are an ideal source of cells, as they can differentiate into any replacement tissue in the body. One example is the embryonic stem cells. These cells have two important remarkable properties: the ability to proliferate in an undifferentiated state, but still pluripotent (self-renewal) and the ability to differentiate into a wide range of specialized cell types. The main disadvantage of using this type of cells is that they tend to form teratomas (tumor-like formations [22]) when implanted in

vivo due to their pluripotent state, and the cells are not autologous, thus limiting their clinical application due to problems with biological recognition and rejection [8].

1.4.3 Adult stem cells

Adult stem cells are the best-understood cell type in stem cell biology. They could be retrieved from different adult tissues, including the brain, heart, lungs, kidney, and spleen. The best characterized source for adult stem cells is the adult bone marrow. Adult bone marrow contains a heterogeneous group of cells, including hematopoietic stem cells, as well as macrophages, erythrocytes, fibroblasts, adipocytes, and endothelial cells. Bone marrow stem cells are commonly called marrow stromal stem cells or mesenchymal stem cells, and more commonly now, mesenchymal stromal cells (MSCs). Originally, MSCs are primitive cells which derive from the mesoderm, being able to differentiate into connective tissues, skeletal muscle cells, and cells of the vascular system. MSCs are non-hematopoietic (they does not form blood and immune cells, known on the contrary as hematopoietic stem cells [23]), multipotent so they are capable of differentiating into both mesenchymal and non-mesenchymal cell lineages. They down-regulate pro-inflammatory cytokines and upregulate anti-inflammatory factors thus modulating the inflammatory response. Moreover, MSCs demonstrate immunosuppressive properties via suppressing T-cells, natural killer (NK) cell functions, and modulating dendritic cell activities [8].

1.4.4 Amniotic-fluid and placental-derived stem cells (AFPS)

Multipotent amniotic-fluid and placental-derived stem (AFPS) cells are capable of extensive self-renewal. They represent 1% of the cells found in the amniotic fluid and placenta. The undifferentiated stem cells expand extensively and double every 36 h.

However, AFPS cells do not form tumors in vivo. These cells could be obtained from amniocentesis in the developing fetus, or from the placenta at the time of birth. AFPS cells represent a new class of stem cells with properties between those of ES and adult stem cell types: they are less active than the last ones but more than adult stem cells [8].

1.4.5 Adipose-tissue derived stem cells (ADSCs)

Adipose-tissue derived stem cells, ADSCs are obtained from adipose tissue that contains a supportive connective tissue containing the pluripotent progenitor cells of ADSCs. They are enormously abundant and easily accessible, unlike other cell types used in tissue engineering. They can be easily obtained via liposuction procedures.

1.5 Applications

Tissue engineering applications are very differentiated, they cover various types of human tissues, including bone and cartilaginous tissue, the firstly investigated, as well as cardiovascular, intestinal, stomach and liver tissues.

1.5.1 Cartilaginous tissue engineering

Cartilage is a connecting soft elastic tissue found in various parts of the body. It is generated by chondrocytes. Its network constituents are primarily collagen Type II, proteoglycans, water and mobile ions; its function is to lubricate joints [2]. Although cartilage is a quite simple tissue, it has a limited spontaneous regenerative capacity after destruction. Repair occurs through the formation of fibro-cartilaginous tissue, with a

different biochemistry and biomechanical profile from native cartilage [24]. In 1988, Vacanti et al. produced new hyaline cartilage from bovine chondrocytes on a polymer scaffold [5]. In subsequent studies with the use of nonwoven polyglycolic acid mesh or copolymers of polyglycolic acid and polylactic acid, the constructs were fabricated into predetermined shapes. Adult cartilage has limited self-healing ability due to non-vascular supply. Supporting matrix has been developed for effective chondrocyte delivery and cartilage repair [25]. An example is the application of a scaffold based on Pluronic F-127. Pluronic® F-127 is a synthetic hydrogel, which is nontoxic and biocompatible (for a more detailed description see Chapter 3); it has been widely used in delivery and controlled release of drugs. Several studies on the use of Pluronic F-127 for cartilage tissue engineering suggested that this polymer seems to be a favoured adhesive material to make the composite scaffold more cell-interactive. Certainly, the type of cell used in engineered cartilage is critical to the long-term success. Different cell populations have been investigated in the experimental studies include matured articular chondrocytes, epiphyseal chondrocytes, mesenchymal stem cells, bone marrow stromal cells, and perichondrocytes [25].

1.5.2 Bone tissue engineering

Tissue engineering applications for helping partial replacement of hard tissues began with cartilage and progressed to bone with the observation that chondrocytes derived from the articular surfaces differentiated in culture to cartilage, whereas chondrocytes from periosteum (a membrane that covers the outer surface of bones [26]) progress in culture to form new bone [2]. A combination of bone and cartilage tissue engineering was used more recently to create a finger replacement [24]. Bioactive ceramics such as HA and calcium phosphates are a major class of biomaterials for bone repair. They showed appropriate osteo-conductivity and biocompatibility in particular they are chemically and structural similar to native bone. However, their inherent brittleness and

the difficulty to shape them are considered disadvantages despite of this manipulation is enough to fit bone defects [9].

1.5.3 Vascular and cardiovascular tissue engineering

Tissue engineering has been an important approach for solutions to small and large vessel replacements. This result is based on tissue engineering vascular work, which began in 1978, when Herring successfully isolated endothelial cells from veins and transplanted them onto synthetic scaffolds. Polyhydroxyalkanoate and polyglycolic acid copolymer seeded with ovine arterial cells were firstly investigated [24]. The ideal goal for cardiovascular tissue engineering is the design of a non-obstructive, non-thrombotic, self-repairing tissue valve that would grow with the patient and remodel in response to in vivo stimuli with improved durability.

1.5.4 Intestinal tissue engineering

The ideal tissue-engineered intestinal substitute would be anatomically and microbiologically constructed to be as similar as possible to the real intestine but, in addition, it has to promote self-repair and self-proliferation. A composite tissue resembling small intestine was generated from "intestinal crypt cells heterotopically transplanted as epithelial organoid units, as firstly reported in 1998" [24]. The polymeric scaffold was based on polyglycolic acid, coated with polylactic acid, and the final biomaterial was implanted into the omentum, a layer of peritoneum [24].

1.5.5 Liver tissue engineering

The liver is a complex and indispensable organ that provides vital functions including metabolism, excretion, detoxification, storage, and phagocytosis. Currently, the only definitive treatment for severe hepatic failure remains liver transplantation. Tissue engineering applications for liver replacement have included direct cellular injection or transplantation through the development of extracorporeal bioartificial liver devices (BAL), and new three-dimensional engineered micro-fabricated constructs intended to be intracorporeal [24]. The main difficulty in this approach is to maintain during time the overall functional capacity of the injected cells. The goals of an extracorporeal BAL are to serve as a bridge to transplantation, reducing postoperative morbidity and mortality. Modern advances in microfabrication together with cellular co-culture may lead to an implantable tissue engineered liver. Actually, vascular ingrowth into transplanted constructs necessary for a complex organ such as the liver, is not adequate yet, thus some improvements are needed [24].

2 Hydrogels

Hydrogels are three dimensional, crosslinked networks of water-soluble polymers with high water content and capable of absorbing large amounts of water or biological fluids [27]. The first work reporting the creation and application of a hydrogel dates back to 1960, when Wichterle and Lim introduced a gel made of poly(2-hydroxyethyl methacrylate)) (HEMA), for biological uses [28]. During the years lots of studies have been based on hydrogels that gained more and more researchers' attention thanks to their unique properties. Hydrogel technology covered many applications in different fields, including drug and gene delivery, tissue engineering and medical devices. Main aspects and characteristic of hydrogels were discussed in this chapter.

2.1 Key aspects in hydrogel design

In the design of a hydrogel the main properties that have to take into account are those listed below. Each property depends specifically on the particular application for which the hydrogel has to be designed.

- Biocompatibility: the material does not interfere on cell function and does present any inflammatory response [29].

- Injectability and in situ crosslinking: the system should be in a sol state before administration. The viscosity of the material has an important role to improve handling of the gel and to give it any desired shape. The sol-gel transition has to

occur in vivo, after injection in the less invasive way as possible to avoid damages to living tissues or cells. In some cases, such as cell microencapsulation or in gel scaffolds, this property is not necessary.

- Mass transport: permeability and diffusion are fundamental properties for the controlled delivery of drugs, transport of oxygen and essential nutrients for cells and their metabolites.

- Biodegradability: it represents the capacity of the matrix to dissolve in a controlled time. The need of long or short degradation time depends strongly on the application, the type of drug to be released and on the targeted drug delivery profile . Release kinetics are dictated primarily by polymer or crosslinks degradation rates when the hydrogel mesh size is smaller than the hydrodynamic radius of the cargo molecule, and by diffusion when mesh size is larger than the hydrodynamic radius of cargo molecule [30].

- Mechanical properties: hardness and viscoelasticity, determined by the elastic and viscous moduli are some of the mechanical parameters that have to be take into account in hydrogel design. They depend on composition, polymer nature and concentration, processing and crosslinking density.

2.2 Main physico-chemical characteristics

In theory, hydrogels can be made from any water-soluble polymer. Their hydrophilic networks can absorb large amounts of water, from 10-20% to 99% by weight; hydrogels containing more than 95% of water are called superabsorbent [27]. Due to their large water content they are very similar to the native extracellular matrix (ECM) so it could

explain their large use in biomedical applications. Despite this high water content they do not dissolve in an aqueous environment but they swell, thanks to the crosslinks between network chains. These crosslinks could be divided in two main types: physical (entanglements or crystallites) and chemical (tie-points and junctions) [28]. Acting on the density of these crosslinks and on the polymer molecular weight, it could be possible to vary the porous structure of the hydrogel: its porosity is an important parameter in drug delivery applications. Biodegradability and hydrogel dissolution can be tuned via enzymatic, hydrolytic or environmental pathways [31].

The network structure of the hydrogel is an important parameter because it influences a lot the behaviour of the gel, for example in terms of swelling, release and degradation. The most important parameters that describe the structure of a hydrogel are polymer volume fraction in the swollen state $\nu_{2,s}$, the crosslinking density ρ and the correlation distance between two adjacent crosslinks, ε [32].

- The polymer volume fraction in the swollen state ($\nu_{2,s}$) describes the amount of liquid that can be imbibed in the hydrogel [32]:

$$\nu_{2,s} = \frac{V_P}{V_G} = \frac{polymer\ volume}{swollen\ volume}$$

- From this volume fraction a volumetric swollen ratio (Q) can be defined, related also to densities of the solvent and the polymer in the matrix [32]:

$$Q = \frac{\frac{Q_m}{\rho_s} + \frac{1}{\rho_p}}{\frac{1}{\rho_p}}$$

Where ρ_s is the density of the solvent

ρ_p is the density of the polymer

Q_m is the mass swollen ratio defined as $W_{swollen}/W_{dry}$, where W is the mass of the polymer in the different state.

- The crosslinking density ρ defined as [33]:

$$\rho = \frac{1}{\bar{v}\overline{M_c}}$$

Where $\bar{v}$ is the specific volume of the bulk polymer

$\overline{M_c}$ is the average molecular weight between two following crosslinking points.

- The correlation distance between two adjacent crosslinks, ε, that represents an estimate of the available space between the macromolecular chains [32]:

$$\varepsilon = v_{2,s}^{-1/3} l \left(\frac{2C_n \overline{M_c}}{M_r} \right)^{1/2}$$

Where, C_n is Flory characteristic ratio; it is constant for each polymer- solvent system and it is related to the short range interaction between polymer chains (gives an idea on the "stiffness" of the network).

l represents the carbon-carbon bond length.

M_r is the weight of the repeating units that constitute the polymer chain.

Despite lots of advantages such as biodegradability, biocompatibility, easy incorporation of cell membrane receptors and growth factors for tissue engineering applications, easy handling and shaping, hydrogels also present several disadvantages for their application as biomaterials. The relatively poor mechanical properties, in particular the low tensile

strength of many hydrogels and their fragility, limits hydrogel use in load-bearing applications and can cause premature polymer dissolution [31].

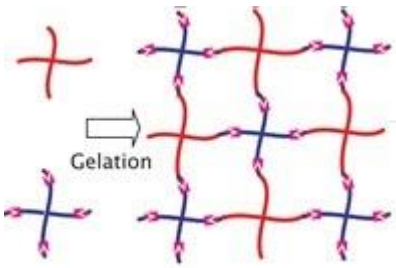

Figure 2.1 Example of a gel network [34].

2.3 Swelling behaviour

The amount of water in a hydrogel can influence permeation and release of nutrients, drugs and cellular products in and out of the gel. When a hydrogel is submerged in water, the first water molecules entering the matrix will hydrate the most polar, hydrophilic groups, leading to "primary bound water". In this way, the gel swells and exposes to water interactions also the hydrophobic groups, leading to hydrophobically-bound water, "secondary bound water". After these first stages, the matrix will absorb additional water, due to the osmotic driving force of the network chains towards infinite dilution. The hydrogel will reach an equilibrium swelling level because this additional swelling is counteracted by the covalent and physical crosslinks, generating an elastic network retraction force [35]. The additional swelling water is called "free water" or "bulk water" and it fills the spaces inside the network. When the swelling occurs, if the network chains are degradable, the gel will begin to dissolve; the rate at which this occurs depends primarily on its composition. In the design and characterisation of an hydrogel matrix it is important to know the amount of free and bound water. The

swelling behaviour, for its important role in determining gel properties and applications, was widely investigated by researchers to find theoretical models.

An equilibrium mathematical model for describing the physics of the swelling was developed by Flory and Rehner and it is known as *theory of the equilibrium swelling* [27]. In their analysis the swelling of the polymer network was dependent on the elastic forces of the polymer chains and the thermodynamic interactions between the polymer and water molecules. Thus, the free energy change of a hydrogel can be expressed as [36]:

$$\Delta G = \Delta G_{el} + \Delta G_{mix} \tag{3.1}$$

Where ΔG_{el} represents the elastic retractive forces

ΔG_{mix} is related to the thermodynamic compatibility of the polymer and the swelling agent.

Differentiating the above equation 3.1 with respect to the number of water molecules at constant temperature and pressure, an expression for the chemical potential change in water relied to swelling contribution is obtained [36]:

$$\mu_1 - \mu_{1,0} = \Delta\mu_{elastic} - \Delta\mu_{mix} \tag{3.2}$$

Where μ_1 is the chemical potential of the swelling agent within the gel

$\mu_{1,0}$ represents the chemical potential of the pure fluid

At equilibrium conditions, the chemical potential of the swelling agent inside and outside the gel must be equal: this corresponds to the equivalence of the elastic and mixing contributions to the chemical potential.
The chemical potential change due to the mixing term is due to two contributions: the heat of mixing and the entropy of mixing. Using appropriate thermodynamic relationships, the chemical potential of mixing can be expressed as [36]:

$$\Delta\mu_{mix} = RT\left(ln\left(1-\nu_{2,s}\right)+\nu_{2,s}+\chi_1\nu_{2,s}\right) \tag{3.3}$$

Where, $\nu_{2,s}$ is the volume fraction of the polymer in the gel in the swollen state;

χ_1 represents a parameter related to polymer-solvent interactions

The statistical theory of rubber elasticity is used to describe the elastic contribution to the chemical potential. The elastic free energy depends on the number of polymer chains in the network and on the linear expansion factor [36]. For gels that are crosslinked in the absence of water, the elastic contribution can be expressed as [36]:

$$\Delta\mu_{elastic} = RT\left(\frac{V_1}{\nu\overline{M_c}}\right)\left(1-\frac{2\overline{M_c}}{\overline{M_n}}\right)\left(\nu_{2,s}^{1/3}-\frac{\nu_{2,s}}{2}\right) \tag{3.4}$$

Where ν is the specific volume of the polymer

V_1 represents the molar volume of the swelling agent

$\overline{M_c}$ the molecular weight of the polymer chains between junction points

$\overline{M_n}$ the molecular weight of the polymer chains if no crosslinks are presented.

For gels that are crosslinked in the presence of water the elastic contribution to the chemical potential is [36]:

$$\Delta\mu_{elastic} = RT\left(\frac{V_1}{v\overline{M_c}}\right)\left(1-\frac{2\overline{M_c}}{\overline{M_n}}\right)\nu_{2,s}\left(\left(\frac{\nu_{2,s}}{\nu_{2,r}}\right)^{1/3}-\frac{\nu_{2,s}}{2\nu_{2,r}}\right) \qquad (3.5)$$

Where the additional parameter is $\nu_{2,r}$ represents the volume fraction of the polymer in the relaxed state (that is the state of crosslinked polymer at the equilibrium, in swollen or non swollen conditions) [36].

By combination equation (3.3), (3.4) and (3.5), the swelling behaviour of neutral hydrogels crosslinked both in the absence of water and in the presence of water are described by the following equations respectively [36]:

$$\frac{1}{\overline{M_c}} = \frac{2}{\overline{M_n}} - \frac{(v/V_1)\left[ln\left(1-\nu_{2,s}\right)+\nu_{2,s}+\chi_1\nu_{2,s}\right]}{\left(\nu_{2,s}^{1/3}-\frac{\nu_{2,s}}{2}\right)}$$

$$\frac{1}{\overline{M_c}} = \frac{2}{\overline{M_n}} - \frac{(v/V_1)\left[ln\left(1-\nu_{2,s}\right)+\nu_{2,s}+\chi_1\nu_{2,s}\right]}{\nu_{2,r}\left(\left(\frac{\nu_{2,s}}{\nu_{2,r}}\right)^{1/3}-\frac{\nu_{2,s}}{2\nu_{2,r}}\right)}$$

There are lots of different methods used by researchers to estimate the previously described parameters of a gel in a swollen state as fractions of the total water content. The three major techniques are: DSC (Differential Scanning Calorimetry), NMR (Nuclear Magnetic Resonance) and those based on the use of small molecular probes [35]. A diffuse parameter used to describe the degree of swelling is the equilibrium weight swelling ratio or degree of swelling. The hydrogel is immersed in distilled water until it reaches its equilibrium state. It is then taken out and after wiping out excess water it is being weighted. The equilibrium swelling ratio of the hydrogel represents the ratio between the weight of swollen hydrogel in equilibrium and the initial dry weight of the hydrogel [27].

2.4 Classification

Hydrogels can be classified into different categories based on [27,37]:

1. Source material, origin: natural and synthetic.
2. Method of preparation: homopolymeric, copolymeric and interpenetrating polymer network.
3. Physical structure: amorphous, semicrystalline and crystalline.
4. Type of crosslinking: physically or chemically crosslinked.
5. Physical appearance: matrix, film, press powder matrices, microsphere or capsule, coatings, membrane or sheets.
6. Network electrical charge: non-ionic (neutral); ionic, both cationic and anionic; amphoteric, i.e. containing both acid and basic groups; zwitterionic, i.e. containing both cationic and anionic groups in each structural unit.
7. Responses to external stimuli: stimulus-responsive and unresponsive.

2.4.1 Natural and synthetic hydrogels

Natural hydrogels include collagen, fibrin, hyaluronic acid (HA), Matrigel, and derivatives of natural materials such as chitosan, alginate and silk fibers. Some of these materials are components of the ECM in vivo, so they are considered natural-derived hydrogels. Disadvantages related to natural hydrogels are that their properties are difficult to control and they have lack of reproducibility due to their natural origin [38]. Other drawbacks in the use of natural hydrogels are their mechanical suboptimal characteristics and possible induced immunogenicity and inflammatory response, due to the presence of immunogen/pathogen moieties [28]. In contrast, natural hydrogels are bioactive and they usually provide spontaneous cell adhesion sites.

The most common synthetic hydrogels are based on poly(ethylene glycol), poly(acryl amide), poly(vinyl alcohol), poly(acrylic acid), poly(propylene fumarate-co-ethylene glycol), and polypeptides. Their physico-chemical properties are more reproducible respect to natural hydrogels, although a rigorous control of the preparation protocol needs to be observed [15]. Chemical composition and mechanical properties can be tuned by varying the concentration or molecular weight of the precursor and/or the crosslinking density. They can also be designed to be hydrolytically or enzymatically degradable over a variable time scale depending on the application. Hydrogel bioactivity can be enhanced by the addition of cell adhesion molecules, ligands or growth factors, by covalent grafting, adsorption or electrostatic interaction. Adhesion molecules can be grafted after hydrogel polymerization, or added to the pre-polymerized mixture and either physically trapped or chemically incorporated during polymerization [38].

2.4.2 Homopolymeric, copolymeric and multipolymer interpenetrating networks

Homopolymeric hydrogels are referred to a polymer network based on a single type of monomer. Their structure depends on the monomer characteristics and on the polymerization technique [37]. Copolymeric hydrogels are constituted of two or more different monomers, with at least one hydrophilic component. The configuration arrangement between different monomers could be random, block or alternating. Interpenetrating polymer hydrogels (IPN) are made of at least two independent crosslinked synthetic and/or natural polymer components, which constitute an interpenetrating gel network [37].

2.4.3 Physically or chemically crosslinked hydrogel

The crosslinks that constitute the hydrogel network can take place after or during the polymerization. If the crosslink is formed by covalent interactions the material is generally called chemical hydrogel; if the interactions are non-covalent, 'physical hydrogel' is the commonly used term.
Physical gelation is free of any chemical reaction, in this way a simple network is formed without involving potentially toxic crosslinkers or initiators [39]. In physical hydrogels junction zones are formed when the separate polymer chains interact over a certain length and not point to point (point crosslinks). Physical hydrogel formation could be obtained through non covalent interactions, such as crystallization, ionic, hydrophobic, electrostatic interactions, hydrogen bonding or a combination of these. Clearly, hydrogen bonds and van der Waals forces are much weaker than covalent ones [27,30].

Chemically crosslinked networks have permanent junctions. Since covalent interactions are much stronger than non-covalent ones, mechanical stability is improved. There are different chemical crosslinking methods such as radical polymerizations, chemical reaction of functional groups, high energy irradiation and enzymatic reactions. One of the most commonly used crosslinking methods involves a free radical mechanism promoted by a photo-initiator or a thermal radical initiator [39]. The presence of chemical elements augmented the risks of cytotoxicity of the hydrogel and their final biocompatibility.

2.4.4 Sensitivity to environmental conditions

Hydrogels characteristics strongly depend on the environmental conditions. " environment sensitive hydrogels" are materials which undergo drastic alteration in their structure and behaviour after changes in the external conditions [28]. We could distinguish between physical, chemical or other complex stimuli. Physical stimuli include

temperature, electric or magnetic field, light, pressure and sound, while the chemical stimuli include pH, solvent composition, ionic strength and molecular species [37].

2.4.4.1 Thermosensitive hydrogel

Among hydrogels responsive to external physical stimuli, particularly interesting are those which are temperature-sensitive, also known as thermosensitive hydrogels. This type of gel goes through a phase transition in response to external temperature stimulus [27]. The structure of thermoresponsive polymers reflects a fine balance between the hydrophobic and hydrophilic interactions among the polymer and water molecules [40]. The phase transition depends on interactions between the polymer network and water, and they can be divided into three types: polymer-polymer, polymer-water and water-water interaction. Thermoresponsive polymers are generally classified into two different types, depending on the presence of an upper critical solution temperature (UCST) or a lower critical solution temperature (LCST) [21]. The critical solution temperature (CST) is the temperature at which the polymer undergoes the sol-gel transition. In the case of a UCST, a phase separation occurs at low temperatures and the polymer solution converts into a gels by cooling , resulting in a 3D network formation via intermolecular interactions [21]. In case of a LCST, below this transition temperature, the hydrophilic domains of the polymer provide sufficient solubility and therefore the polymer-solvent dispersion is in a solution state. As the temperature increased, to above the LCST, hydrophobic interactions increase and the polymer becomes insoluble, thus causing a collapse into a gel form or a precipitate. Gelation based on UCST is generally not used in biomedical applications, as this sol-gel transition takes place at temperatures that are too high to preserve good cell viability [21]. On the other hand, thermally induced gelation based on LCST represents an attractive approach for obtaining an in situ injectable material for cell and drug delivery; in particular, systems are designed to gel at physiological temperature. The phase transition temperature can be altered by varying the composition of co-monomers in the polymer structure: with the addition of

hydrophobic co-monomers, the LCST can be decreased while increasing of hydrophilic content results in an augmented LCST. Furthermore, polymer concentration influence the sol-gel transition temperature: increasing polymer concentration, the temperature of gelation generally decreases.

A hypothesis to explain the existence the LCST is based on the presence of local structural transition, which involves the presence of water molecules around a specific portion of the polymer in solution. At low temperatures, the water molecules tend to be structured around the polymer chain and do not possess sufficient energy to alter the bonding pattern. With an increase in temperature, the water molecules gain energy resulting in an increase of motion which causes hydrogen bonding disruption. This causes exposure of hydrophobic monomers that consequently leads to more chances of mutual interactions and entanglements, and thus, formation of a gel [41].

Thermodynamically, the change in solubility necessary to obtain gel formation by LCST is related to the free energy of mixing. Considering the definition of the variation of the free energy, $\Delta G = \Delta H - T\Delta S$, where ΔG is the change in free energy of the system, ΔH is the change in the enthalpy of the system, T is the absolute temperature and ΔS is the change in entropy. Below the LCST, the entropy term (ΔS) is positive, thus the free energy term (ΔG) becomes negative and the mixing is favoured. On the contrary, above the LCST the change in entropy (ΔS) is negative leading to a positive free energy change (ΔG) which makes polymer–water association unfavourable, allowing interactions between polymer chains encouraging phase separation, thus gel formation [40].

2.4.4.2pH-sensitive hydrogel

pH-sensitive polymers are produced by adding acidic or basic functional groups to the polymer backbone; these groups either accept or release protons in response to appropriate pH and ionic strength changes in aqueous media [27]. The degree of ionization of these hydrogels depends on the number of pendant acidic or basic in the hydrogel. Neutral polymer gels show less swelling than polyelectrolyte ones. The more ionized a hydrogel is, the more charges will have, the higher electrostatic repulsion between the polymer chains will exist. Clearly, the swelling degree increases due to electrostatic repulsions [27]. Anionic materials contain pendant groups which are generally carboxylic acids or sulfonic acids. Ionization occurs when the pH of the environment is above the pK_A of the ionizable group [36]. When the pH of the system increases, the number of fixed charges increases, resulting in more electrostatic repulsion between the chains. This, in turn, results in an increased swelling. Conversely, cationic materials contain pendant groups such as amines. They ionize in media at pH below the pK_a values of the ionizable species. Thus, if the pH of the system decreases, ionization will increase, causing increased electrostatic repulsions and increased swelling [36].

2.5 Methods of characterisation

Due to the demand of hydrogels with characteristic more and more specifically tuned for every applications also methods of properties characterisation are developed and improved. Some methods of characterisation are listed below.

Sensor transducers are components, which convert the nonelectrical changes of properties of the stimuli-responsive hydrogel into an electrical signal. Transducers can exploit the mechanical work performed by hydrogels or observe alteration in hydrogel properties such as density, volume and stiffness. Various transduction methods are

available to study the variation in hydrogel properties; these include optical, conductometric, amperometric and mechanical methods [27].

The optical methods for detecting the volume change of hydrogels have been widely explored with different techniques. Two similar optical techniques are fluorescence resonance energy transfer (FRET) and non-radiative energy transfer (NRET). Both techniques involve a donor fluorescent dye emitting a photon which is consumed by another dye. Distance between the dyes, and thus of the swelling, can be measured with these techniques [27].

Among mechanical techniques micro-cantilevers can transduce changes of mass, temperature, heat, or stress, into bending (static mode) or a change in resonance frequency (dynamic mode). Hydrogel swelling leads to alteration of surface stress, which in turn statically bends the micro-cantilever. For dynamic mode, a change in the measure alters the resonant frequency which is measured after proper excitation of the structure [27].

2.6 Applications

Hydrogel applications cover a vast quantity of different discipline and scientific fields. This is probably due to their unique properties and to the possibility of tuning their parameters to optimize their final performance. The improvements during the years have largely influenced hydrogel application possibilities rendering it very versatile.

The hydrogel technologies may be applied to hygienic products, agriculture, drug delivery systems, sealing, coal dewatering, artificial snow, food additives, pharmaceuticals, biomedical applications, tissue engineering and regenerative medicines, diagnostics, wound dressing, separation of biomolecules or cells and barrier materials to regulate biological adhesions, and biosensor [37]. They were used in early agricultural water absorbents based on biopolymers through grafting of hydrophilic monomers onto starch and other polysaccharides [37]. Hydrogel products for hygienic applications are

mainly based on acrylic acid and its salts [37]. Pharmaceutical hydrogels could be categorized according to a variety of criteria mainly including, route of administration, type of material being delivered or release kinetics. Depending on the route of administration, pharmaceutical hydrogels can be classified as: oral hydrogel systems , transdermal and implantable hydrogel systems, topical and transdermal hydrogel systems, hydrogel devices for gastrointestinal (GI) drug delivery, hydrogel-based ocular delivery systems [28]. Drug delivery systems are one of the major applications of the hydrogel. This is due to their biocompatibility and controlled biodegradability. When they enter the human body they slowly degrade, releasing the drug they carry. However, poorly soluble drugs are difficult to entrap in the hydrogel matrix [27].

Hydrogel also find applications not directly related to biomedical field; they are used as materials for sensors, such as in pH sensors: micromechanical pH sensors, having an ability to sense a change of 5×10^{-5} pH by using an atomic force microscope for deflection measurement [27]. Many medically significant sensors have been produced including carbon dioxide sensors, lactate sensors, sensors for rheo-chemical characterisation of solutions, oxygen sensors and ion sensors.

In cell microencapsulation applications, cells are immobilized within microbeads or microcapsules. These micro constructs can be implanted in patients to restore organ or tissue functions, by mean of the activity of the encapsulated cells (which, for example, release therapeutic metabolites or proteins). A semi-permeable membrane is needed to protects cells from immune system rejection, by preventing permeation of antibodies, complement system components, thus avoiding the use of immune-suppressants [27].

3 Poloxamers (Pluronics)

3.1 General properties and applications

Poloxamers are nonionic triblock copolymers developed by BASF in 1973. They are build up with a central hydrophobic chain of *poly(propylene oxide)* (usually called PPO) tied with two hydrophilic chains of *poly(ethylene oxide)* (usually called PEO).

Different trade names, such as *Pluronics* or *Synpernonics* are possible.

Because the chain length of PEO and PPO is customizable and various PEO and PPO unit ratios are possible, different types of poloxamers exist.

Poloxamers are commercialized by BASF with different names, which are composed by a letter, *P*, and three digits: the first two digits represent, multiplied by 100, the molecular weight of the poly(propylene oxide) chain; the last digit, multiplied by 10, means the percentage of poly(ethylene oxide) in the copolymer. For example P188 is a non-ionic triblock copolymer build up with a poly(propylene oxide) molecular mass of 1800 g/mol and 80% of poly(ethylene oxide).

Pluronics nomenclature is different: the first letter indicates the physical form of the product, e.g. P=paste, L=liquid, F=flakes; the first (or the first two digits, if the name is a three-digits name), multiplied by 300, indicates the molecular weight of the poly(propylene oxide); the last digit, multiplied by 10, gives the percentage of poly(ethylene oxide).

Poloxamers are synthetized by condensation of ethylene oxide and propylene oxide [42].

Because of their molecular structure poloxamers have surfactant properties, which means that poloxamer molecules form micelles in water. They are soluble in water and in many polar and non-polar organic solvent.

For these properties poloxamers have been widely explored as carriers in drug delivery applications and are commonly used in the pharmaceutical and cosmetic industry.

3.2 Physics of block copolymers

In liquid medium, at low concentrations, i.e. 10^{-4} – 10^{-5} % w/v , Poloxamer molecules form monomolecular micelles [42,43] while, at higher concentrations, they form multimolecular aggregates, made up of an inner hydrophobic core surrounded by a hydrophilic poly(ethylene oxide) outer corona. This micellization phenomenon occurs above a critical concentration, known as *critical micellar concentration* (*cmc*), which values depend on the molecular weight of hydrophilic and hydrophobic block, the nature of the solvent and temperature. Above cmc the micelles can arrange in a lattice structure: the concentration at which this happens is called *critical gel concentration* (*cgc*).

The sequence is well explained in Figure 3.1.

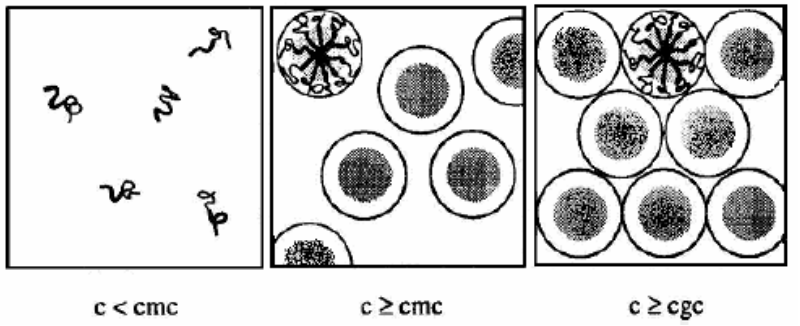

Figure 3.1 Poloxamer micelles behaviour with concentration [42].

This micellization behaviour and the presence of a LCST (see Chapter 2.4.4.1) guarantees the interesting, and widely applied, characteristic of reversible thermal gelation, i.e. the poloxamer suspensions are liquid at refrigerated temperatures but gel upon warming to room temperature.

Poloxamer micellization behaviour has been widely explored using various characterisation techniques, and correlations between the *molecular structure*, i.e. composition, molecular weight, structure, and *micellar characteristics*, i.e. cmc, cmt (the temperature at which micelles begin to form), micelle size and enthalpy, association number, have been found [44].

For example, using SAXS (*small-angle X-ray scattering*), it was demonstrated that depending on molecular weight, composition, temperature, concentration and salt content, not only spherical but also rod-like micelles are possible.

Booth and co-workers [45] studied the behaviour of the diblock copolymers PEO-PBO (PBO are block copolymers with poly(butylene oxide) instead of poly(propylene oxide)), PBO-PEO-PBO, and PEO-PBO-PEO copolymer and came to the conclusion that, at a certain composition, the CMC varies according to the following rule:

$$(PEO)_m\text{-}(PBO)_n << (PBO)_{n/2}\text{-}(PEO)_m\text{-}(PBO)_{n/2} \leq (PEO)_{m/2}\text{-}(PBO)_n\text{-}(PEO)_{m/2}$$

while the aggregation number Z (the number of molecules per micelle) increases with *n* and is highest for a diblock-copolymer.

Increasing temperature the hydrophilic domains of the chains will be desolvated due to the breakage of hydrogen bonds that have been established between these domains and the solvent. This leads to an increase in hydrophobic interactions between poly(propylene oxide) domains and to gel formation [46].

For most poloxamers of the series PEO-PPO-PEO, the cmt is usually between 20-50°C and its value increases with decreasing copolymer concentration [47,45].

Under the hypothesis of a large aggregation number Z and a narrow distribution, the standard free energy ΔG° and the standard enthalpy of micelle formation ΔH° are related to critical concentration cmt and temperature [48]:

$$\Delta G^\circ = RTln(cmt) \tag{4.6}$$

$$\Delta H^\circ = R\frac{dln(cmt)}{d(1/T)} \tag{4.7}$$

Where cmt is a molar concentration.

By integrating this equation we obtain [47]:

$$ln(cmt) \simeq \Delta H^\circ/RT + costant \tag{4.8}$$

that is ΔH° is approximately a constant in the temperature range involved.

For example, by evaluating *cmt* for Pluronic R17R4 using Dynamics Light Scattering as reported in [47], it is possible to plot the right line obtained in Equation (4.3), Figure 3.2: the line slope will represent ΔH°.

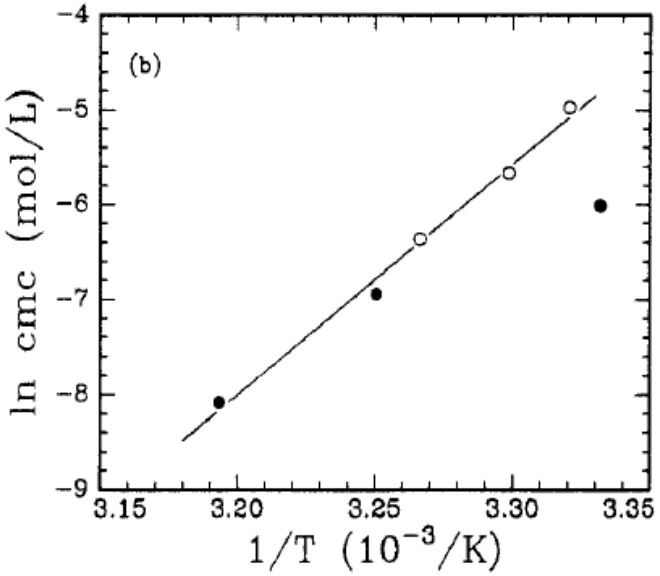

Figure 3.2 ln (cmc) vs 1/T plot for R17R4.

Once known the assumed constant value for ΔH°, that is $\Delta H^{\circ} = 115 \pm 6\ kJ/mol$, it was possible to evaluate other thermodynamic standard quantities: $\Delta G^{\circ} = -9\ kJ/mol$ and $T\Delta S^{\circ} = 124\ kJ/mol$.

The obtained results show us that:

1. In an aqueous medium micelle formation is endothermic.
2. in PEO-PPO-PEO the association process is usually *entropy driven*.

3.3 Pluronic F-127

One of the best known and widely used Poloxamer is Pluronic F-127, a linear triblock copolymer made up with a 13000 g/mol poly(propylene oxide) and 70% of poly(ethylene oxide).

Pluronic F-127 (or PF-124 or Poloxamer 407) aqueous solutions behaviour have been studied quite extensively.

In particular, aqueous solutions of F-127 with concentrations ranging from 20% and 30% are in liquid form when refrigerated and gel at room temperature, as previously studied by Schmolcka [49].

The molecular structure of Pluronic F-127 is illustrated in Figure 3.3 (m=68 ; n= 231).

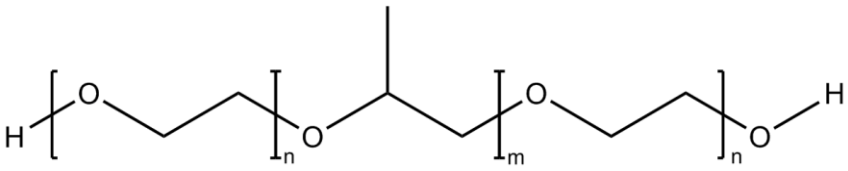

Figure 3.3 Pluronic F-127 molecular structure.

It is supposed that gels are micellar in nature: as previously seen, at low temperature a liquid micellar solution phase form is stable, while, increasing the temperature, due to the dehydration process we observe a cubic structure for micelles. A further increase in temperature leads to a hexagonal-packed cylinders form.

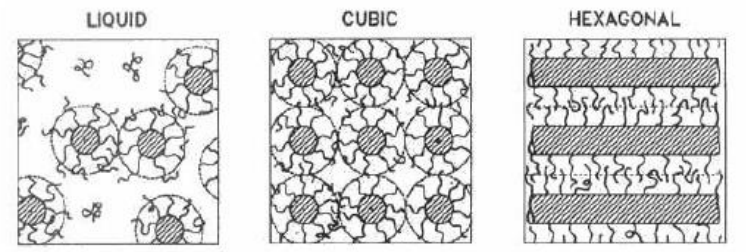

Figure 3.4 Thermal behaviour of Pluronic micelles [46].

Low toxicity and reversible thermal gelation at temperature close to the physiological one, for solution ≥ 20% wt, make F-127 solutions an important candidate for drug delivery and tissue engineering application [42].

For example, Miyazaki, et al [50] have shown that F-127 is a winning vehicle for topical administration of Indomethacin. Chi, et al [51] have developed a *ketoprofen* containing gel and have demonstrated prolonged anti-inflammatory and analgesic activities; more recently Want, *et al* [52] have studied the *in vivo* and *in vitro* skin absorption of *capsaicin* and *nonivamide.*

3.4 Tetronic

Tetronic are tetra functional block copolymers based on *poly(ethylene oxide)* and *poly(propylene oxide).*
Their tetra arms structure allows to use Tetronics as crosslinking molecules in chemical crosslinked gels (e.g. via Michael-addition [53])

An example of Tetronic molecule is Tetronic 701, Figure 3.5 (m=10, n=50).

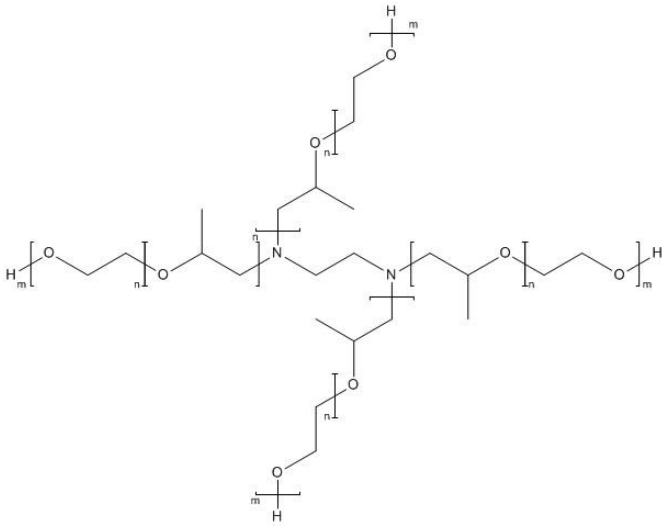

Figure 3.5 Tetronic 701 molecular structure.

4 Crosslinking methods to design hydrogels

It is important to ensure a crosslinking between the polymer molecules in hydrogels, with the aim to control their mechanical properties and durability.

Two crosslinking methods are here discussed:

- Physical crosslinking.
- Chemical crosslinking.

4.1 Physical crosslinking

We have a *reversible* or *physical* gel when the molecular networks are held together by molecular entanglements and/or secondary forces (i.e. ionic, H-bonding or hydrophobic forces) [35].

For example, as previously seen in Chapter 4, Pluronic solutions gel above a certain temperature known as *cmt* (*critical micellar temperature*), due to desolvation of PEO chains and more effective hydrophobic interactions between PPO groups.

Another example of this type of gel is sodium alginate, that represented for more than two decades the most common polymer for encapsulation purposes [54]: in this case the gelation is due to the combined presence of a polyelectrolyte and a multivalent ion of the opposite charge; these kinds of gels are also known as *ionotropic*.

However *physical gels* are usually not stable and present weak mechanical properties because of the weak forces involved in the crosslinks, besides their formation is quicker than the chemical gels.

4.2 Chemical crosslinking

Gels whose networks have been covalently-crosslinked are called *permanent* or *chemical* gels.

Like physical gels, in most cases chemical-crosslinked gels present regions which are not homogeneous: microscopically they present high-crosslinked and partially swollen regions, called *cluster,* dispersed within highly swollen and low crosslinked regions. However chemical-crosslinking guarantees stronger mechanical properties and stability.

In order to have a chemical-crosslinking it is required the presence of multifunctional groups in the polymers that, once reacted, generate crosslinking points and therefore a gel network; various chemical strategies can be used to covalently couple functional groups (Figure 4.1).

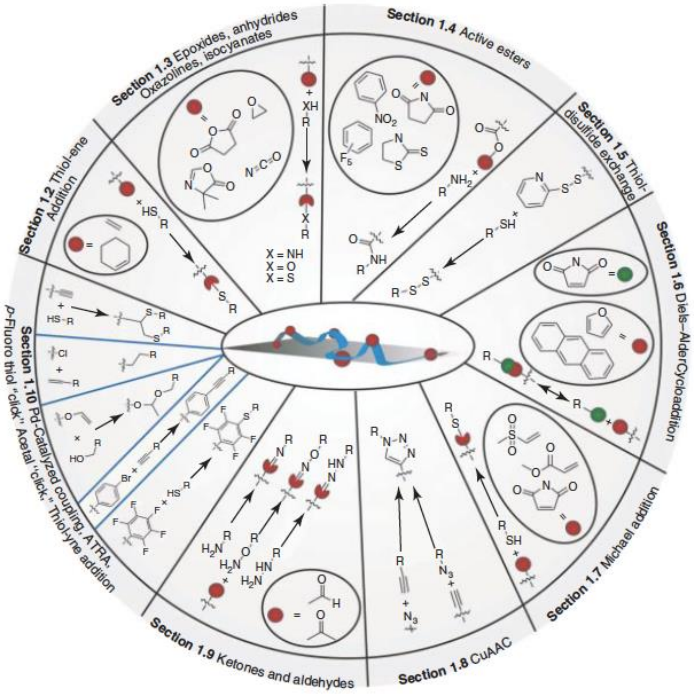

Figure 4.1 Various reaction that can be used for the preparation of functionalized polymers [55].

4.3 Free Radical Polymerization (FRP)

Photopolymerization is a method that enables *in situ* formation of crosslinked networks at physiological pH an temperature [56].

Researchers have focused their studies on the photopolymerization of PEG-based monomers in presence of appropriate photoinitiator molecules that generate free radicals when irradiated with UV light, interacting with end chain groups of polymers and starting a polymerization *via* radical pathway.

Many studies have been performed on photopolymerization of poly(ethylene glycole)-diacrylate (PEGDA) and poly(ethylene glycole)-dimethacrylate, modified PEG molecules with unsaturated double C final bonds that make them photopolymerizable. Additional molecule, e.g. poly(vinyl)alcohol can be mixed with PEG-monomers solution in order to control properties of the final hydrogel.

Hydrogels produced by photopolymerization pathway show high biocompatibility and studies have been carried out to test their use as vehicle for cell delivery applications.

4.4 Introduction to Click Chemistry

Click chemistry is a term widely used in organic chemistry to describe a set of reactions which generate the target molecules quickly and reliably, by conjugating small modular units. The term was coined by K. Barry Sharpless in 1998. As reported by Sharpless [57]: "*The required process characteristics include simple reaction conditions (ideally, the process should be insensitive to oxygen and water), readily available starting materials and reagents, the use of no solvent or a solvent that is benign (such as water) or easily removed, and simple product isolation. Purification - if required - must be by nonchromatographic methods, such as crystallization or distillation, and the product must be stable under physiological conditions.*"

The use of click chemistry approaches has significantly improved the chemical toolbox for producing functional biomaterials and hydrogels in the last decade. An overview on click chemistry principal reaction is reported hereafter.

4.4.1 Thiol-ene reaction

It is the addition of a thiol to an "ene" bond, usually a carbon-carbon double bond, through either a radical or a nucleophilic pathway [55].

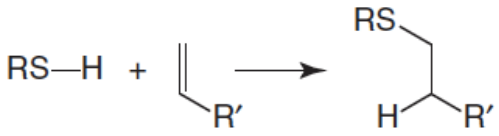

Figure 4.2 Addition of a thiol to an olefin [55].

4.4.2 Radical pathway

The radical addition of a thiol to an unsaturated C-C double bond proceed *via* three steps:

- Initiation.
- Propagation and chains transfer.
- Termination.

The general reaction scheme is synthetized in Figure 4.3.

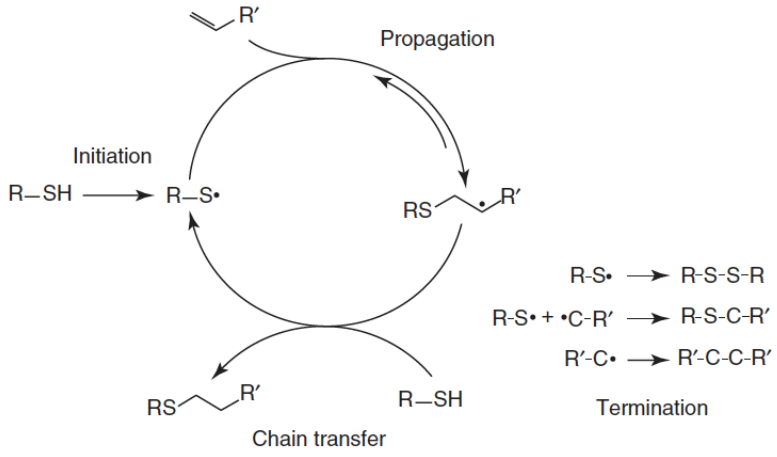

Figure 4.3 General radical thiol-ene addition mechanism [55].

4.4.3 Nuocleophilic thiol-ene addition: Michael-type reaction

As previously discussed, the thiol-ene addiction can also proceed via a nucleophilic route in aqueous solutions where a mild base act as catalyst.

The general nucleophilic mechanism proposed is shown in Figure 4.4.

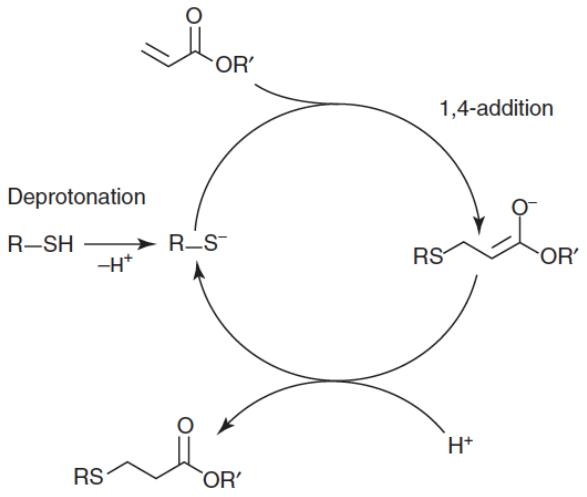

Figure 4.4 Proposed nucleophilic thiol-ene reaction mechanism [55].

The key step is the Michael reaction, that consists in the addition of a strongly nucleophilic thiolated anion to an activate C-C double bond. The double bond activation is usually due to the presence of electron-withdrawing groups (i.e. esters, amides, nitriles) next to the double bond.

This reaction is powerful in polymers functionalization and crosslinking, and two pathways are possible, as shown in Figure 4.5.

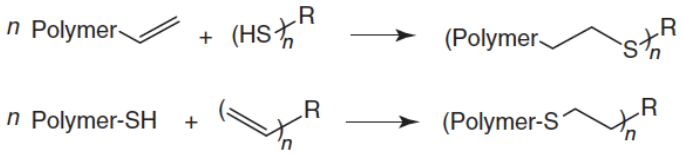

Figure 4.5 Polymer-end functionalization via Michael-type reaction [55].

In the years this reactions has been widely investigated for biomedical applications due to its cell friendly chemistry [58]. In fact the reaction do not generate any toxic by-products, it is relatively fast at physiological pH and temperature, and can reach quantitative conversion [59].

4.4.4 Azide-Alkyne reaction (CuI-catalyzed azide/alkyne cycloaddition (CuAAC))

Garamon in his fundamental work [57] refers to this reaction as the *cream of the crop* of click chemistry.

It is an evolution of the non catalized Huisgen reaction between an azide and a terminal or internal alkyne that produces at about 100°C a mixture of 1,4 and 1,5-disubstitution products.

Differently the Cu(I) catalised reaction at room temperature is completely selective in the formation of 1,4 and 1,5-disubstitution products [60], as shown in Figure 4.6.

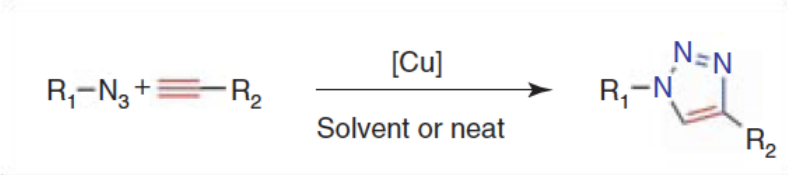

Figure 4.6 Reaction pathway for a typical copper catalized Huisgen cycloaddition [61].

The presence of copper catalyst is an important limit in biological due to its toxicity [62].

4.4.5 Oxime chemistry

This reaction involves the reaction between an aminoxy group and an aldehyde or keton.

An application is reported in Figure 4.7, where an eight-armed aminooxy functionalized poly(ethylene glycol) was mixed with glutaraldehyde to form oxyme-linked hydrogel [63].

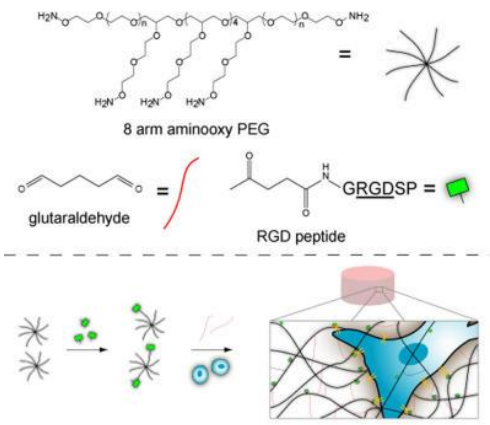

Figure 4.7 Eight-arms PEG aminooxy functionalized crosslinked with glutaraldehyde [63].

5 Cell Adhesion

Although polymeric hydrogels are materials that can efficiently mimic the extracellular matrix (ECM) in their physic-chemical properties, hey are often non-adhesive to cells. This lack of adhesion is generally due to the absence of adhesive cell signals, i.e. biomolecules that bind specific proteins on the cell membrane (namely integrins) and transduce mechanical stresses from the gel to the cells.

Commonly used strategies to improve cell adhesion are:

- The addition of *cell adhesive peptides* (e.g. RGD).
- Usage of *block co-networks*.
- The addition of *alkyl amine functionality*.

These strategies will be briefly discussed hereafter.

5.1 Cell Adhesive Peptides

Mammalian cells are hold in tissues via binding of integrins, displaced on cell surface, and specific amino acid sequences present in the proteic components of the extracellular matrix. Researchers have tried to mimic this mechanism in order to design cell adhesive hydrogel scaffolds to use in Tissue Engineering [64].

The most studied peptide-functionalize materials mimic the integrin binding arginine-glycine-aspartic acid (RGD) sequence [65].

It is possible to include RGD via:

- **Physical methods** (deposition, adsorption, precipitation into or onto a material)
- **Chemical methods** that involve covalent bonds between the functionalized-peptide and the substrate (e.g. interactions with hydroxyl, amino, carboxyl groups)

Two different RGD molecular structures are possible: *linear* and *cyclical*; the cyclical one is more stable and selective over the linear one.

In the following various RGD types produced by Peptide International are reported in the following [66]:

- **cyclo (Arg-Gly-Asp-$_D$-Phe-Cys).** structure is reported in Figure 5.1. It can be conjugated through the cysteine via Michael-type addition for example using acrylates, methacrylates and maleimide [67].

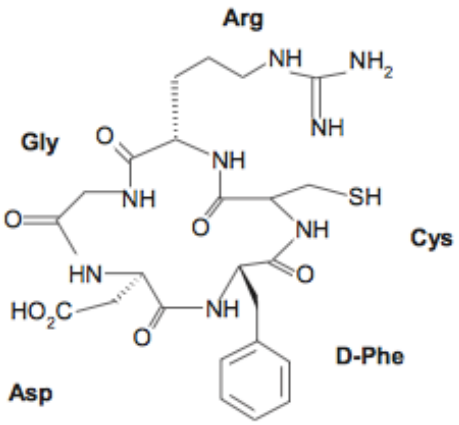

Figure 5.1 Cyclo (Arg-Gly-Asp-$_D$-Phe-Cys)

- **Cyclo [Arg-Gly-Asp-D- Phe-Lys(Ac-SCH2CO)]**, reported in Figure 5.2, contains a S-acetilthioacetil group that, after deprotection, can be used to form thioether bonds [68].

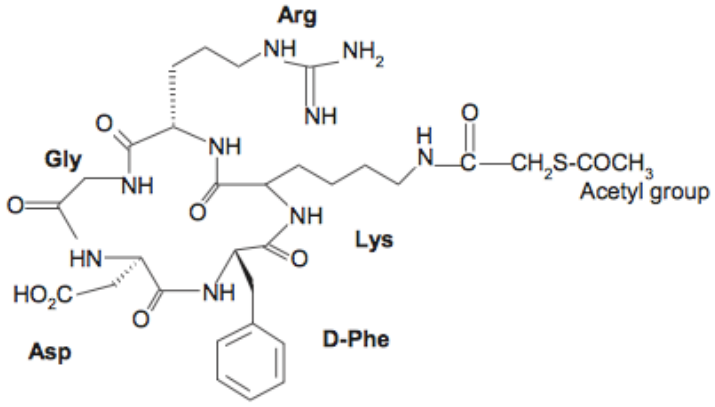

Figure 5.2 Cyclo [Arg-Gly-Asp-D- Phe-Lys(Ac-SCH2CO)]

- **GRGDSPC, H-Gly-Arg-Gly-Asp-Ser-Pro-Cys-OH**: This peptide is an ideal novel targeted non-viral gene delivery vector, which was easy to be synthesized, high efficient and low cytotoxicity. The integrin-binding heptapeptide GRGDSPC can be easily linked to carriers or surfaces this is possible thanks to the presence of the end –SH group [69]. In particular, this peptide sequence is the one used in our experiments linked to our polymer gel via Michael-type addition.

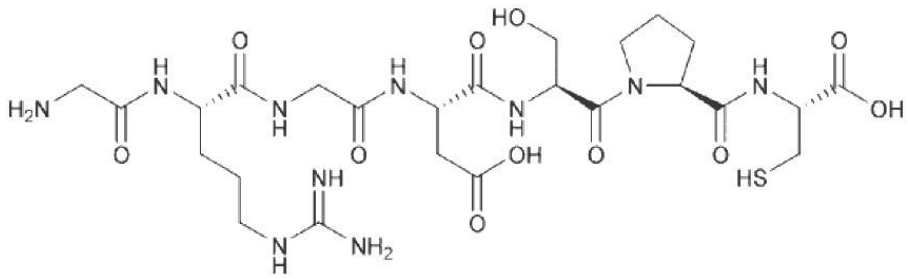

Figure 5.3 H-Gly-Arg-Gly-Asp-Ser-Pro-Cys-OH

Other arginine-glycine-aspartic acid motif containing molecules, with different properties, are possible.

6 Cells

As discussed in Chapter 1, the unique characteristics of stem cells have been widely exploited in tissue engineering. Anyway, several other cell types are commonly used in tests with biomaterials and as biomaterial constituents for biomedical applications. Cell lines of differentiated cells offer several advantages over primary cells and stem cells, including robustness, easy culture protocols, availability and contained lab costs. In particular, in this thesis work we used fibroblast, endothelial cell and podocyte cell lines for a fast screening of our gel properties. While fibroblasts are considered a standard for cytotoxicity tests on drugs and biomaterials, kidney glomerular cells, i.e. endothelial cells and podocytes, were chosen to assess their biological response in presence of soft biomaterials. In fact, we were interested in selecting hydrogels for future applications in *in vitro* 3D-models of kidney glomeruli..

6.1 Fibroblasts

Fibroblasts are a heterogeneous population of cells found in numerous tissues and are of mesenchymal origin. Fibroblasts from different anatomical sites have all a similar morphology but DNA-microarray studies have demonstrated that a specific gene-expression profile corresponds to each different anatomical source. For example, dermal fibroblasts have numerous functions, not only in synthesizing and depositing ECM components, but also proliferation and migration in response to chemotactic, mitogenic and modulatory cytokines, and also autocrine and paracrine interactions [70].

The development of techniques for culturing fibroblasts was long established prior to the discovery made in 1975 by Rheinwald and Green for culturing and expanding keratinocytes, which require growth-arrested murine 3T3 fibroblast cells to support their proliferation [70]. Dermal fibroblasts can be extracted from skin biopsies either through enzymatic degradation or by explant culture, which is particularly useful for obtaining cells from smaller specimens. Growth parameters and the characteristics of fibroblasts in culture are influenced by passage number, age of the donor, subtype of fibroblast (reticular or papillary dermis) being cultured and anatomical site. Older donor skin fibroblasts compared with younger skin fibroblasts tend to migrate more slowly, reach cell culture senescence earlier and have a prolonged cell population doubling time [70]. Other factors that influence fibroblast behaviour in culture include vitamins, such as vitamin C, and antioxidants, including coenzyme Q10. Fibroblasts used in tissue engineering may be allogeneic or autologous. In contrast to allogeneic cells, autologous fibroblasts carry no risk of rejection or risk of cross-infection. However, there is often a delay in culturing autologous cells in order to obtain sufficient cell numbers, whereas allogeneic cells are cryopreserved and therefore readily available [70].
In the present experiment a specific type of commercialized fibroblasts was utilized. The 3T3 cell line (CLS order No. 400103) was established from 17 to 19 days old mouse embryos. The cells are contact inhibited. The cells should be grown in plastic flasks; they do not grow well on some types of glass surfaces [71].

6.2 Endothelial cells

Endothelium is an integral component of a number of physiological and pathophysiological processes, including neovascularization, wound healing, thrombosis, atherosclerosis, tumor growth, and diabetic retinopathy [72]. Endothelial cells (EC) line the blood vessels and are present throughout the vasculature in the human body. These cells have the ability to self-assemble into vascular tubes when isolated and then cultured in protein materials such as collagen and fibrin. Endothelial cells can be

extracted from numerous tissue sources, including umbilical cords, dermal tissue and the saphenous vein [20]. Endothelial cells can be divided in different types depending on their source: a commonly used macrovascular cell type is human umbilical vascular endothelial cells (HUVEC), human dermal microvascular endothelial cells (HMVEC). An advantage of HMVEC is that they potentially represent an autologous cell source for therapeutic neovascularization [20]. Other sources of EC such as those isolated directly from the bone marrow (bmEC) and EC derived from an original progenitor cell source were explored. Although these cell types are less commonly used, they have potential advantages in terms of availability and use as an allogeneic cell source. However, the methods for isolating these cells are still being developed [20]. Glomerular endothelial cells are another type of these cells greatly studied. This specific type of endothelial cells present fenestrations [73]. Although several other endothelial cells (EC) possess these transcytoplasmic holes, those of the glomerular endothelium have a unique constellation of structural features. Furthermore, they perform a unique and vital physiological function in allowing filtration of the blood in the glomerulus [73].

Endothelial cells used in our experiments are derived from Mus musculus hemangioendothelioma (mouse). This endothelial cell line, EOMA (Cell Line Designation: EOMA ATCC Catalogue No. CRL-2586) has been isolated in 1980 from a mouse hemangioenthotelioma [68]. Endothelioma cells synthesize angiotensin-converting enzyme, express surface receptors for acetylated low density lipoprotein, produce thrombospondin and show intracellular staining with an antibody to von Willebrand antigen. Eoma cells secrete Catepsine L. Although these cells can constitutively express the genes for the cytokines, mRNA IL-6, their levels are particularly increased after incubation with Liposome Encapsulated Hemoglobin (LEH) [69]. Eoma cells have all the properties of endothelial cells, such as the capacity of organized themselves in tubular structures when cultured in protein materials such as Matrigel. Their behaviour in vitro is the same as microvascular endothelial cells.

6.3 Podocytes

Podocytes are unique cells with a complex cellular organization. In the kidney, glomerular podocytes are highly differentiated cells with a complex ramified structure, [74]. The glomerular basement membrane (GBM) provides the primary structural support for the glomerular tuft. The basic unit of the glomerular tuft is a single capillary. Endothelial and mesangial cells are located inside the GBM, while podocytes are attached outer [75]. Podocytes are exposed to a wide variety of chemical and mechanical stimuli, both from the blood stream and the urinary space. To constantly maintain proper glomerular filtration, they need to communicate among themselves and with the other glomerular cells [74]. Kidneys receive 20% of cardiac output, meaning that the whole blood of the organism passes at the glomerular filtration barrier every 5 min [74]. Therefore, glomerular cells are exposed to a highly changing microenvironment, in terms of blood pressure and content, and must rapidly identify and react to physiological and pathological changes, to maintain the integrity of the filtration process. Thanks to their location and a highly ramified structure, podocytes can accomplish this process, and appear to utilize to this purpose a highly informative and fast neuron-like system of communication to signal between themselves and with the other glomerular cells [74].

In the present experiment a specific type of commercialized podocytes was utilized. Podocytes cells SVI (CLS order No. 400495) cloned from the outgrowth of glomeruli which were isolated from H-2kb-tsA58 transgenic mice. Cells proliferate at 33°C, and they mature at 37°C. At present, the cells have been cultured successfully for more than 40 passages without noting phenotypic changes [76].

6.4 Cellular medium

All the cell media were prepared under sterile conditions, that is, all the activities were carried out under laminar flow cabinet to prevent contaminations. Once prepared, culture media can be stored at 4°C and heated in a thermal bath before being used. The main components of cell media were the same for the different types of cell and are listed below:

- Fetal bovine serum FBS (Sigma-Aldrich) : it is a fetal bovine serum. Serum is the centrifuged fluid component of either clotted or defibrinated whole blood. Bovine serum comes from blood taken from domestic cattle. Bovine serum is categorized according to the age of the animal from which the blood was collected because this property influences the characteristics of the fluid. *Fetal bovine serum* comes from fetuses, *newborn calf serum* comes from calves less than three weeks old, *calf serum* comes from calves aged between three weeks and 12 months and *adult bovine serum* comes from cattle older than 12 months [77]. Fetal bovine serum is the most widely used growth supplement for cell culture media because of its high content of embryonic growth promoting factors, proteins. The most important protein among them is BSA, Bovine serum albumin, a globular protein. This serum promotes cells growth, proliferation and differentiation.

- Antibiotics (PS:Penicillin – Streptomycin) : they ensure the sterility avoiding contaminations by microorganisms. Their presence is necessary for preventive purposes.

- Hydrocortisone and sodium selenite: they are hormones added to the culture medium of the cells to promote cells growth.

- L-glutamine, insulin and transferrin: they are important factors that allow the growth of cells and promote their metabolism.

6.5 Cells transfer from a flask/plate in confluence-trypsinization

When cells reach a certain level of growth in a flask, they must be detached and transferred to a new flask with fresh medium to prevent overcrowding that can cause their death. Trypsin and EDTA are used to detach the cells. Cell-matrix-interactions are mediated by a variety of adhesion molecules, in particular by integrins. The integrins are a family of at least 20 different heterodimeric cell surface receptors that mediate adhesion to various extracellular matrix components as well as to other cells. Integrins transduce signals from the extracellular environment to the cytoskeleton and to the nucleus of cells, thereby inducing gene expression of matrix-degrading metalloproteinases and other genes. The binding of integrins to their specific ligands is dependent on the presence of divalent cations, such as Mg^{2+}, Mn^{2+} and Ca^{2+}. These cations presumably exert their effects by binding to three to five cation-binding regions within all integrin α subunits and possibly also within distinct β subunits [78] thereby enabling cell adhesion. EDTA can bind divalent ions such as Mg^{2+} and Ca^{2+}, acting on adhesion and deadhesion mechanism of cells. Trypsin is an enzyme, belonging to the class of hydrolytic enzymes, that catalyzes the proteolytic cleavage with selectivity for arginine and lysine. In its active site, trypsin presents a specific sequence named "catalytic triad", i.e. Ser195-His57-Asp102. The substrate of trypsin is a basic protein. The optimal pH for its catalytic activity is in a range of 7 and 9, at different pH the hydrolysis mediated by this protease is too slow. Cells adhesion and aggregation need interactions between specific proteins present on the cells surface and known as "adhesion receptors". There are at least three different mechanisms of molecular recognition between cells: a mechanism based on homophilic interactions, in which a receptor of a cell binds an equal receptor on adjacent cell; an heterophilic mechanism, which occurs when the receptors that mediate the interaction between adjacent cells are

of different types; one mediated by a bifunctional molecule that acts as a bridge between the two receptors on adjacent cells. The receptors that mediate the recognition and adhesion between cells belong to two separate groups for structure and properties: cadherins (Ca^{2+} -aderine), which work only in the presence of calcium ions (Ca^{2+}) and molecules (CAM, cell adhesion molecules), belonging to the immunoglobulin superfamily, which mediate the adhesion in the absence of Ca^{2+}. Trypsin, as mentioned before, is a proteolytic enzyme, that is, it removes the proteins on cell surface causing cells detachment because the adhesion mechanism explained are forbidden . Before its use, the culture medium must be removed because it contains a trypsin inhibitor (alpha-1 antitrypsin) [79].

6.6 Cell preservation methods

Cell growth is fast and often the quantity of cells needed during an experiment is not elevated, particularly in the starting phases of the project. Then, it is useful to freeze cells: this operation allows to store cells ideally for an unlimited time period keeping constant their properties and characteristics. Freezing cells can be easily reused if necessary by simply thawing them as explain below.

6.7 Material and methods

In this section we exposed the techniques to prepare cell medium, to preserve cells and all the activities necessary for culturing cells in order to allow them to survive and grow. The quantity and particular factors vary among endothelial cells and podocytes, but for the latter is the same of that for fibroblasts. All quantities and reagents are listed below:

Materials. Dulbecco's Modified Eagle's Medium/Nutrient F-12 Ham (DMEM/F12)(D6421), Dulbecco's phosphate buffered saline (PBS)(D8537), fetal bovine serum (FBS) (F9665-500 mL), Collagen from human placenta (Bornstein and Traub Type IV, C5533-5 mg), Penicillin-Streptomycin (PS)(P4333-100 mL), L-Glutamine solution (G7513-100 mL), trypsin-EDTA solution (1x, T3924-100 mL), Apo-transferrin human (T5391-10 mg), hydrocrtisone (H0135-1 mg), sodium selenite (S9133-1 mg), dimethyl sulfoxide (DMSO)(D1435-500 mL), HEPES (H3375) were purchased by Sigma-Aldrich; Humulin 100U/mL human insulin purchased by Eli Lilly.

- Endothelial cells medium

Base Volume	**100 mL**
DMEM/F-12 (1:1)	100 mL
FBS 10%	11 ml
Penicillin 100000 U/ml and Streptomycin 100 μg/ml	1 mL
L-glutamine 4mM	2.2 mL

- Podocyte/fibroblast medium

Base Volume	**100 mL**
DMEM/F-12 (1:1)	100 mL
FBS 10%	11 ml

Penicillin 100000 U/ml and Streptomycin 100 μg/ml	1 mL
L-glutamine 2mM	1.1 mL
Transferrin 5 μl/ml	1 mL
Hydrocortisone 10^{-7}M	72μL
sodium selenite 5ng/mL	25 μL
Insulin	0.12 U/mL

6.7.1 Podocytes culture flask preparation

A tablet of collagen type IV was dissolved in 5 mL of acetic acid 0.25% (1mg/mL) (Sigma-Aldrich); the mixture was left under stirring overnight to promote complete protein dissolution. An optimal collagen coating is achieved at a surface concentration of 6 μg/cm^2 , therefore the amount of collagen solution added to the flask depends on the surface area of the flask used:

- T75 (75cm^2): 450 μl collagen solution in 5 ml PBS(Phosphate buffered saline, pH 7.4. Life Technologies).
- T25 (25cm^2): 150 μl collagen solution in 3 ml PBS.
- 35 mm Petri (10 cm^2): 60 μl collagen solution in 1 ml PBS.
- well, volume 0.3-0.45 ml culture area 0.8 cm^2 : 4.8 μl collagen solution.
- 4 well, volume 0.7-1.0 ml culture area 1.8 cm^2 :10.8 μl collagen solution.
- 2 well, volume 2.0-2.5 ml culture area 4.2 cm^2:25.2 μl collagen solution.

Once the collagen solution was added, the flask was incubated at 37 °C for 2 hours or at 4 °C overnight. Before culturing the cells in the flask, the collagen solution was removed and the flask washed two times with PBS.

Procedure. Before starting trypsinization it is necessary to verify at the optical microscope that the cells in the flask are grown enough to reach the confluence condition. The medium was removed from the flask and cells washed two times with PBS or Hank's solution without Mg^{2+} and Ca^{2+} (the volume depends on the surface area of the flask used). A solution of trypsin and EDTA 0.05% / 0.02% in Hank's solution without Mg^{2+} and Ca^{2+} (the appropriate amount indicated before for each flasks) was added to the cells and the flask was incubated at 37 °C for two minutes. After controlling the real detachment of the cells from the surface, cell medium was added to the flask (5 mL of medium for T75 or 2.5 mL for T25). A cell rubber was then used to scraper the cells, and this operation was repeated twice after removing the cells and their medium. The cells were storage in a test tube; then, they were spin-dried at 22 °C for 10 minutes, 1200 rpm. After removing the supernatant, the pellet was dissolved in the medium. All the operations have to be done under laminar flow cabinet to prevent contaminations and to maintain a sterile environment.

6.7.2 Cell freezing in liquid nitrogen

Materials. PBS (Sigma-Aldrich), Trypsin/EDTA, complete medium for the specific type of cell, DMSO solution (Solution A : medium+ 20% FBS. Solution B : medium + 20% FBS + 20% DMSO . Solution B must be filtrated before use).

Procedure. Solution A and solution B were storage at 4 °C before starting trypsinization process (see previous paragraph). After this, cells were stored in a test tube and then counted with a Bürker chamber. Cells were then centrifuged for 10

minutes at 4 °C, 10000 rpm. After the spin cycle, the supernatant was removed slowly and cells were dissolved in 300-500 μL of solution A. Cells were then transferred in a cryovial (2 mL capacity) and the same quantity of solution B was added drop by drop. The cryovial was covered with cotton and put in a styrofoam box and storage at -80 °C. After 10-15 hours the vial was put in liquid nitrogen.

Freezing process has to be done very slowly. For this reason, cells were put before at -80 °C and after in liquid nitrogen. Also, the first passage from room temperature, 4 °C and then -80 °C must be gradually. DMSO is a cryoprotective substance used to prevent the freezing of the cytoplasm.

6.7.3 Thawing frozen cells in liquid nitrogen

Materials. Complete medium for the specific type of cell.

Procedure. Cells frozen in liquid nitrogen were transferred in dry ice and then the cryovial was put directly in a thermal bath at 37 °C to complete thawing. Cells were then transferred in a test tube (50 mL volume), dispersed in 10 mL of medium very slowly and shaking weakly. Cell solution was centrifuged at 22 °C, for 10 minutes, 10000 rpm. Supernatant was removed and fresh medium was added to start the culture of the cells. Cells must be unfreezed as rapidly as possible (time maximum 2-3 minutes).

7 Hydrogel via Michael-type addition: F-127 TA-HA

Aim of this work was to develop biocompatible hydrogels based on Pluronic and synthesized with different crosslinking techniques, in order to evaluate the tuneable physico-chemical and biological properties of these gels, in view of specific biomedical applications. As seen in Chapter 4, it is important to ensure chemical crosslinking between the polymer chains to assure good mechanical properties and stability; moreover appropriate end-chain reactive groups are needed to provide functionality, for instance to allow peptide attachment for cell adhesion.

Two chemical crosslinking strategies will be discussed: radical crosslinking (see Chapter 1) and via Michael-type addition.

In this chapter, Pluronic hydrogels prepared through Michael-type additions are presented. Materials and methods developed for the synthesis of polymeric precursors, hydrogels formation, and their characterisation are reported and summarised. Firstly we wanted to develop a gel chemically crosslinked via Michael-type addition combining Pluronic F-127 thioacetate (as protected Michael donor) and Tetronic 701 acrylate (as Michael acceptor). Then, we also studied an alternative formulation utilizing Michael-type reaction but combining Pluronic F-127 thioacetate (as protected Michael donor) with Pluronic F-127 hexaacrylate (as Michael acceptor). The use of Michael-type addition has been widely used in biomaterials preparation. It is a well-known reaction mechanism which allows to fabricate a variety of macromolecular architectures including step-growth polymers, dendrimers and crosslinked networks; this last category is our objective. The proposed polymer functionalization, which is required to synthesize the polymeric precursors, does not required tedious reaction steps. Furthermore, Michael-type reaction is cell friendly as it can proceed quantitatively and selectively in aqueous media at room temperature without formation of toxic

byproducts [80]. The use of alternative crosslinking reactions could present a disadvantage because very accurate purification steps may be necessary to obtain hydrogels for biological applications.

The physico-chemical properties of the hydrogels obtained via Michael-type addition can be tuned by varying the composition of the polymeric precursors. In particular, in our study both types of hydrogel formulation were tested, the one based on Pluronic F-127 only and the other based on Pluronic F-127 and Tetronic 701 mixture. Both formulations were designed to obtain a tandem gelation. In tandem gelation two processes take place independently: a very rapid physical gelation obtained by an increase of temperature, combined with a chemical gelation mechanism that provide a chemically and mechanically stable crosslinked polymer network [81]. By coupling physical gelation with a chemical crosslinking mechanism it is possible to exploit the advantages of both processes: a fast thermal gelation is particularly appealing when in situ gel formation is required (for instance in tissue engineering and cell microencapsulation [54]), while stability and good mechanical properties can be obtained by a slower but covalent crosslinking [81].

7.1 Experimental Part

Synthesis of the precursors

All the functionalized polymers obtained were characterised using an 400 MHz Bruker ^{1}H NMR spectrometer and a Thermo Scientific Nicolet iS50 FT-IR spectrometer in ATR mode. DLS measurements were carried out with Malvern Zetasizer ZS. GPC analysis were performed with Jasco GPC System in tetrahydrofuran at 35°C.

7.1.1 Synthesis of Pluronic F-127 allyl ether (F-127 ALL)

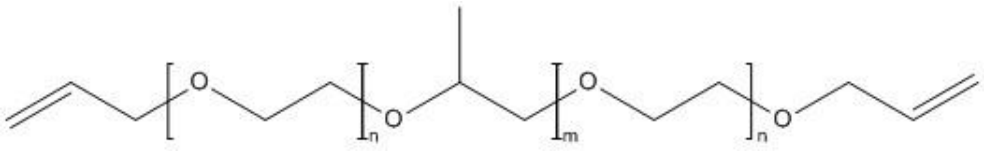

Figure 7.1 F-127 ALL molecular structure (n=231, m=68).

Materials. Pluronic F-127 (MW=12600, 70% PEG), allyl bromide, sodium hydride and toluene were purchased from Sigma-Aldrich (composition confirmed by ^{1}H NMR Spectroscopy) and used as received.

Synthesis. 10 g of Pluronic F-127 (0,794 mmol, 1.59 meq of –OH groups) were dissolved in 150 mL of toluene under nitrogen atmosphere and dried refluxing toluene through a Soxhlet extractor filled with 4 Å molecular sieves. After 3 hours the solution was cooled at room temperature and then immersed in an ice bath. The polymer was then deprotonated using 57 mg of NaH (1.5 eq per –OH group) and stirred for about 15 minutes. 0.687 mL of allyl bromide (7.94 mmol, 5 eq per ONa group) dissolved in 10 mL of toluene were dropped in the solution using a dropping funnel, and additional 10 mL of toluene were dropped in the solution by the dropping funnel in order to transfer

all the allyl bromide into the reactor. The reaction mixture was stirred overnight at room temperature.

In order to purify F-127 ALL, the precipitated sodium bromide was filtered away using Buchner filter and the solvent evaporated at the rotary evaporator. The resulting viscous oil was dissolved in 200 mL of DCM and washed two times with 30 mL of deionized water saturated with sodium chloride. The solution was dried with sodium sulphate, filtered, the solvent evaporated and then precipitated two times in cold diethyl ether. Conversion = 100 % (from ^{1}H NMR data). Yield = 80%.

^{1}H NMR ($CdCl_3$): δ=1.1 (m, 206H, PPG C**H**$_3$ = 69 monomeric units), 3.4 (m, 68H, PPG C**H** = 68 monomeric units), 3.5 (m, 131H, PPG C**H**$_2$ = 66 monomeric units), 3.65 (m, 924H, PEG chain protons = 231 monomeric units), 4.01-4.04 (dd, 4H, –CH_2OC**H**$_2$–$CH=CH_2$), 5.15-5.30 (m, 4H, –$OCH_2CH=C$**H**$_2$), 5.85-5.98 ppm (m, 2H, –OCH_2C**H**CH_2).
FT-IR (film on ATR plate): 2990-2790 (ν C-H), 1467 (δ_s CH_2), 1342, 1279,1242, 1097 (ν_{as} C-O-C), 962, 841 (ν_s C-O-C)cm^{-1}.

7.1.2 Synthesis of Pluronic F-127 thioacetate (F-127 TA)

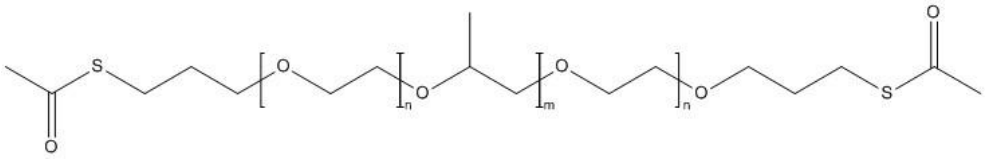

Figure 7.2 F-127 TA molecular structure (n=231, m=68).

Materials. F-127 ALL was produced as previously described; 2,2'-Azobis(2-methylpropionitrile) (AIBN), thioacetic acid (purum, ≥95.0% (GC)) and toluene were purchased from Sigma-Aldrich (composition confirmed by ^{1}H NMR Spectroscopy) and used as received.

Synthesis. 7 g of F-127 ALL (0.5 mmol, 1.11 meq of allyl groups) were dissolved in 150 mL of previously degassed toluene. After the addition of 0.91 g of AIBN (5.55 mmol; MW=164.2; 5 fold excess compared to allyl groups) the solution was heated to 60-65 °C and 0.13 mL of thioacetic acid was added repeatedly every 2 hours (4 times 0.13 mL; 1.78 mmol, 1.6 fold excess per addition). After repeating these additions 4 times, the solution was stirred overnight at room temperature. The series was then repeated by adding 0.83 g of fresh AIBN. After the last series the reaction mixture was stirred overnight at room temperature.

In order to purify F-127 TA, the solvent was evaporated at the rotary evaporator. The resulting viscous oil was dissolved in 200 mL of DCM and washed two times with 30 mL of deionized water saturated with sodium chloride. The solution was dried with sodium sulphate, filtered, the solvent evaporated and then precipitated three times in cold diethyl ether. Conversion = 91 % (from ^{1}H NMR data). Yield= 87%.

^{1}H NMR ($CdCl_3$): δ=1.1 (m, 206H, PPG C**H**$_3$ = 69 monomeric units), 1.81-1.90 (broad q, 4H, –OCH$_2$C**H**$_2$CH$_2$S–), 2.32 (s, 6H, –SCOC**H**$_3$), 2.92-2.97 (t, 4H, –

C**H₂**SCOCH₃), 3.4 (m, 68H, PPG C**H** = 68 monomeric units), 3.49-3.52 (t, 4H, –OC**H₂**CH₂CH₂S–), 3.5 (m, 131H, PPG C**H₂** = 66 monomeric units), 3.65 ppm (m, 924H, PEG C**H₂** = 231 monomeric units).

FT-IR (film on ATR plate): 2990-2790 (ν C-H), 1692 (ν C=O), 1467 (δ_s CH_2), 1342, 1279,1242, 1097 (ν_{as} C-O-C), 962, 841 (ν_s C-O-C)cm^{-1}.

7.1.3 Synthesis of Tetronic 701 acrylate (T701 ACR)

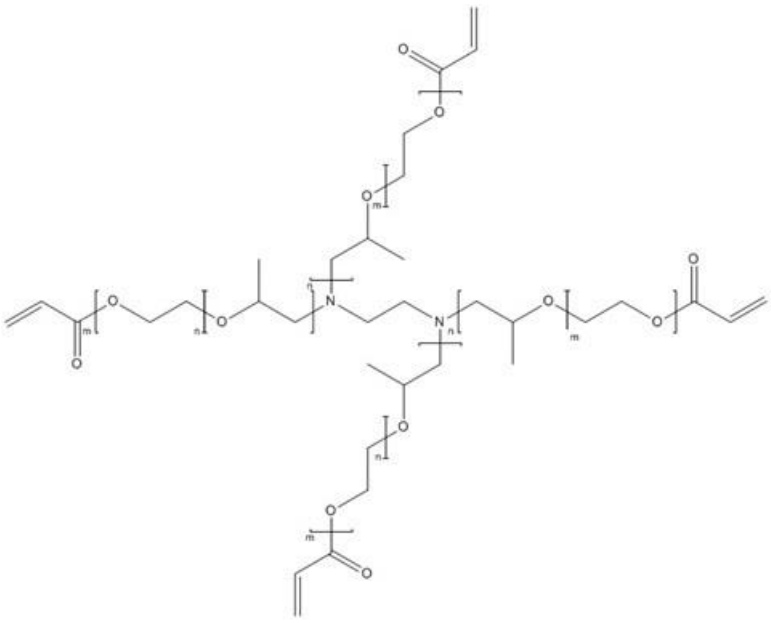

Figure 7.3 T701 ACR molecular structure (m=10, n=50).

The synthetic procedure, similar to that described in [82], was carried out as follow:

Materials. Tetronic 701 (MW = 3600, 10% PEG), acryloyl chloride (purity: 97.0%, contains <210 ppm MEHQ as stabilizer), triethylamine (purity ≥99.5%) and toluene were purchased from Sigma-Aldrich (composition confirmed by ^{1}H NMR Spectroscopy) and used as received.

Synthesis. 10 g of T701 (2.78 mmol, 11.1 meq –OH groups) were dissolved in 150 mL of toluene under nitrogen atmosphere and dried refluxing toluene through a Soxhlet extractor filled with 4 Å molecular sieves. After 3 hours the solution was cooled at room temperature and then immersed in an ice bath. 5.3 mL (38.2 mmol, 1.5 mol per mol acryloyl chloride) of TEA were added into the reactor, 2 mL of acryloyl chloride (25.5 mmol, 2.3 eq per –OH group) diluted in 10 mL of toluene were dropped using a

dropping funnel. The dropping funnel was washed with additional 10 mL of toluene, which were dropped into the reactor under nitrogen flux, and the mixture was stirred overnight at room temperature.

In order to purify T701 ACR, the precipitated triethylammonium hydrochloride was filtered away using Buchner filter and the solvent evaporated at the rotary evaporator. The resulting viscous oil was dissolved in 200 mL of DCM and washed two times with 30 mL of deionized water saturated with sodium chloride. The solution was dried with sodium sulphate, filtered, the solvent evaporated and then precipitated two times in cold diethyl ether. Conversion = 100 % (from ^{1}H NMR data). Yield = 80%.

^{1}H NMR ($CdCl_3$): δ=1.1 (m, 159H, PPG C**H**$_3$ = 53 monomeric units), 3.4 (m, 50H, PPG C**H** = 50 monomeric units), 3.5 (m, 89 H, PPG C**H**$_2$ = 45 monomeric units), 3.65 (m, 40H, PEG C**H**$_2$ = 10 monomeric units), 4.3 (t, 4H,–CH_2C**H**$_2$–O–CO–CH=CH_2), 5.8 (dd, 4H, CH_2=C**H**–COO–), 6.15 and 6.4 ppm (both dd, 4H, C**H**$_2$=CH–COO).
FT-IR (film on ATR plate): 2990-2790 (ν C-H), 1467 (δ_s CH_2), 1724 (ν C=O), 1342, 1279, 1242, 1097 (ν_{as} C-O-C), 962, 841 (ν_s C-O-C) cm^{-1}.

7.1.4 Synthesis of pluronic F-127 hexaacrylate (F-127 HA)

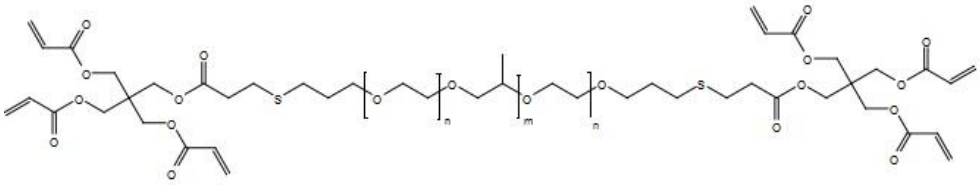

Figure 7.4 F-127 HA molecular structure (n=231, m=68).

Materials. F-127 TA was produced as previously described; pentaerythritol tetraacrylate (Tetra ACR) (MW = 352.34), tris(2-carboxyethyl)phosphine hydrochloride (TCEP) (MW=286.65, purity 98%), sodium hydroxide (MW=40.00, ACS reagent, purity ≥97%, pellets), hydrochloric acid (MW=36.46, 37%), N,N-Dimethylformamide (MW=73.09) were purchased from Sigma-Aldrich (composition confirmed by ^{1}H NMR Spectroscopy) and used as received.

Synthesis. *Pluronic-thiol deprotection*: 2 g of F-127 TA were dispersed in 10 mL of NaOH 0.2 M solution and the mixture was left in an ice bath (2-3°C) for 1.5 h under stirring. The cold polymer solution was buffered with 7 mL of HCl 0.6 M solution and 1.5 mL of HCl 0.2 M solution to obtain a pH equal to 7.4. 1.11 g of Tetra ACR (315 mmol; equivalent tetraacrylate/equivalent thioacetate = 40) dissolved in 18.5 mL of DMF were then added to the polymer solution. Finally, 90 mg of TCEP (0.315 mmol; 1 equivalent per equivalent of thioacetic group) were added to the solution to prevent disulfide formation during the reaction. The pH solution was checked and eventually NaOH solution was added to maintain the reactant pH solution between 7 and 8, cause of the strong acidity of the phosphine powder. After warming at room temperature the solution was stirred overnight.

In order to purify F-127 HA the reactant solution was saturated with 8 g of sodium chloride (1.2 excess respect the NaCl given solubility in water, 357 mg/mL at 25 °C from Sigma specification sheet) and after adding 200 mL of DCM a liquid-liquid

extraction was carried out. The organic phase was dried with sodium sulphate, filtered, the solvent evaporated and then precipitated four times in cold diethyl ether to remove the unreacted Tetra ACR. Conversion = 100 % (from ^{1}H NMR data). Yield = 60%.

^{1}H NMR ($CdCl_3$): δ=1.1 (m, 206H, PPG C**H**$_3$ = 69 monomeric units), 3.4 (m, 68H, PPG C**H** = 68 monomeric units), 3.5 (m, 131H, PPG C**H**$_2$ = 66 monomeric units), 3.65 (m, 924H, PEG C**H**$_2$ = 231 monomeric units), 4.3 (t, 6 H,–CH_2C**H**$_2$–O–CO–CH=CH_2), 5.8 (dd, 6H, CH_2=C**H**–COO–), 6.15 and 6.4 ppm (both dd, 6H, C**H**$_2$=CH–COO).

FT-IR (film on ATR plate): 2990-2790 (ν C-H), 1724 (ν C=O), 1467 (δ_s CH_2), 1342, 1279, 1242, 1097 (ν_{as} C-O-C), 962, 841 (ν_s C-O-C) cm^{-1}.

Hydrogel formulation

7.1.5 Pluronic F-127 thioacetate - Tetronic 701 acrylate hydrogel formulation

A gel via Michael-type addition was synthesized based on Pluronic F-127 TA and T701 ACR.

Materials. F-127 TA and T701 ACR were produced as previously described; sodium hydroxide (MW=40.00, ACS reagent, purity ≥97%, pellets), hydrochloric acid (MW=36.46 37%), potassium phosphate monobasic (MW=136.09, ACS reagent, purity ≥99.0%), sodium phosphate dibasic (MW=141.96, for molecular biology, purity ≥98.5%, (titration)) were purchased by Sigma-Aldrich (composition confirmed by ^{1}H NMR Spectroscopy) and used as received.

Procedure. 0.25 g of F-127 TA were dispersed in 800 µL (solution concentration: 31% w/v) of NaOH 0.2 M solution and the mixture was left in an ice bath (2-3°C) for 1.5 h under stirring. The cold polymer solution was buffered with 597 µL of HCl 0.2 M solution to obtain a pH equal to 7.4 (it is always necessary to check the pH value and eventually modified the HCl or NaOH quantities to adjust it). After the pH neutralisation, 0.143 g of T701 ACR were added to the cold polymer solution (0.04 mmol, molar ratio T701 ACR/F-127 TA = 2). This reacting solution, forming an hexaacrylate precursor for the final gel was left under stirring for 2 hours. At the same time, 0.75 g (equivalent ratio Hexaacrylate/F-127 TA = 1) of F-127 TA were dispersed in 1.8 mL of NaOH 0.2 M solution and the mixture was left in an ice bath (2-3°C) for 1.5 h under stirring. The cold polymer solution was buffered with 1.2 mL of HCl 0.2 M solution to obtain a pH equal to 7.4. After the neutralisation of the cold polymer solution and the check of the pH value, 1.3 mL of PBS 10 mM (pH 7.4) were added to the F-127 TA solution to reduce its concentration, in order to obtain a final gel concentration of 20% w/v. The two cold solutions, Hexaacrylate (F-127 TA+T701

ACR) and F-127 TA deprotected, were rapidly mixed and stirred. The gelling solution was transferred in a vial (maximum volume 8 mL) and left overnight at 37°C.

7.1.6 F-127 thioacetate– F-127 hexaacrylate hydrogel formation (F-127 TA-HA)

A gel via Michael-type addition was synthesized using F-127 TA and F-127 HA as precursor.

Materials. F-127 TA and F-127 HA were produced as previously described; sodium hydroxide (MW=40.00 97%), hydrochloric acid (MW=36.46 37%), potassium phosphate monobasic (MW=136.09 99.0%), sodium phosphate dibasic (MW=141.96 98.5%) were purchased by Sigma-Aldrich (composition confirmed by ^{1}H NMR Spectroscopy) and used as received.

Processing. 0.057 g of F-127 TA were dispersed in 180 μL (polymer solution concentration: 32% w/v) of NaOH 0.2 M solution and the mixture was left in an ice bath (2-3°C) for 1.5 h under stirring. At the same time, 0.024 g (ratio F-127 HA equivalents/F-127 TA equivalents = 1) of F-127 HA were dissolved in 110 μL (polymer solution concentration: 22% w/v) of PBS 10 mM (pH 7.4): the mixture was left in an ice bath under stirring. The cold polymer solution was buffered with 100 μL of HCl 0.6 M solution and 50 μL of HCl 0.2 M solution to obtain a pH equal to 7.4 (it is always necessary to check the pH value and eventually modified the HCl or NaOH quantities to adjust it). The final volume of the aqueous solution was adjusted by adding PBS to finally obtain the target polymer concentration 10, 13, 20, 27% w/v. The two cold solutions, F-127 TA deprotected and F-127 HA, were rapidly mixed and stirred. The gelling solution was transferred in a vial or into a 24-well plate (50 μL for each well, to obtain a centred drop) and left overnight at 37°C.

Physico-chemical characterisation

7.1.7 F-127 thiol deprotection: kinetic study

Materials. F-127 TA produced as previously described; sodium hydroxide (MW=40.00 97%) purchased by Sigma-Aldrich; Deuterium Oxide (D_2O) purchased by euriso-top.

Procedure. The deprotection kinetics was tested for a 20% w/v F-127 TA (i.e. the typical polymer concentration which provides thermal gelation). 0.15 g of F-127 TA were dissolved in 675 µL of D_2O. The polymer solution was left under stirring in an ice bath (2-3°C) until the complete dissolution of the polymer powder. Then, 75 µL of NaOH 2 M solution were added by drops under stirring. The total time period investigated was 1.5 hour: the F-127 TA mixture was sampled every 2 minutes for the first 10 minutes of reaction, every 5 minutes between 10 and 20 min and every 10 minutes until the end (1.5 h) of the entire period. The conversion was calculated through ^{1}H NMR spectroscopy by evaluating the hydrolysis of the thioester bonds.

7.1.8 Crosslinking kinetics

The crosslinking kinetic was studied with Dynamic Light Scattering analysis, Malvern Zetasizer Nano ZS.

Materials. Hydrogels based on F-127 TA and F-127 HA were produced as previously described and pegylated gold nanoparticles were obtained as follows.

7.1.8.1 Synthesis of pegylated gold nanoparticles

Materials. Gold NPs (10 nm and 20 nm diameter, stabilized suspension in 0.1 mM PBS, reactant free), poly(ethylene glycol)methyl ether thiol (MW=2000) were purchased from Sigma-Aldrich and used as received.

Synthesis. 2 mL of gold NPs were mixed with 54 μg of poly(ethylene glycol)methyl ether thiol (ligand concentration 0.0135 μmol/NPs mL). The solution was stirred at room temperature for two hours.

Dialysis. The NPs solution was purified with dialysis against deionized water for 24 hours (Dialysis membrane: Cellu-Sep T1/Nominal MWCO: 3500, purchased by Membrane Filtration Products, Inc.). After the purification, pegylated gold NPs were transferred in vials and stored in the fridge.

Procedure. F-127 TA and F-127 HA solutions with a polymer concentration of 10% w/v and 20% w/v were prepared as described above. For the DLS measurements the minimum sample volume required is 1 mL. In order to obtain a final gel concentration in the DLS cuvette of 10% w/v, we prepared a gelling solution with an initial polymer concentration (F-127 TA+F-127 HA) of 20% w/v. Then 500 μL of 10 nm pegylated gold NPs suspension were dispersed in 500 μL of the gelling solution, and the mixture was quickly stirred and transferred in a DLS cuvette. Differently from the 10% w/v, to assure a final gel concentration in the DLS cuvette of 20% w/v, the gelling solution was prepared by dissolving the F-127 HA directly in the pegylated gold NPs suspension instead of PBS. F-127 TA deprotected solution and F-127 HA + pegylated gold NPs were mixed quickly and transferred in a DLS cuvette. The kinetics crosslinking was studied evaluating the increase in apparent viscosity, by measuring the size variation of the nanoparticles, using the Stokes-Einstein equation. For each gelling solution concentration (10% and 20% w/v) a series of size measurements (every 150 s and 300 s) were performed at 15 °C (for more details see Results and Discussions 8.2.4).

7.1.9 Swelling measurements

In order to evaluate swelling capacity of F-127 TA-HA gels, the following tests were carried out.

Procedure. A series of F-127 TA-HA gelling solutions were prepared according to the procedure described above with different polymer concentration 10, 20 and 27% w/v. Each gelling solution was transferred in the moulds (obtained shaping an agarose gel, diameter 1.2 cm) shown in Figure 7.5, using 140 μL per each cylindrical mould. The mould was left overnight in an oven at 37°C to allow the complete hydrogel formation. Then, every gel was extracted from the mould and their weight was measured by a high precision balance. Afterwards, gels were transferred in a 6-wells plate, and filled with 5 mL of PBS 10 mM solution (pH 7.4). The weight measurements of the swollen gels were carried out after 24 hours, expecting that this time was sufficient to achieve an equilibrium condition.

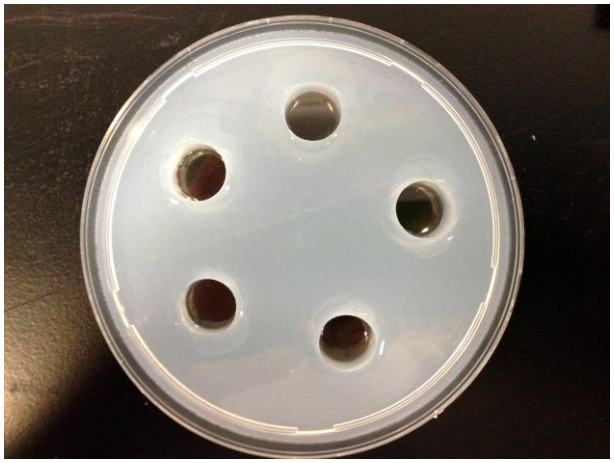

Figure 7.5 Agarose gel mould.

The swelling degree was defined as:

$$\%\ degre\ of\ swelling = \frac{\Delta w}{w_0}$$

Where, w_0 is the initial gel weight

w is the gel weight in the swollen condition

and $\Delta w = w - w_0$ is the weight variation .

The $\%\ degree\ of\ swelling$ was measured at room temperature (≈25°C) and physiological temperature (37°C). Three different samples were tested at each temperature to obtain mean values and standard deviations. The weight measurements of the swollen gels were carried out after removing the excess of water, which was often present around the gel surface, with blotting paper.

7.1.10 Diffusion tests

The release mechanism of a drug in the F-127 TA-HA gel was investigated with ^1H high resolution magic angle spinning (HR MAS) technology.

Materials. F-127 TA and F-127 HA produced as previously described; ibuprofen (MW=206.28, 98%, purchased by Sigma-Aldrich), PBS 10mM (pH 7.4), deuterium oxide (D_2O) purchased by Euriso-Top.

Procedure. A series of F-127 TA-HA gelling solutions with a polymer concentration of 10, 20 and 27% w/v, were prepared with the procedure described above, but in this case all the solutions (NaOH 0.2 M, HCl 0.6 and 0.2 M and PBS 10 mM) were prepared with

D_2O instead of deionized water: the deuterated solvent allowed NMR analysis to quantify ibuprofen diffusion. A stock solution of ibuprofen in PBS, 300 mg/mL was prepared and mixed with F-127 TA and F-127 HA to reach a drug concentration inside the gel of 60 mg/mL (0.27 M). The gelling solutions were left in a thermal bath overnight at physiological temperature (37°C) to obtain the final gel. After gel formation, 15 µL of the gels were used to perform the experiments. The specimen was put with a spatula in a Bruker zirconium HR-MAS rotor represented in Figure 7.6:

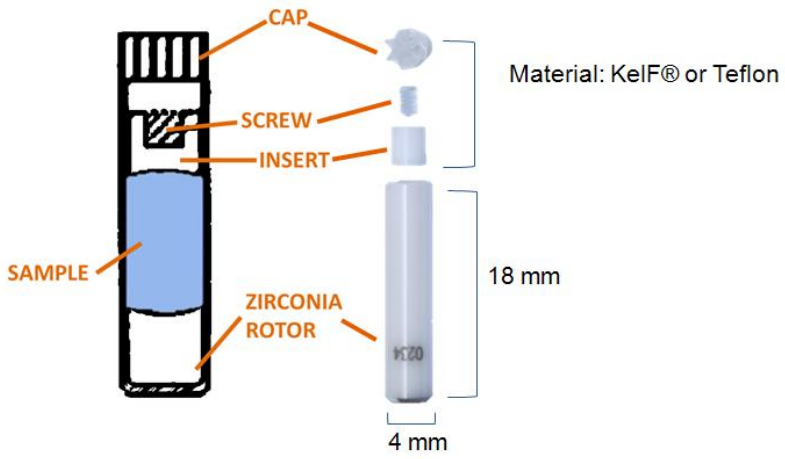

Figure 7.6 HR-MAS rotor.

Biological tests

7.1.11 Cell culture

Materials. Both podocytes, fibroblast and endothelial cell type (see cells specification in Chapter 6) were cultured over F-127 TA-HA gel layer and cell adhesive properties were investigated.

13% w/v F-127 TA-HA gelling solutions were tested in presence of cells according to the following three procedures:

- Non pre-treated gel (**Procedure 1**).
- Pre-treated gel with cell medium (**Procedure 2**).
- Functionalized gel with RGD (**Procedure 3**).

The experimental details of the three procedures are reported hereafter. All the activities were conducted under sterile conditions to prevent microorganisms contamination.

Materials. F-127 TA and F-127 HA were produced as previously described; sodium hydroxide (MW=40.00 97%), hydrochloric acid (MW=36.46 37%), Tris(2-carboxyethyl)phosphine hydrochloride (MW 286.65, powder, purity ≥98%) and PBS were purchased by Sigma-Aldrich (composition confirmed by ^{1}H NMR Spectroscopy) and used as received. Steryl H_2O and PS antibiotic solution were purchased by Sigma-Aldrich (for commercial specifications see Chapter 6). RGD (synthetic peptide, sequence GRGDSPC, MW=690.74, purity 96.15%) purchased by CASLO.

Procedure 1. 0.057 g of F-127 TA were deprotected in 180 μL (concentration 32% w/v) of NaOH 0.2 M solution prepared with steryl H_2O and the mixture was left in an ice bath (2-3°C) for 1.5 h under stirring. At the same time, 0.024 g (ratio between F-127 HA equivalents and F-127 TA equivalents equal to 1) of F-127 HA were dissolved in 110 μL (concentration 22% w/v) of PBS+PS, antibiotic solution: the mixture was left in an ice bath (2-3°C) under stirring. The cold polymer solution was buffered with 100 μL of HCl 0.6 M solution and 50 μL of HCl 0.2 M solution to obtain a pH equal to 7.4. F-127 HA concentration was then adjusted to reach the final gel concentration needed (13% w/v). 50 μL of the gelling solution were transferred in 24-well plate to generate a gel spot at the centre of each well. The plate was incubated at 37°C overnight and the gel was washed six times with 500 μL PBS+PS (every 10 minutes) before cell seeding. In particular, 16000 cells/well were seeded on each well and incubated with 500 μL of cell medium (composition described in Chapter 6).

Procedure 2. The gelling solution was prepared as described above and then 50 µL were transferred in 24-well plate creating a gel centred drop. The plate was incubated at 37°C. After 10 minutes from the starting formation of the gel, the gel drops were pre-treated overnight with 500 µL of cell medium. The gel was then washed six times with 500 µL PBS+PS (every 10 minutes) before culturing cells. In particular, 16000 cells/well were deposited on each well with 500 µL of cell medium (composition described in Chapter 6).

Procedure 3. 0.057 g of F-127 TA were deprotected in 180 µL (concentration 32% w/v) of NaOH 0.2 M solution prepared with sterile H_2O and the mixture was left in an ice bath (2-3°C) for 1.5 h under stirring. At the same time, 0.04 g (3/5 equivalent ratio F-127 HA/F-127 TA) of F-127 HA was dissolved in 110 µL (concentration 36% w/v) of PBS+PS: the mixture was left in an ice bath (2-3°C) under stirring. The cold polymer solution was buffered with 100 µL of HCl 0.6 M solution and 50 µL of HCl 0.2 M solution to obtain a pH equal to 7.4. F-127 HA concentration was then adjusted to reach the final gel concentration needed (13% w/v). 50 µL of the gelling solution were transferred in 24-well plate create a gel centred spot. The plate was incubated at 37°C overnight. 2 hours before cell seeding, 42.27 µL (2/5 equivalent ratio F-127 HA/F-127 TA) of RGD stock solution with PBS+PS (20 mg/mL) and 13.4 µL (equimolar ratio with RGD) of TCEP stock solution (13 mg/mL) with PBS+PS were added on the gel surface, and finally 500 µL of PBS+PS were added in each well. Each gel was washed six times with 500 µL PBS+PS (every 10 minutes) before culturing cells. In particular, 16000 cells/well were deposited on each well with 500 µL of cell medium (composition described in Chapter 6).

7.2 Results and Discussions

Synthesis of the precursors

7.2.1 Pluronic F-127 allyl ether (F-127 ALL)

Mechanism. NaH is a strong base that easily deprotonates hydroxyl (-OH) groups, leading to production of gaseous H_2 and end chain hydroxyl anion groups. Then hydroxyl anion attacks allyl bromide groups leading to F-127 ALL and sodium bromide.

This mechanism is summarized in Figure 7.7

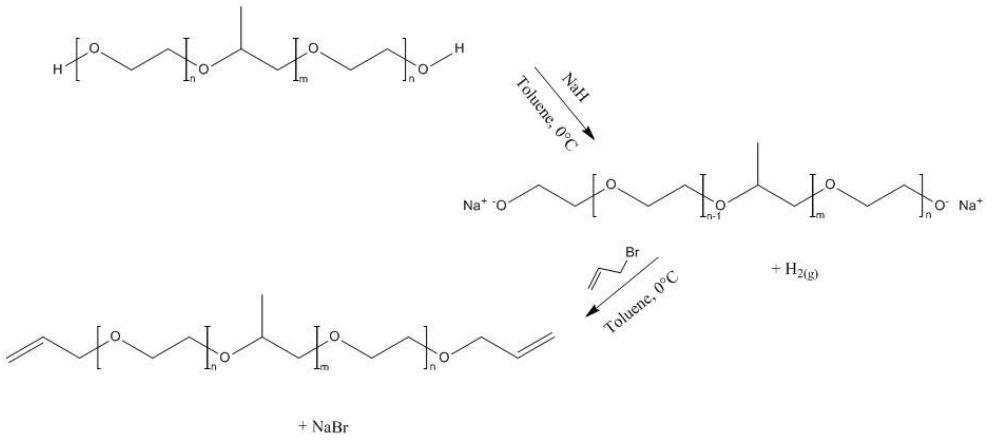

Figure 7.7 F-127 ALL synthesis mechanism.

The functionalization of Pluronic F-127 was confirmed by FT-IR and ^{1}H NMR analysis as we can see in figures below.

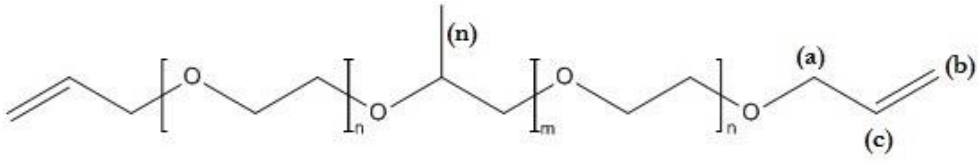

Figure 7.8 F-127 ALL structure with ^{1}H NMR peaks identification.

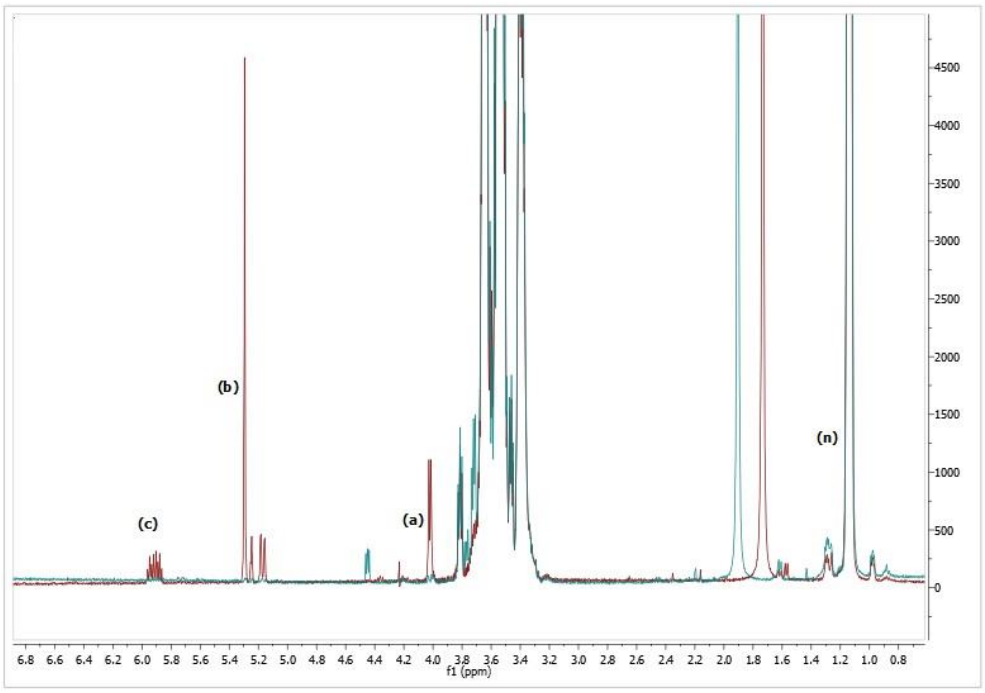

Figure 7.9 ^{1}H NMR F-127 ALL (red line) vs. pure F-127 (blue line).

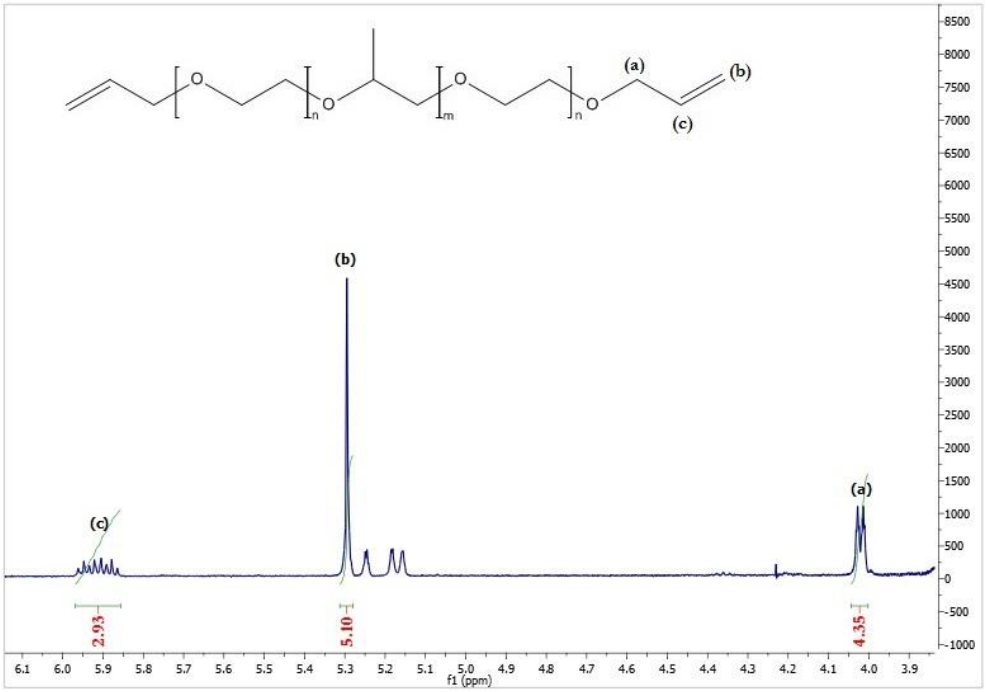

Figure 7.10 F-127 ALL ^{1}H NMR.

^{1}H NMR ($CdCl_3$): δ=1.1 (m, 206H, PPG C**H**$_3$ = 69 monomeric units), 3.4 (m, 68H, PPG C**H** = 68 monomeric units), 3.5 (m, 131H, PPG C**H**$_2$ = 66 monomeric units), 3.65 (m, 924H, PEG chain protons = 231 monomeric units), 4.01-4.04 (dd, 4H,–CH_2OC**H**$_2$–$CH=CH_2$), 5.15-5.30 (m, 4H, –$OCH_2CH=C$**H**$_2$), 5.85-5.98 ppm (m, 2H, –OCH_2C**H**CH_2).

The peaks integral was normalised with respect to the first peak at δ=1.1 (m, 206H, PPG C**H**$_3$ = 69 monomeric units).

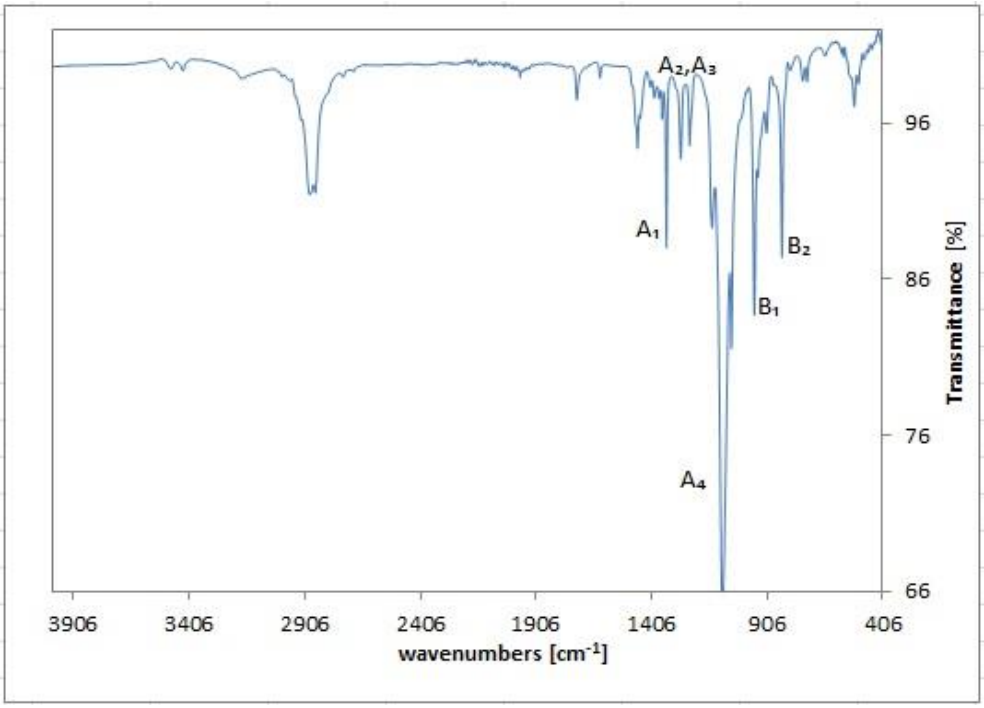

Figure 7.11 F-127 ALL FT-IR.

FT-IR (film on ATR plate): 2990-2790 (ν C-H), 1467 (δ_s CH_2), A_1-A_4: 1342, 1279, 1242, 1097 (ν_{as} C-O-C) B_1-B_2: 962, 841 (ν_s C-O-C) cm^{-1}.

FT-IR analysis allowed to obtain qualitatively information on the chemical composition of the polymer. In particular, the resultant spectrum in Figure 7.11 is in agreement with data reported in literature [82].

7.2.2 Pluronic F-127 Thioacetate (F-127 TA)

Mechanism. The reaction proceeds via a radical activation of allyl groups in the polymer chains and thiol groups in thioacetic acid, as shown in Figure 7.12.

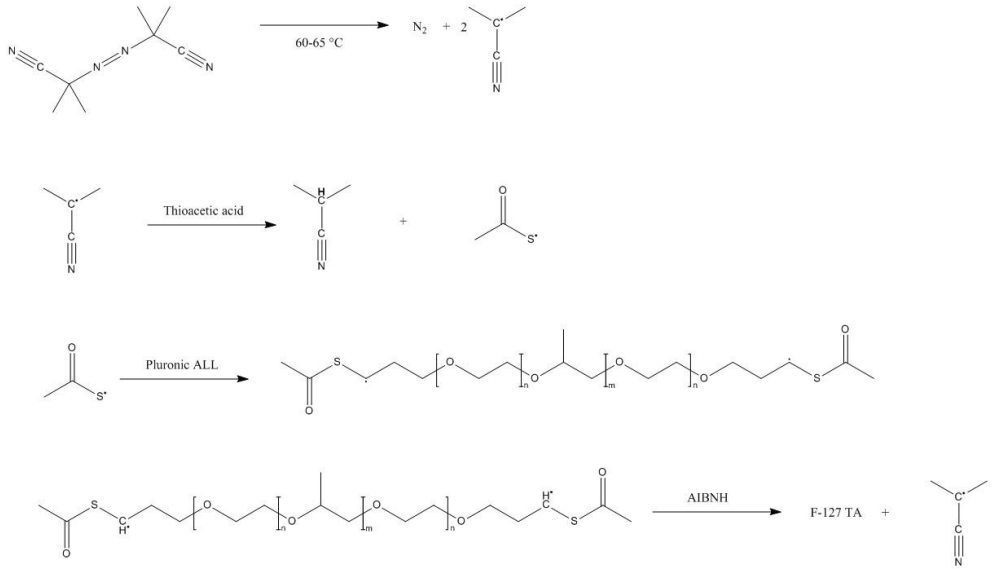

Figure 7.12 Thioacetilation radical pathway.

AIBN decomposes by generating a molecule of nitrogen gas to form two 2-cyanoprop-2-yl radicals that, activating thioacetic acid through a radical pathway, generate F-127 TA.

The formation of the product was confirmed from the analysis exposed in figures below:

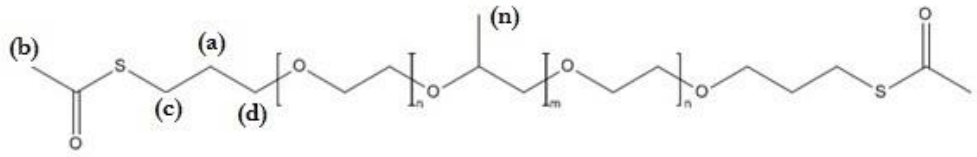

Figure 7.13 F-127 TA structure with ^{1}H NMR peaks identification.

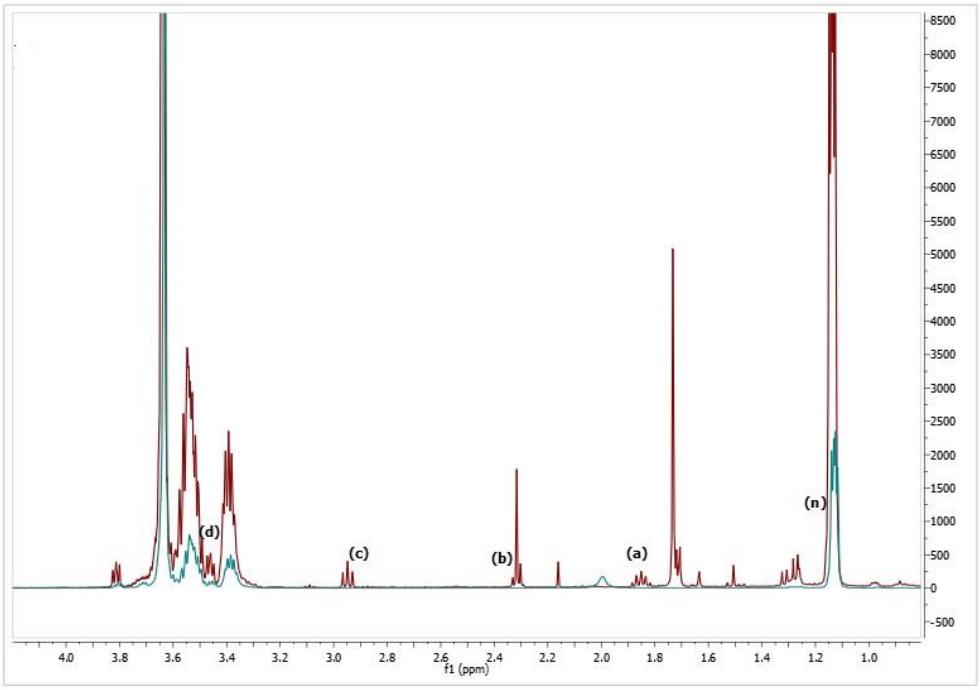

Figure 7.14 ^{1}H NMR F-127 TA (red line) vs. pure F-127 (blue line).

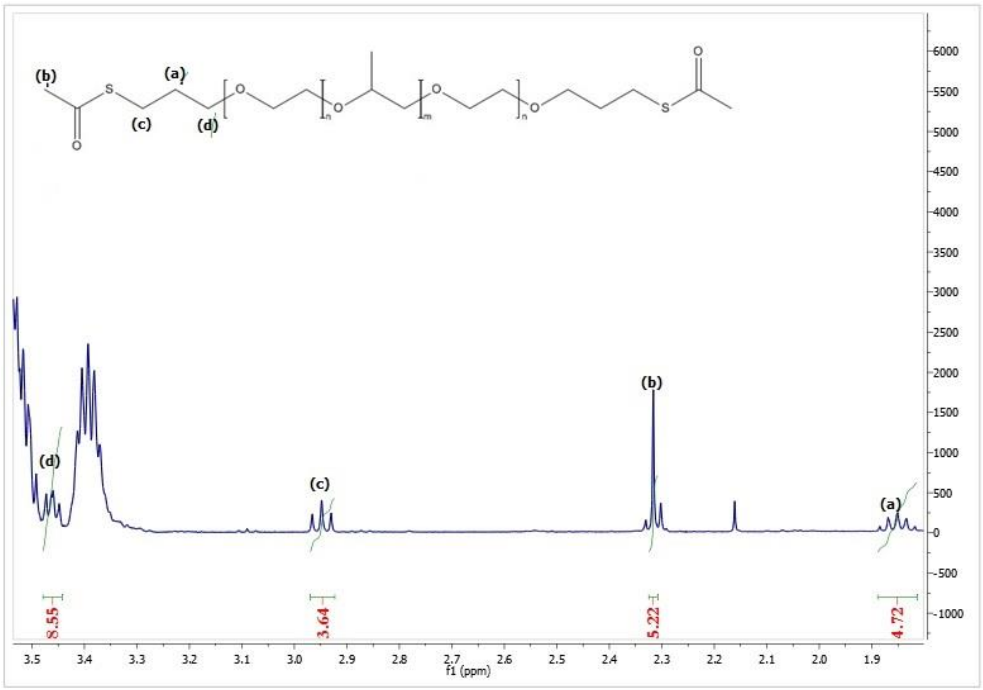

Figure 7.15 F-127 TA ^{1}H NMR.

^{1}H NMR ($CdCl_3$): δ=1.1 (m, 206H, PPG C**H**$_3$ = 69 monomeric units), 1.81-1.90 (broad q, 4H, –OCH$_2$C**H**$_2$CH$_2$S–), 2.32 (s, 6H, –SCOC**H**$_3$), 2.92-2.97 (t, 4H, –C**H**$_2$SCOCH$_3$), 3.4 (m, 68H, PPG C**H** = 68 monomeric units), 3.49-3.52 (t, 4H, –OC**H**$_2$CH$_2$CH$_2$S–), 3.5 (m, 131H, PPG C**H**$_2$ = 66 monomeric units), 3.65 ppm (m, 924H, PEG C**H**$_2$ = 231 monomeric units).

As reported in Figure 7.15, by normalizing the integrals respect to the first peak at δ=1.1 (m, 206H, PPG C**H**$_3$=69 monomeric units) that remains constant during the reaction, we calculated reaction conversion. In this case the normalised peaks intensity (a) and (d), should be equal to 4, however values are overestimated; in particular, peak (d) 3.49-3.52 (t, 4 H, –OC**H**$_2$CH$_2$CH$_2$S–) has a doubled value respect to the theoretical one, possibly cause of the interference of the bigger peaks of PPG. Peaks (b) and (c) present respectively a conversion of 91% and 87%.

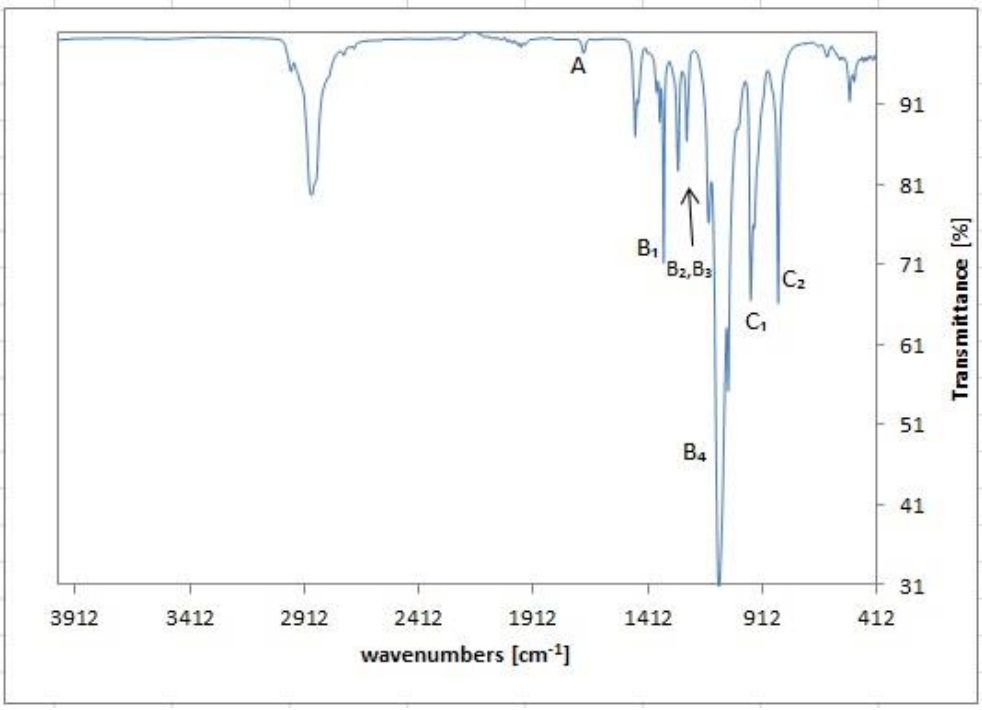

Figure 7.16 F-127 TA FT-IR.

FT-IR (film on ATR plate): 2990-2790 (ν C-H), A: 1692 (ν C=O), 1467 (δ_s CH_2), B_1-B_4: 1342, 1279,1242, 1097 (ν_{as} C-O-C), C_1,C_2: 962, 841 (ν_s C-O-C) cm^{-1}.
FT-IR analysis revealed new chemical bonds formation due to F-127 functionalization, as exposed in Figure 7.16 that is in agreement with data reported in literature [82].

7.2.3 Tetronic 701 acrylate (T701 ACR)

Tetronic 701 was successfully functionalized with acrylate end groups, in order to obtain a polymeric 4-arm crosslinker for Michael addition – based hydrogels.

Mechanism. Acryloyl chloride attacks –OH group in Tetronic chains leading to T701 ACR and hydrogen chloride. Triethylamine, commonly used as a base in organic synthesis, remove hydrogen chloride, producing salt triethylamine hydrochloride (or triethylammonium hydrochloride) and thus reaction proceeds to completion.

This mechanism is summarized in Figure 7.17:

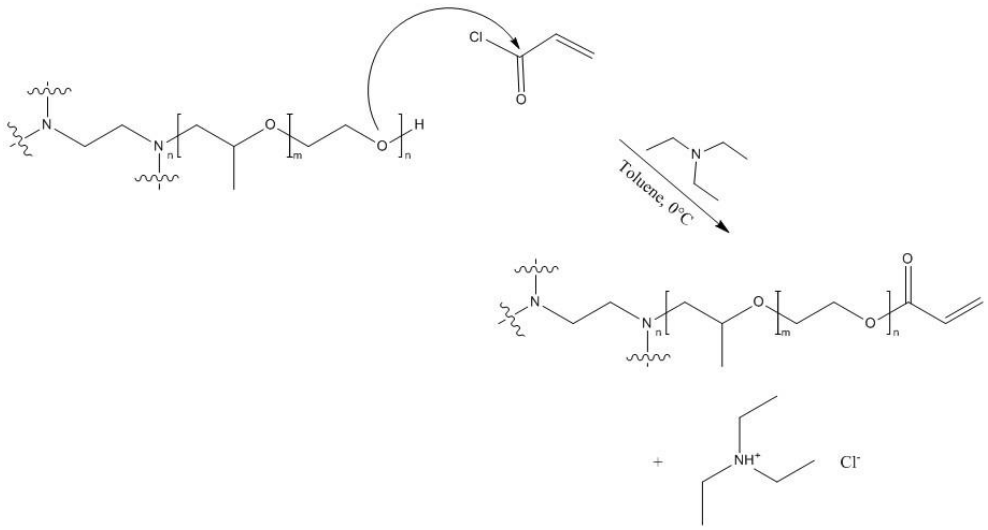

Figure 7.17 T701 acrylation mechanism.

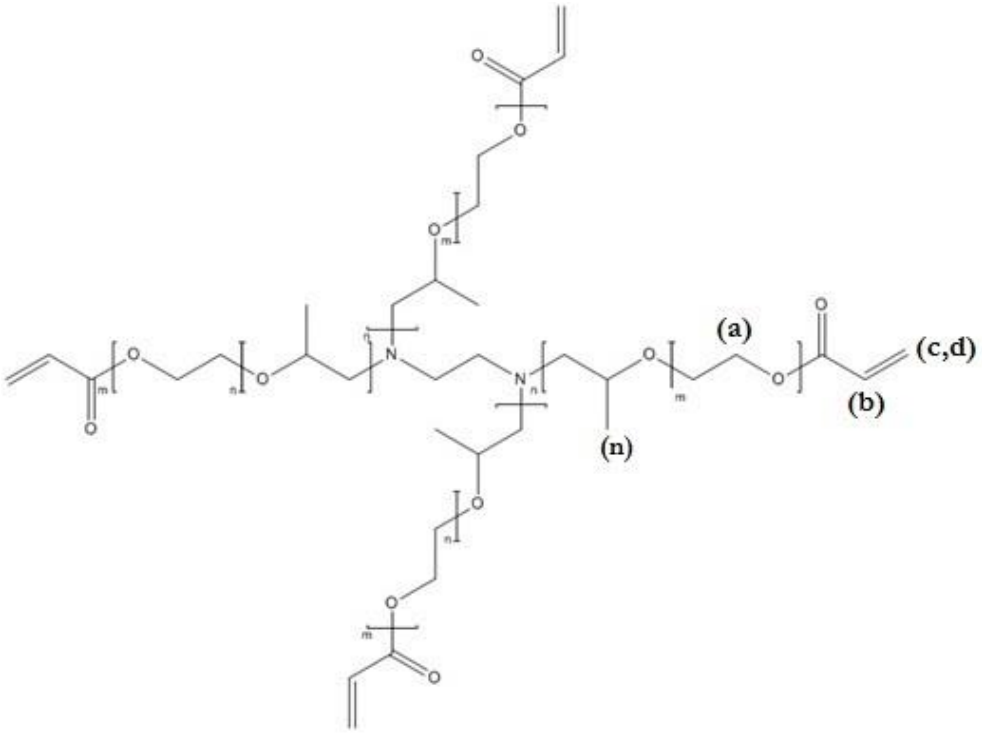

Figure 7.18 T701 ACR structure with ^{1}H NMR peaks identification.

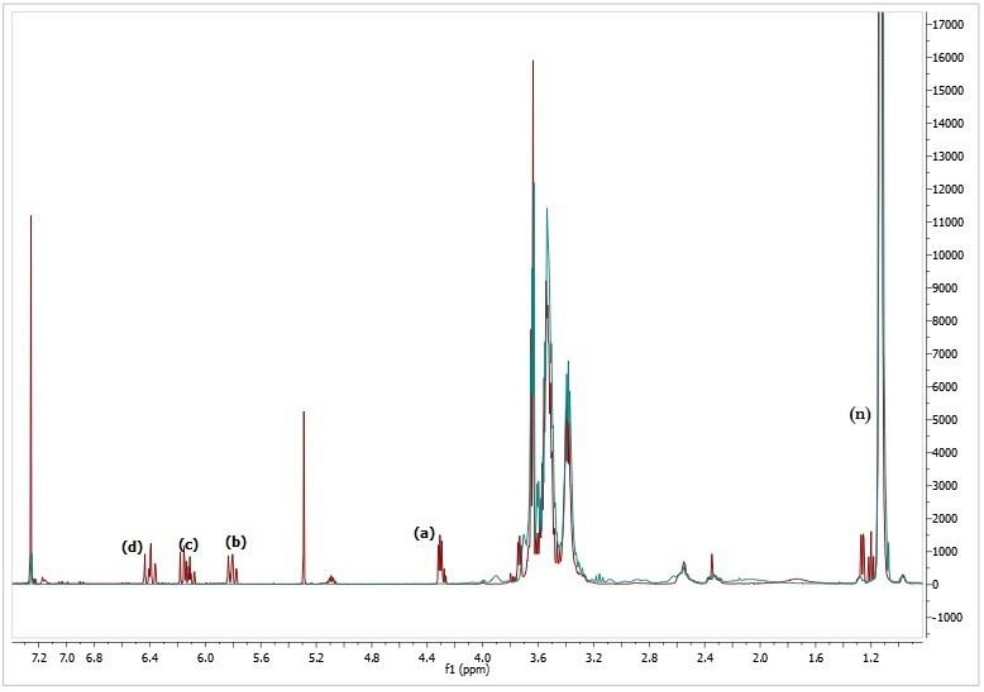

Figure 7.19 ^{1}H NMR T701 ACR (red line) vs. pure T701 (blue line).

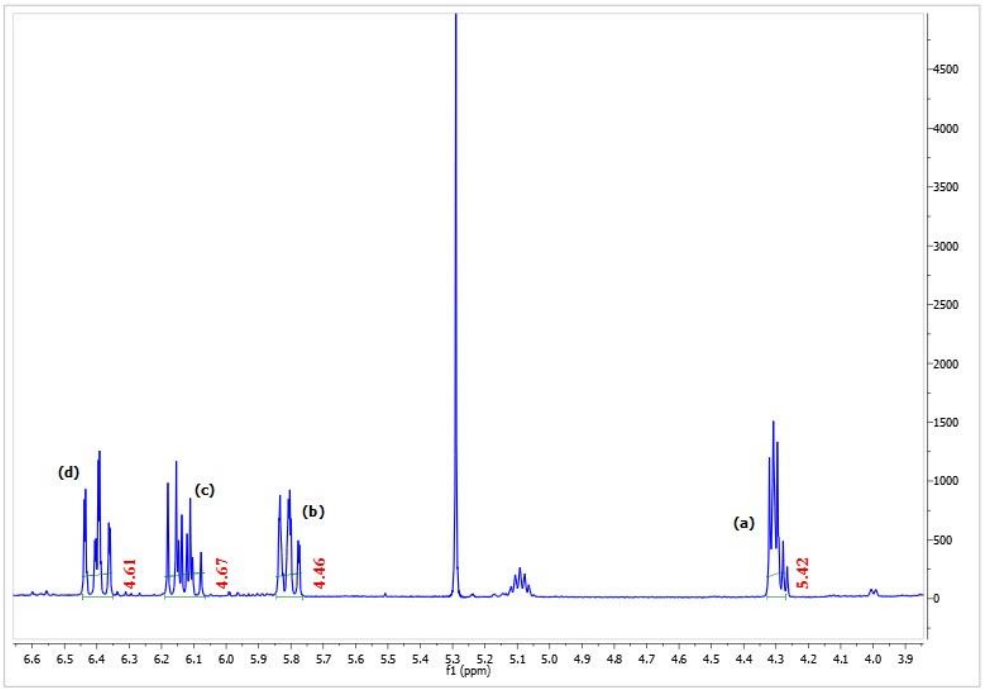

Figure 7.20 T701 ACR ^{1}H NMR.

^{1}H NMR ($CdCl_3$): δ=1.1 (m, 159H, PPG C**H**$_3$ = 53 monomeric units), 3.4 (m, 50 H, PPG C**H** = 50 monomeric units), 3.5 (m, 89H, PPG C**H**$_2$ = 45 monomeric units), 3.65 (m, 40H, PEG C**H**$_2$ = 10 monomeric units), 4.3 (t, 4H,–CH_2C**H**$_2$–O–CO–CH=CH_2), 5.8 (dd, 4H, CH_2=C**H**–COO–), 6.15 and 6.4 ppm (both dd, 4H, C**H**$_2$=CH–COO).

The peaks integral was normalized with respect to the first peak at δ=1.1 (m, 206H, PPG C**H**$_3$=69 monomeric units).

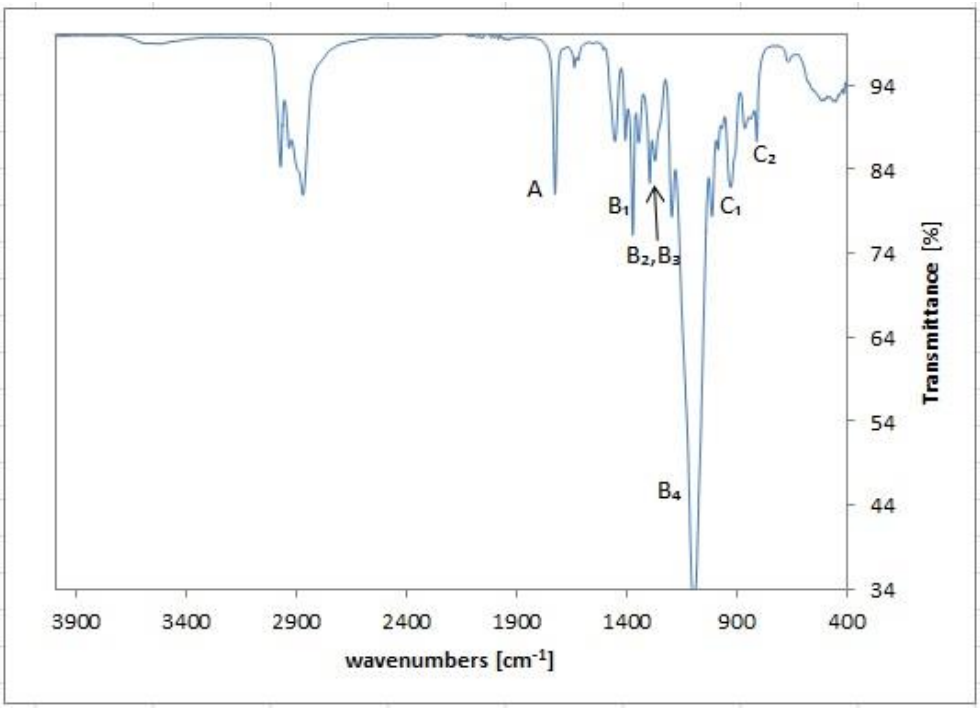

Figure 7.21 T701 ACR FT-IR.

FT-IR (film on ATR plate): 2990-2790 (ν C-H), 1467 (δ_s CH_2), A: 1724 (ν C=O), B_1-B_4: 1342, 1279, 1242, 1097 (ν_{as} C-O-C), C_1, C_2:962, 841 (ν_s C-O-C) cm^{-1}.

FT-IR analysis revealed new chemical bonds formation due to F-127 functionalization, as exposed in Figure 7.21 that is in agreement with data reported in literature [82]

7.2.4 Pluronic F-127 hexaacrylate (F-127 HA)

Mechanism. F-127 TA was deprotected using a NaOH solution 0.2 M. The hydrolysed F-127 TA reacted with a great excess of Tetra ACR (equivalent Tetra ACR/equivalent TA = 40) via Michael-type addition reaction to obtain functionalized polymer, F-127 HA.

This mechanism is summarized in Figure 7.22.

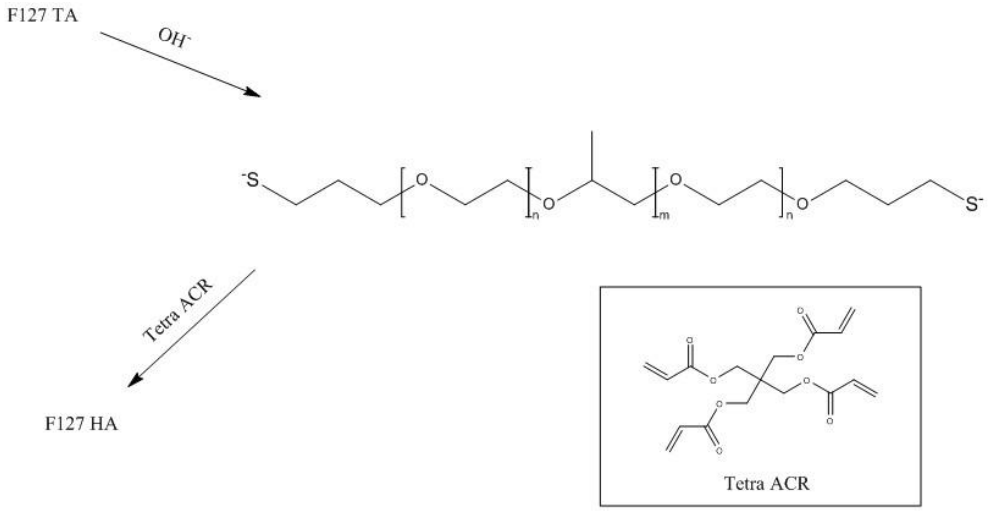

Figure 7.22 F-127 HA formation mechanism.

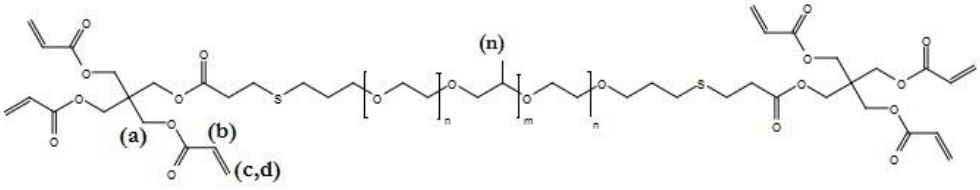

Figure 7.23 F-127 HA structure with ^1H NMR peaks identification.

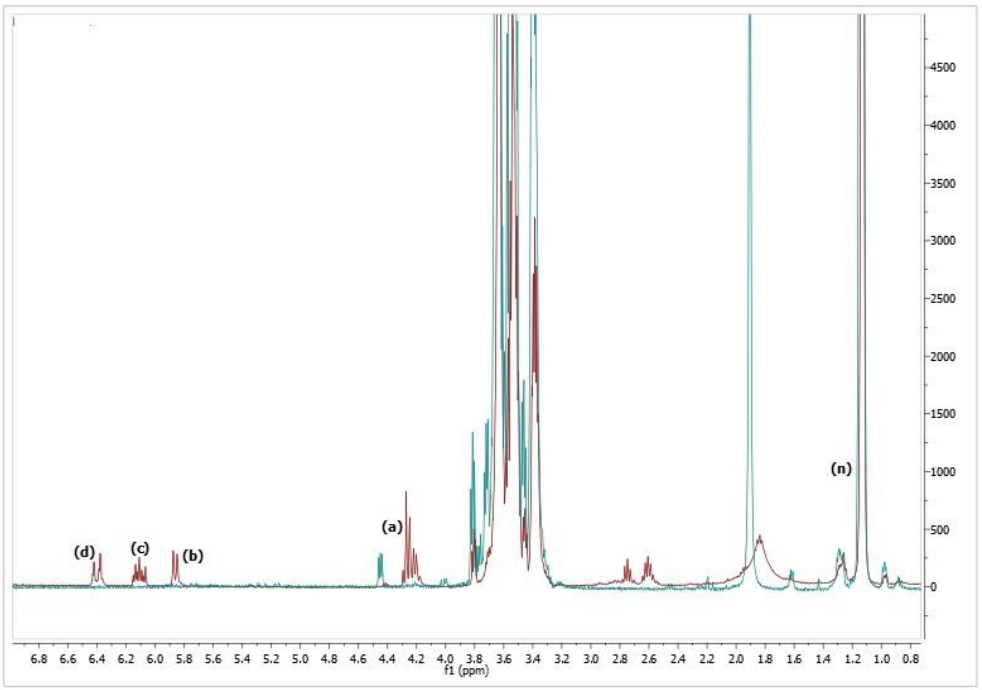

Figure 7.24 ^{1}H NMR F-127 HA (red line) vs. pure F-127 (blue line).

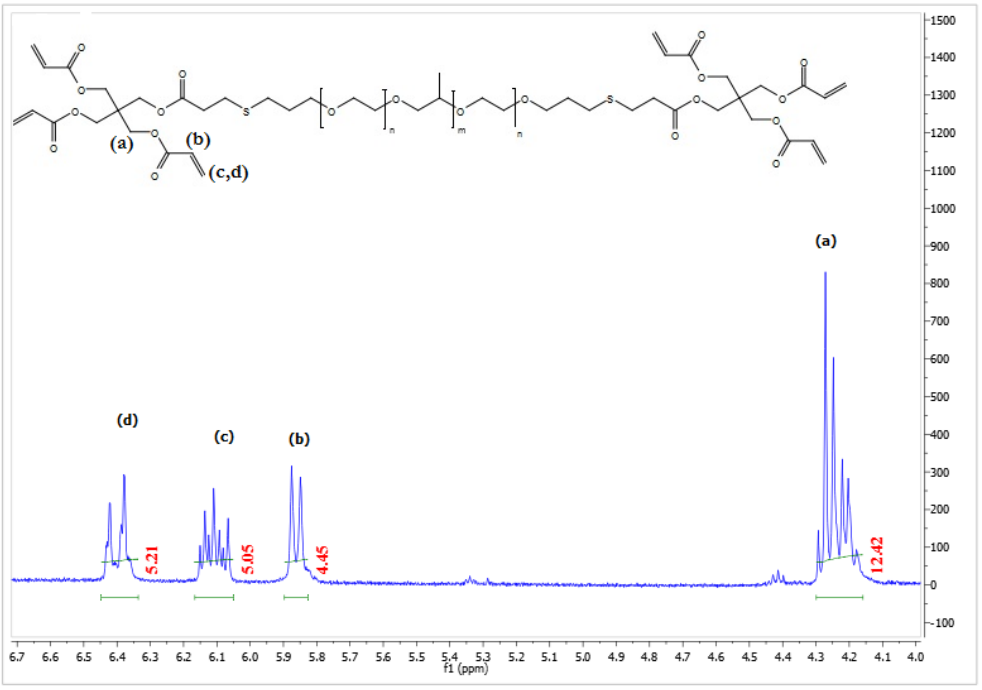

Figure 7.25 F-127 HA ^{1}H NMR.

^{1}H NMR ($CdCl_3$): δ=1.1 (m, 206H, PPG C**H**$_3$ = 69 monomeric units), 3.4 (m, 68H, PPG C**H** = 68 monomeric units), 3.5 (m, 131H, PPG C**H**$_2$ = 66 monomeric units), 3.65 (m, 924H, PEG C**H**$_2$ = 231 monomeric units), 4.3(t, 6H, –CH_2C**H**$_2$–O–CO–CH=CH_2), 5.8 (dd, 6H, CH_2=C**H**–COO–), 6.15 and 6.4 ppm (both dd, 6H, C**H**$_2$=CH–COO).

In NMR analysis it is worth to note that all the normalised peak integrals except (a) at 4.3 (t, 6H,–CH_2C**H**$_2$–O–CO–CH=CH_2) are lower than the theoretical values. This is due to the formation of a polymeric specie from an inner Michael reaction between two F-127 -SH molecules and a tetracrylate bridge. This is confirmed by GPC analysis (see next paragraph for further details).

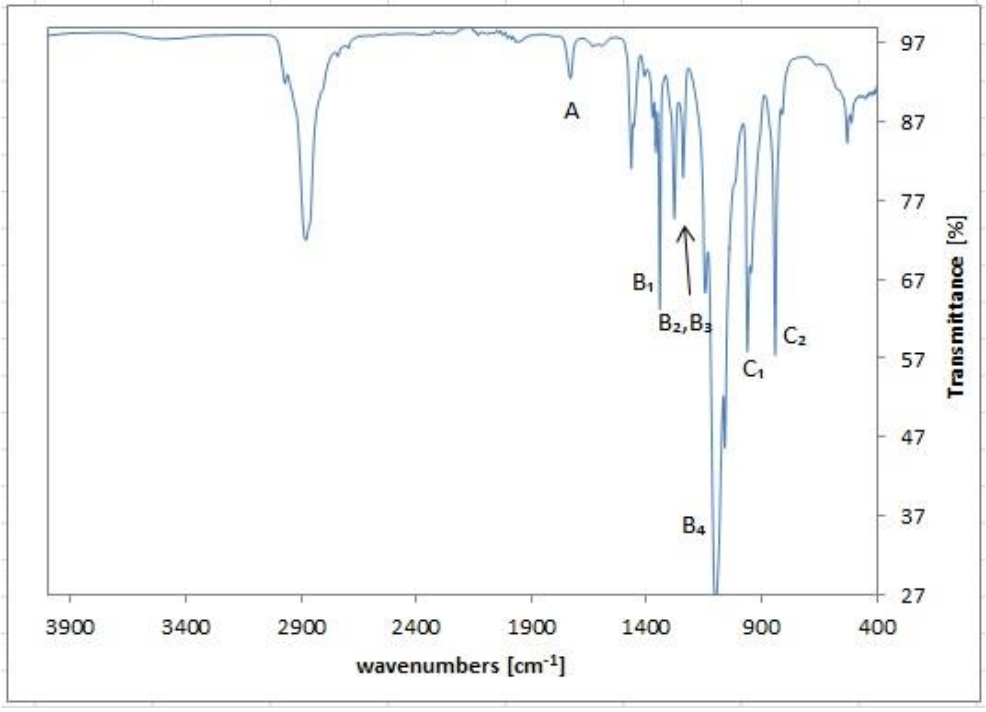

Figure 7.26 F-127 HA FT-IR.

FT-IR (film on ATR plate): 2990-2790 (ν C-H), A: 1724 (ν C=O), 1467 (δ_s CH_2), B_1-B_4: 1342, 1279, 1242, 1097 (ν_{as} C-O-C), C_1-C_2: 962, 841 (ν_s C-O-C) cm^{-1}.

FT-IR analysis allowed to check the presence of new chemical bonds generated from F-127 functionalization, as exposed in Figure 7.26, that is in agreement with data reported in literature [82].

1.1.1 Gel Permeation Chromatography (GPC) of F-127 HA

The F-127 HA, as well as commercial F-127 were analysed by GPC in THF and their chromatograms are shown in Figure 7.27.

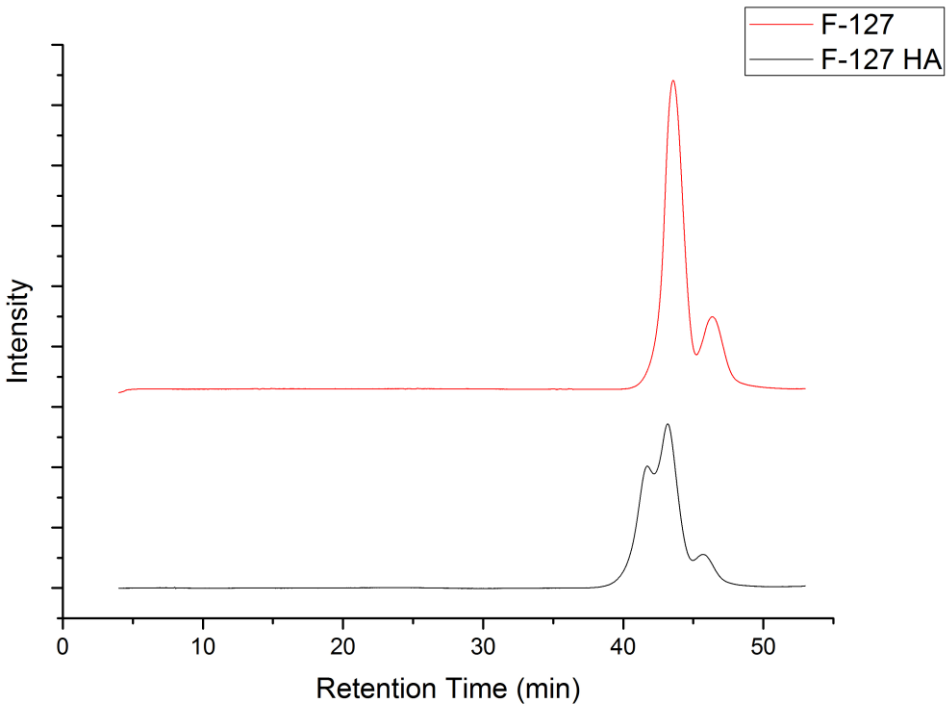

Figure 7.27 F-127 HA (black line) and pure F-127 (red line) GPC chromatograms.

We can observe the presence of three different peaks in the F-127 HA chromatogram, and two peaks in non functionalized F-127.

By integrating the whole F-127 HA chromatogram, we evaluated the following value for $\overline{M_n}$, $\overline{M_w}$, and the polidispersity index PDI :

Table 7.1 $\overline{\mathbf{M_n}}$, $\overline{\mathbf{M_w}}$, **PDI** values for F-127 HA.

$\overline{M_n}$	$\overline{M_w}$	PDI
19935	23645	1.19

The expected $\overline{M_n}$ for F-127 HA, evaluated by adding the Tetra ACR MW to the value extrapolated for non-functionalized F-127, reported in the following table, was: $\overline{M_n}$= 13940.

Table 7.2 $\overline{\mathbf{M_n}}$, $\overline{\mathbf{M_w}}$, **PDI** values for pure F-127.

$\overline{M_n}$	$\overline{M_w}$	PDI
13240	15526	1.12

The difference between expected and evaluated $\overline{M_n}$ in F-127 HA, together with the presence of an additional peak in its GPC chromatogram, suggested us the presence of unknown polymer species. In order to determine these species nature we decomposed the peaks in F-127 HA and non-functionalized F-127 chromatogram using the *Multiple Peak Fit* functions in *Origin 9.1* software.

The used algorithm was a Non-Linear curve fitting, where the fitting curve was assume to be a sum of gaussian curves (one for each peak). The *Gaussian* equation representing a single peak is reported below:

$$y = y_0 + \frac{A}{w \cdot \sqrt{\frac{\pi}{2}}} \cdot e^{-\frac{2(x-x_0)^2}{w^2}}$$

Where y_0: baseline offset

A: total area under the curve from the baseline

x_0: center of the peak

w: equal to 2 times "sigma", approximately 0.849 the width of the peak at half height

The centre x_0 represents the "mean", while $w/2$ is the standard deviation.

The algorithm return the fitting parameters reported in Table 7.3 and Table 7.4, and the resulting curve is shown in Figure 7.28 and Figure 7.29.

Table 7.3 Values of the adopted model for peaks decomposition of F-127 HA GPC chromatogram.

	Peak 1		Peak 2		Peak 3	
Model Parameter	*Value*	*Standard Error*	*Value*	*Standard Error*	*Value*	*Standard Error*
y_0	257.4	10.2	257.4	10.2	257.4	10.2
x_0	41.6	0.0045	43.3	0.003	45.5	0.007
A	15500.0	108.6	18591.0	103.0	4116.5	54.0
W	1.6	0.008	1.4	0.006	1.7	0.02

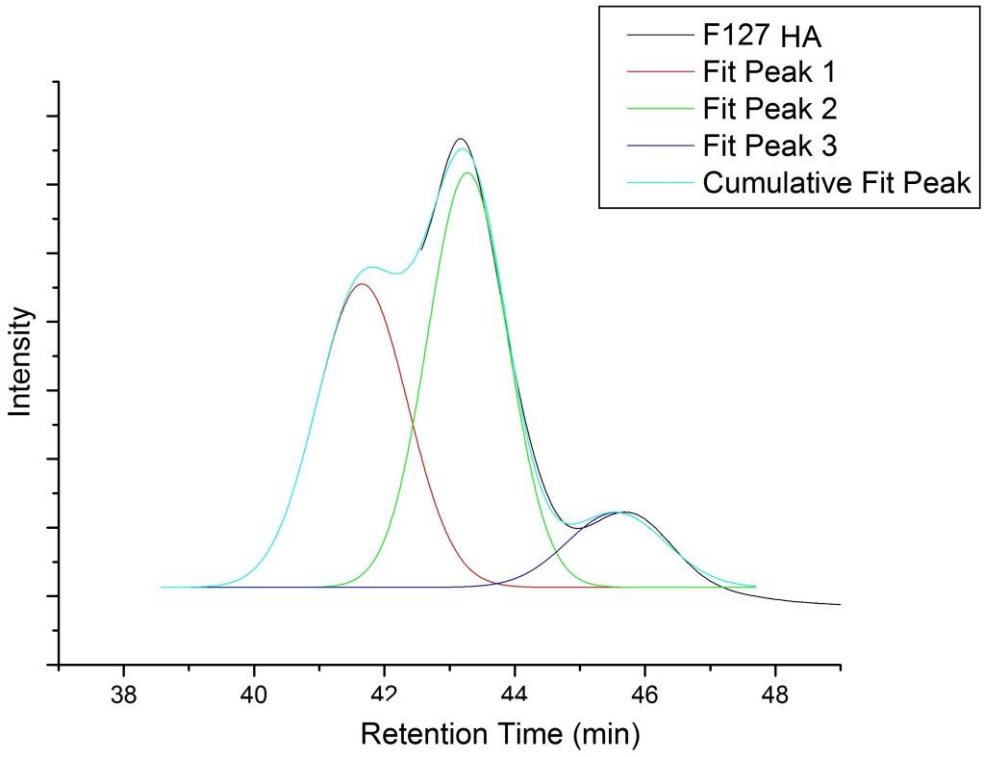

Figure 7.28 Peaks decomposition of F-127 HA GPC chromatogram.

Table 7.4 Values of the adopted model for peaks decomposition of F-127 GPC chromatogram.

	Peak 1		Peak 2	
Model Parameter	*Value*	*Standard Error*	*Value*	*Standard Error*
y_0	86.0	11.1	86.0	11.1
x_0	43.6	7.6E-4	43.3	0.003
A	40244.6	53.3	9675.6	56.8
W	1.5	0.002	1.6	0.009

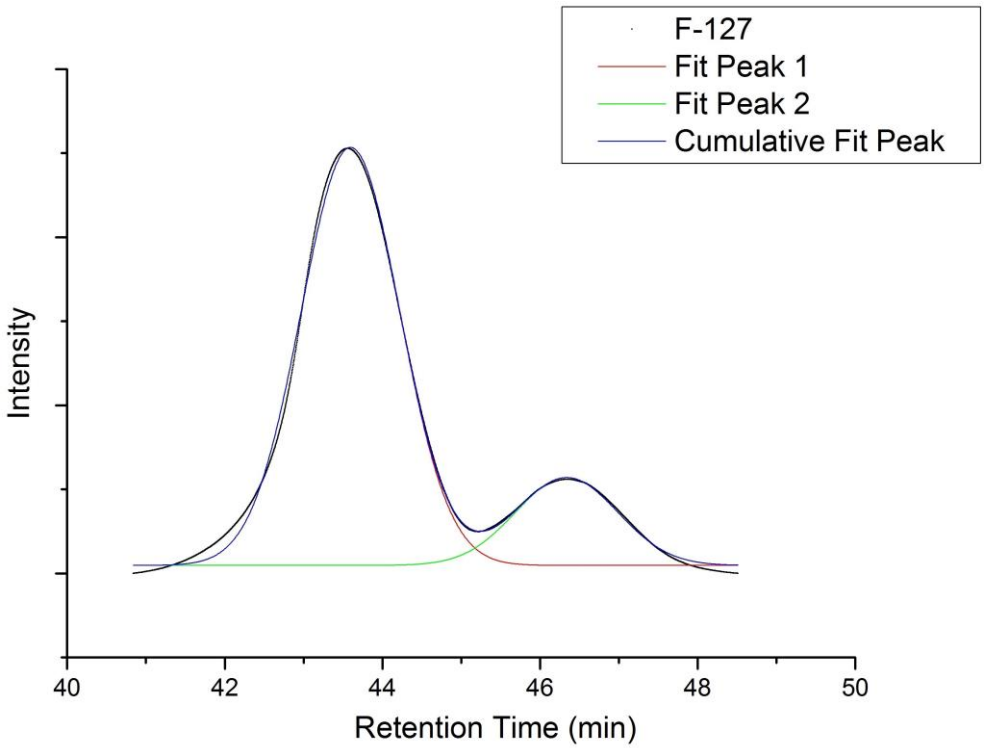

Figure 7.29 Peaks decomposition of pure F-127 GPC chromatogram.

As evident from Figure 7.28 and Figure 7.29, especially from the cumulative fit peak curve, the chromatograms are well fitted by the assumed model.

The average molecular weights and PDI were therefore calculated for each peak after their deconvolution, assuming a *gaussian* distribution with the fitting parameters previously calculated.

The non-functionalized F-127 (Figure 7.29) reveals the presence of an high Mw specie and a low Mw specie, as evident by the $\overline{\mathbf{M_n}}$ and $\overline{\mathbf{M}_w}$ evaluated for the two peaks (Table 7.5).

Table 7.5 $\overline{\mathbf{M_n}}$, $\overline{\mathbf{M_w}}$, **PDI** values for the two peaks of pure F-127.

	Peak 1	**Peak 2**
$\overline{\boldsymbol{M_n}}$	16528	7059
$\overline{\boldsymbol{M_w}}$	17226	7492
PDI	1.04	1.06

Regarding F-127 HA, we have identified three different species (as summarised in Table 7.6):

Table 7.6 $\overline{\mathbf{M_n}}$, $\overline{\mathbf{M_w}}$, **PDI** values for the three peaks of F-127 HA.

	Peak 1	**Peak 2**	**Peak 3**
$\overline{\boldsymbol{M_n}}$	29689	18213	8952
$\overline{\boldsymbol{M_w}}$	31328	19009	9627
PDI	1.05	1.04	1.07

Due to the relatively high molecular weight of the first F-127 HA peak ($\overline{M_n}$=29689, $\overline{M_w}$=31328), we hypothesized that it may correspond to a polymer specie generated by a F-127 'dimerisation', i.e. by a two macromolecules of F-127 thiol (obtained from F-127 TA) coupled with an intermediate tetraacrylate group, as summarised in Figure 7.30: a side reaction of a F-127 HA molecule ($\overline{M_n}$=18213, $\overline{M_w}$=19009) and a F-127 TA ($\overline{M_n}$=13440, $\overline{M_w}$=15726) molecule via Michael addition.

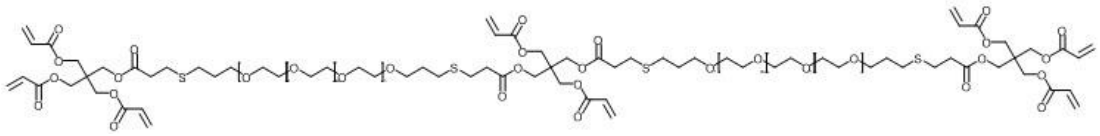

Figure 7.30 Mechanism for the generation of the mono-reacted specie between F-127 TA and F-127 HA.

The second and the third peak correspond to the tetraacrylate functionalization, respectively, of the high and low Mw species present in non-functionalized F-127.
By integrating the intensities (proportional to monomer units concentration) of peak 1 and peak 2, respectively, we obtained the following peak areas:

Table 7.7 Peak areas by integrating intensities.

	Peak 1	**Peak 2**
Area	15332	18533

Since the area of the two peaks is almost comparable, we can assume that the corresponding two polymer species (one with 6 acrylates and another with 4 acrylates per F-127 molecule, respectively) are almost equimolar, and this is in agreement with the the ^{1}H NMR spectrum of F-127 HA, by which a mean value of 5 acrylates per F-127 molecule (instead of 6) was calculated.

Physico-chemical characterisation

7.2.5 Deprotection of Pluronic thioacetate

Since F-127 TA converts easily and *in situ* in F-127 dithiol via base treatment the synthesis of F-127 TA as thiol-protected form was preferred to minimise disulphide bonds formation during storage. For its application in the F-127 HA production and for the gel formation, it is therefore necessary to deprotected it with the mechanism described in Figure 7.31:

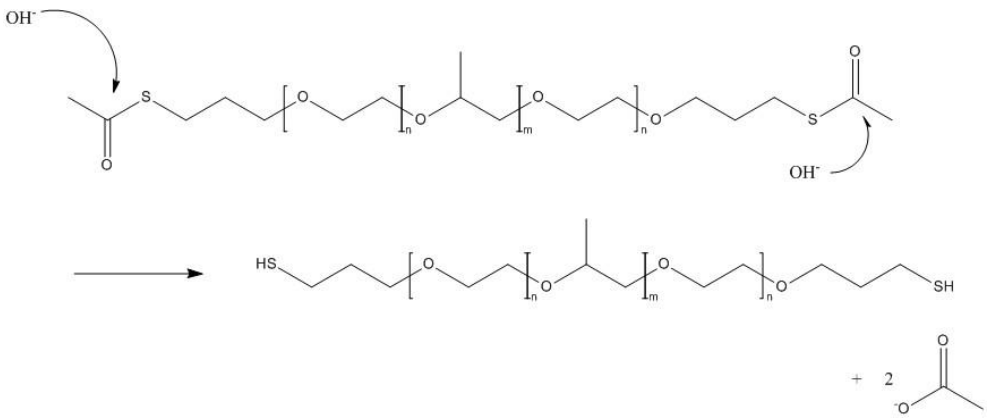

Figure 7.31 F-127 TA deprotection scheme.

Thioacetate groups are readily hydrolyzed by strong bases, such as NaOH, in a pseudo first-order reaction, as reported in [53] and confirmed in Figure 7.32.

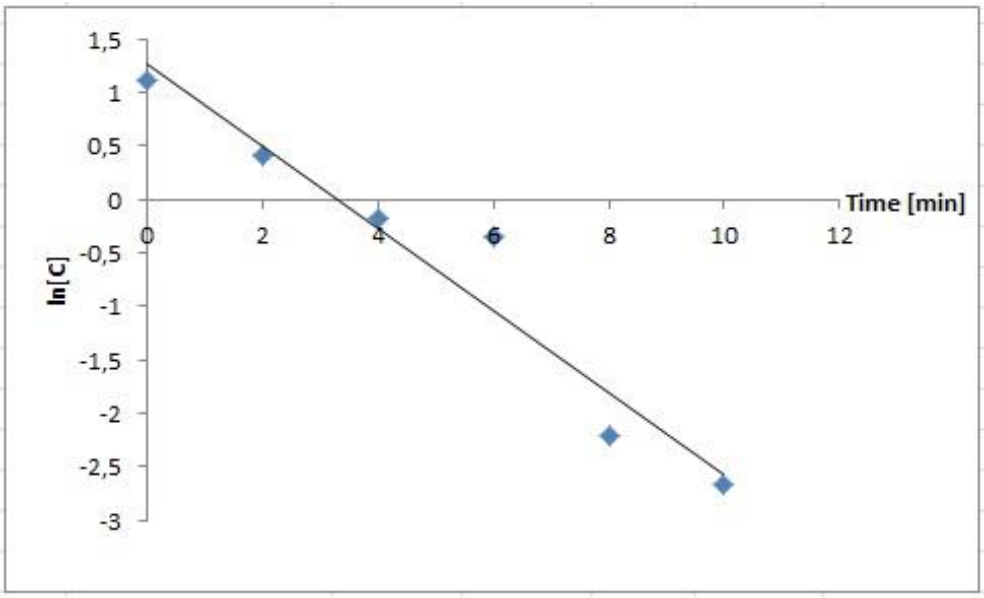

Figure 7.32 ln(concentration) vs time.

Therefore, this hydrolytic process depends on three main variables: the concentration of the base, the concentration of the protected macromolecule and the reaction time. The target is to obtain a quantitative F-127 TA deprotection in the shortest reaction time, in order to minimize oxidation of thiols to disulfides, which would affect the efficiency of the Michael-type addition during gel formation. This could be achieved by maximizing the concentration of the base. However, at high base concentration the polymer could be damaged and loss its reactive characteristics, and the final buffering at physiological pH could be extremely complicated. A fast deprotection could also be obtained by decreasing the concentration of the polymer while keeping a relatively mild concentration of OH^-.

The kinetics study was conducted for a solution concentration of F-127 TA equal to 20% w/v. The NaOH solution was prepared with D_2O: the deuterated solvent allowed NMR analysis to quantify thioacetate hydrolysis. We choose a NaOH 0.2 M solution, i.e. a base concentration which is relatively easy to buffer to physiological pH after the deprotection step.

The ^{1}H NMR results and the progress of the conversion are reported in the following figures:

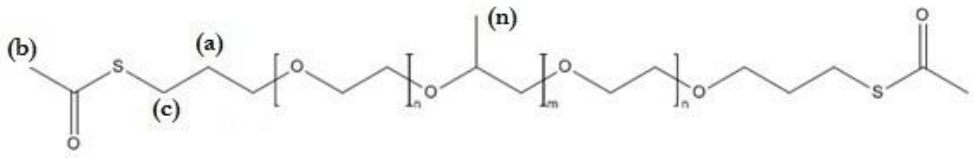

Figure 7.33 F-127 TA structure with ^{1}H NMR peaks identification.

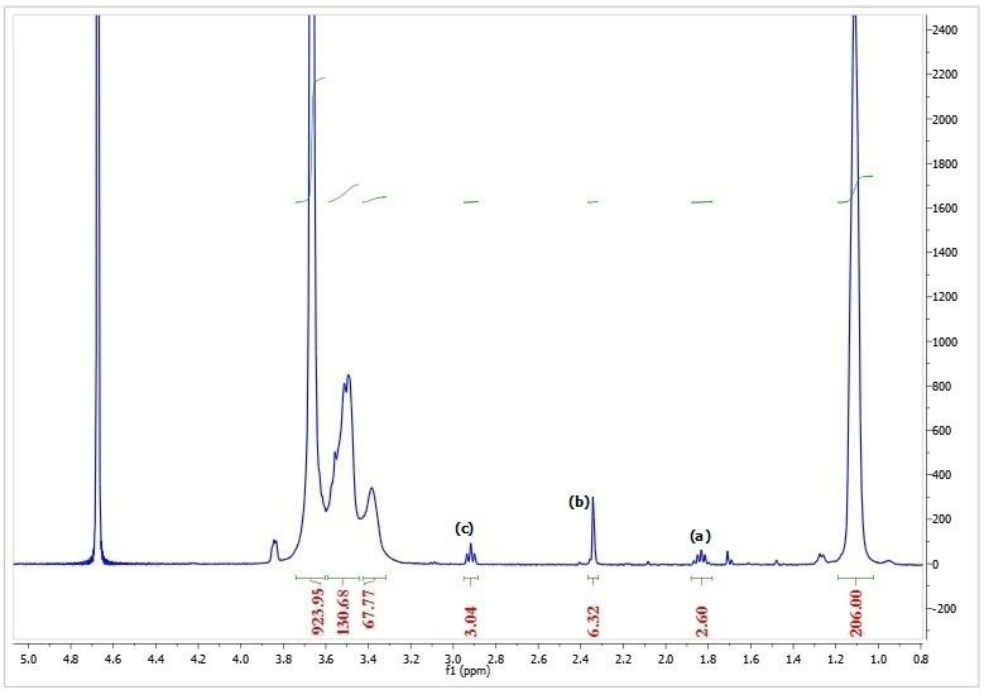

Figure 7.34 F-127 TA ^{1}H NMR in D_2O.

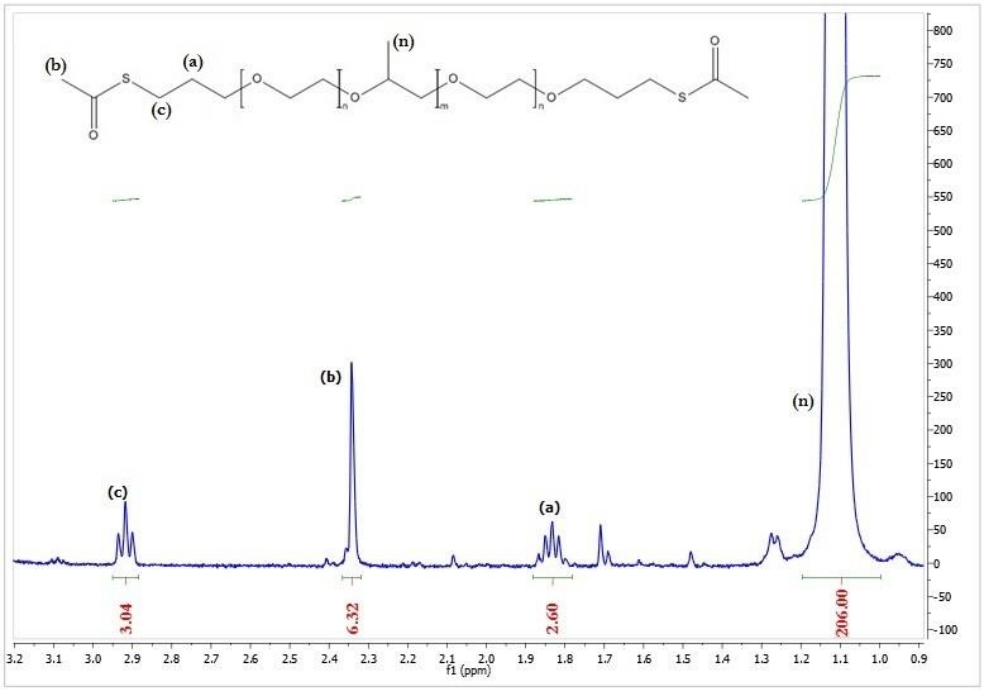

Figure 7.35 F-127 TA ^{1}H NMR in D_2O; magnified view of the NMR spectrum within the region $1<\delta<3.2$

The value of the peaks that correspond to the end functional groups were normalized respect to the value of the protons corresponding to PPG C**H**$_3$, which remain constant during the reaction.

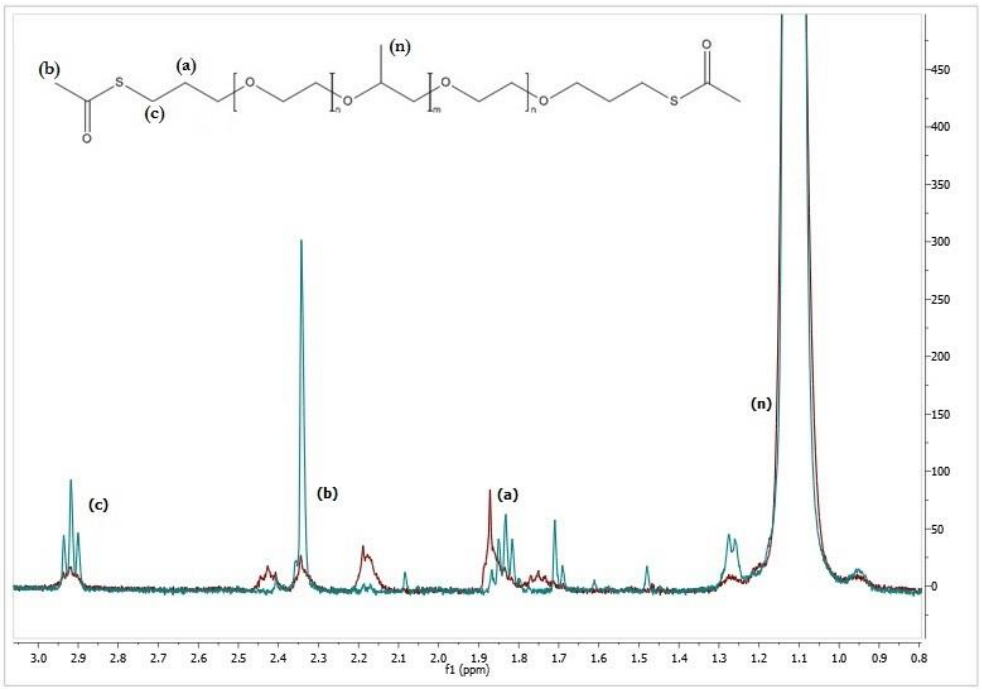

Figure 7.36 F-127 TA ^{1}H NMR in D_2O at time zero vs. F-127 TA after 2 minutes of reaction.

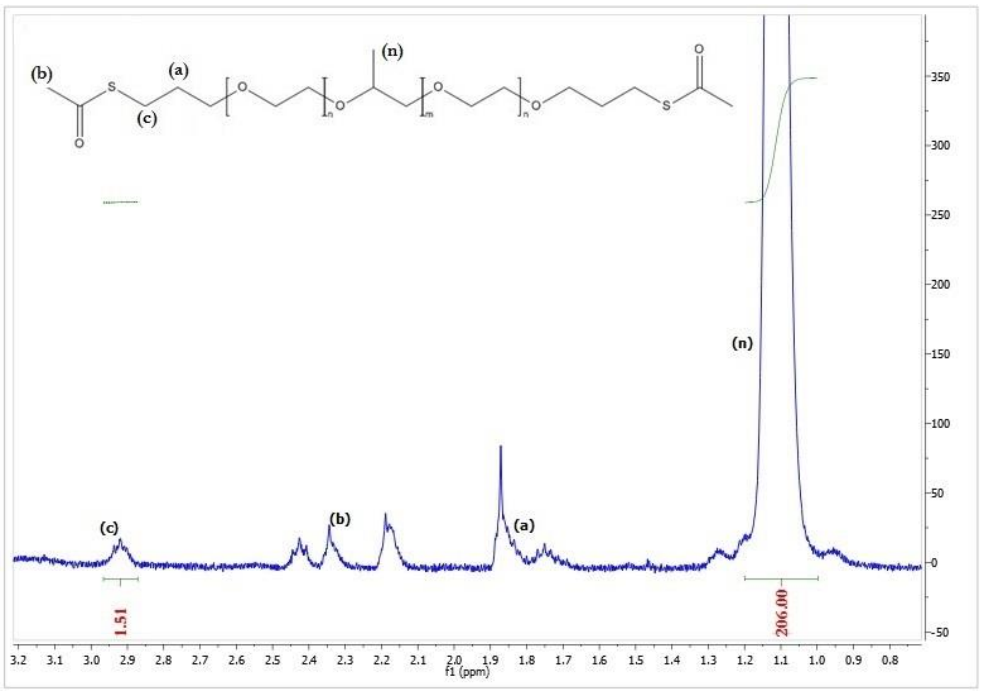

Figure 7.37 ^{1}H-NMR spectrum of F-127 TA after 2 minutes of reaction. Magnified view of the spectrum region $0.7<\delta<3.2$, to highlight the effect of the reaction on peak variations.

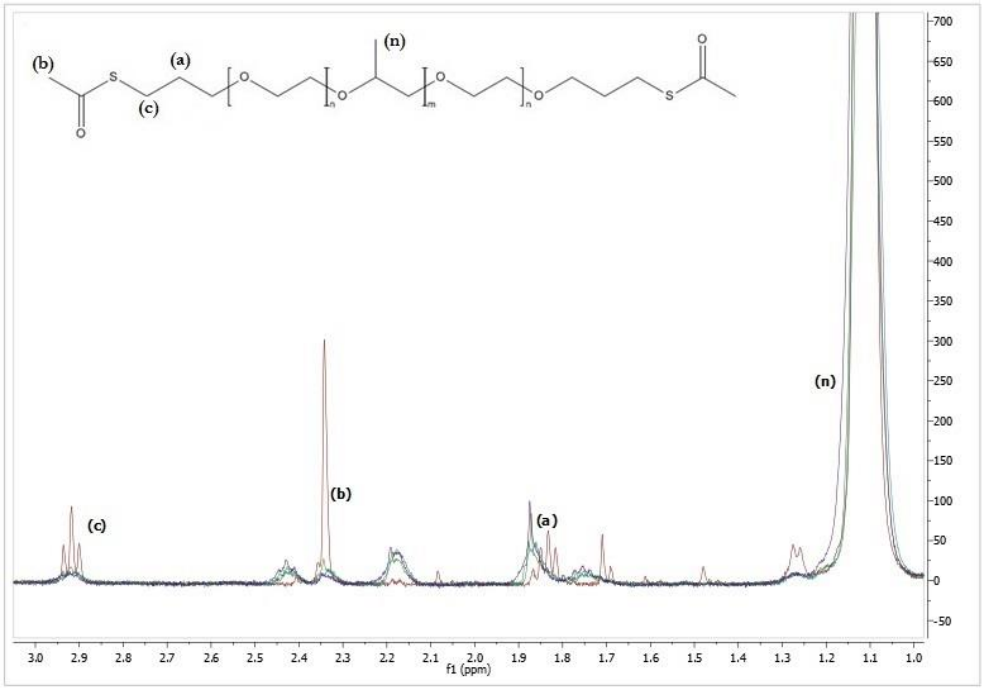

Figure 7.38 Overlap of the ^{1}H-NMR spectrum of the first 6 minutes of reaction.

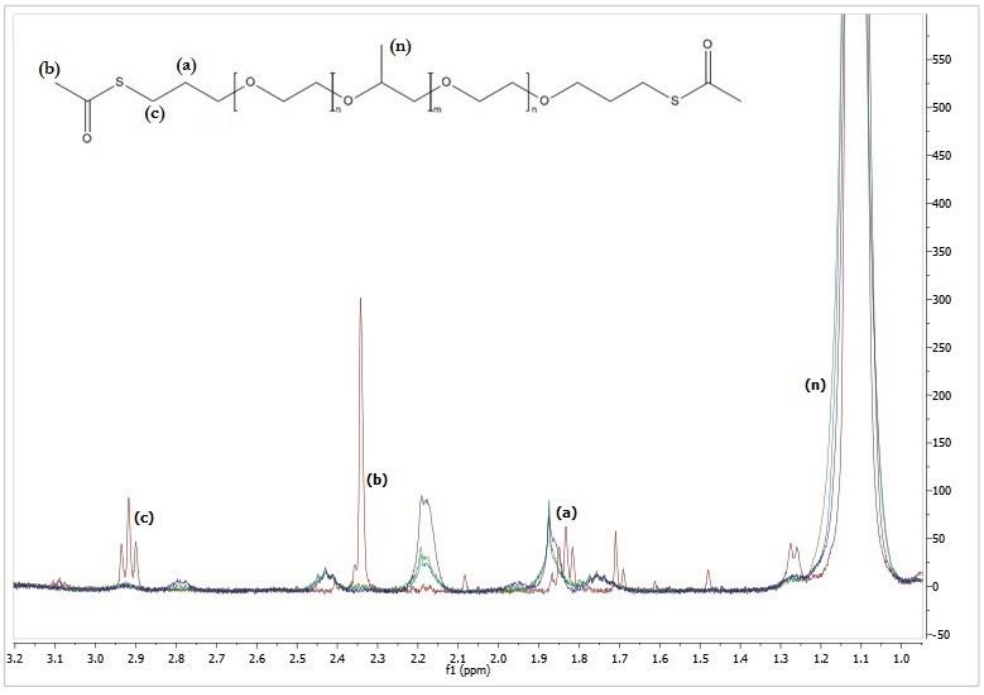

Figure 7.39 Overlap of ^{1}H-NMR of the deprotection reaction of F-127 TA from minute 8 to minute 14.

From the previous images we noticed that the peak (c) C**H**$_2$SCOCH$_3$ was the best to calculate the reaction conversion over time, as reported in Table 7.8.

Table 7.8 CH_2SCOCH_3 conversion.

Time[min]	Integral Value	Conversion%
0	3.04	0
2	1.51	50
4	0.83	73
6	0.71	77
8	0.11	96
10	0.07	98
14	0.00	100

As we can see in Figure 7.40 under these reaction conditions, complete deprotection was achieved in roughly 10 min.

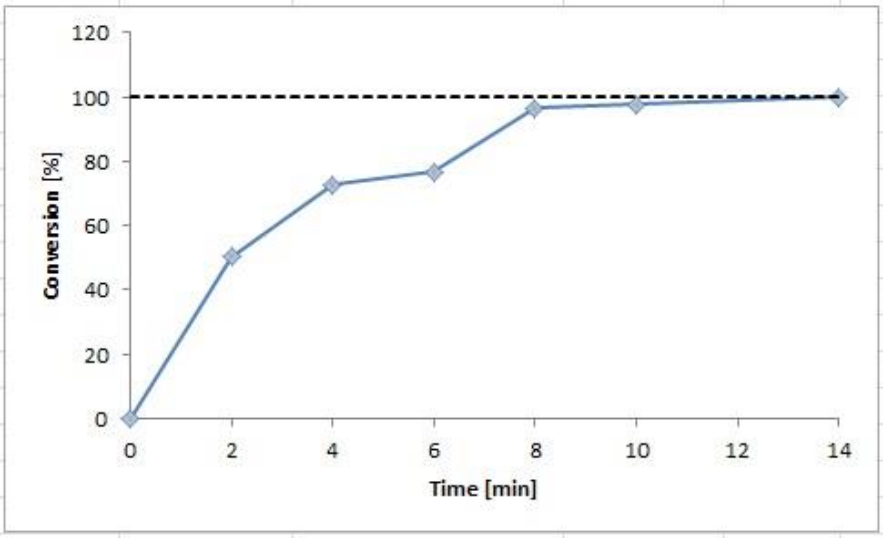

Figure 7.40 Conversion diagram.

7.2.6 Pluronic F-127 thioacetate - Tetronic 701 acrylate hydrogel characterisation

As previously mentioned, we investigated the feasibility of obtaining chemically crosslinked gels via Michael-type addition between Pluronic F-127 di-thiol, generated in situ by deprotection of F-127 TA, and T701 ACR, used as a 4-arm crosslinker. A chemical hydrogel was obtained (as presented in the experimental section 0) but its physico-chemical characteristics were no acceptable to any further investigation or application. In fact, the final gel was opaque, sticky, soft and with low elastic characteristics. The poor quality of the material may be ascribed to the possible presence of unreacted reagents and solvents, due to the difficulties encountered in T701 ACR purification. The presence of unreacted or low molecular weight compounds could also compromise biological tests, because of their high toxicity.

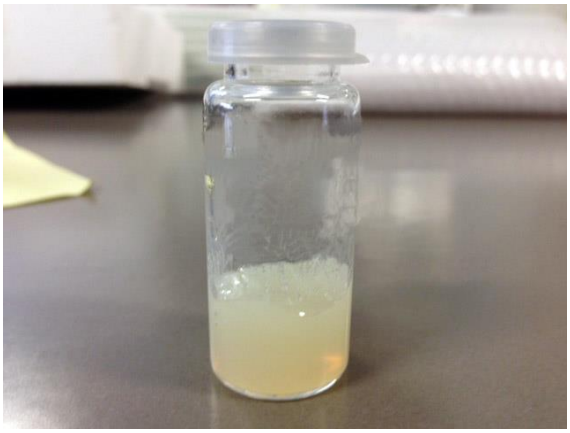

Figure 7.41 Hydrogel based on F-127 TA and T701 ACR.

Pluronic F-127 thioacetate -Pluronic F-127 hexaacrylate hydrogel characterisation

7.2.7 Crosslinking kinetics

The kinetics of radical crosslinking was studied by Dynamic Light Scattering (Malvern Zetasizer Nano ZS), evaluating the increase of the viscosity of the reacting polymer solution.

The polymer solution viscosity can be easily calculated by dispersing in the sample gold NPs of well-defined size (10-20 nm) and measuring by DLS the apparent variation of particle size due to the viscosity increase during the crosslinking process. In fact, the viscosity can be calculated by rearranging the Stokes-Einstein equation:

$$\mathcal{D} = \frac{k_b T}{6\pi\eta r} \tag{8.1}$$

into

$$\eta = \frac{k_b T}{6\pi\mathcal{D} r} \tag{8.2}$$

Where η is the solution viscosity, $k_b T$ is the product of the Boltzmann constant and the temperature, $\mathcal{D}$ is the diffusion coefficient of the gold NPs in the medium, and r is the hydrodynamic radius of the gold NPs.
The DLS is able to calculate the diffusion coefficient $\mathcal{D}$ from the autocorrelation function, however the Zetasizer software returns an apparent hydrodynamic radius r_{app} by setting the viscosity value as the viscosity of pure water η_w at temperature T, according to the Stokes-Einstein equation:

$$r_{app} = \frac{k_b T}{6\pi\eta_w \mathcal{D}} \tag{8.3}$$

From equation (8.2) and (8.3) the solution viscosity can be calculated as follow:

$$\eta = \frac{k_b T}{6\pi \mathcal{D} r} = \frac{k_b T}{6\pi r} \frac{6\pi\eta_w r_{app}}{k_b T} \tag{8.4}$$

Thus,

$$\eta = \eta_w \frac{r_{app}}{r} \tag{8.5}$$

As reported in the experimental section we synthesized pegylated gold NPs from the simpler commercial gold NPs. This is necessary to avoid interactions between gold and F-127 thiol which may cause unpredictable results from the DLS measurements. The apparent hydrodynamic radius was taken from the average size from Zetasizer output taking into account that gold NPs were monodisperse.

7.2.7.1 Pegylated gold nanoparticles

The hydrodynamic radius of the pegylated gold NPs was verified by DLS measurements. As mentioned in the experimental section, pegylation was carried out for monodisperse 10 nm and 20 nm gold NPs. The average size of 10 nm pegylated gold NPs, as obtained from the Zetasizer measurements, was equal to 17 nm, and used in the viscosity calculation of 10% w/v F-127 TA-HA gel. The average size of 20 nm pegylated gold NPs was equal to 27nm and used in the viscosity calculation of 20% w/v F-127 TA-HA gel.

The recorded viscosity vs. reaction time for 10% w/v and 20% w/v gelling solution at 15°C are reported in Figure 7.42:

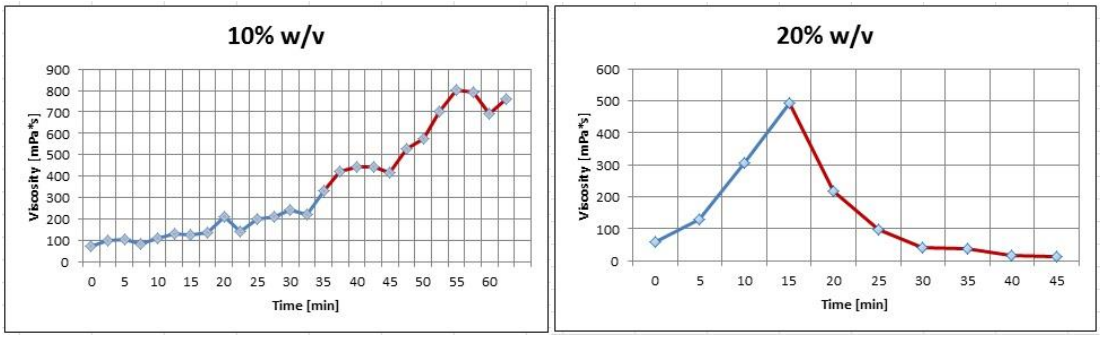

Figure 7.42 Recorded viscosity vs. reaction time for 10% w/v gelling solution (left) and for 20% w/v gelling solution (right).

In the graphs above the blue lines represent reasonable viscosity values, whereas red lines represent viscosity values calculated by the Zetasizer software from poor quality autocorrelation functions as reported in Figure 7.43 and Figure 7.44. We interpreted the onset of poor autocorrelation function as an effect of the sol-gel transition around the gel point, which makes the calculations of the apparent nanoparticle size in viscoelastic materials unfeasible.

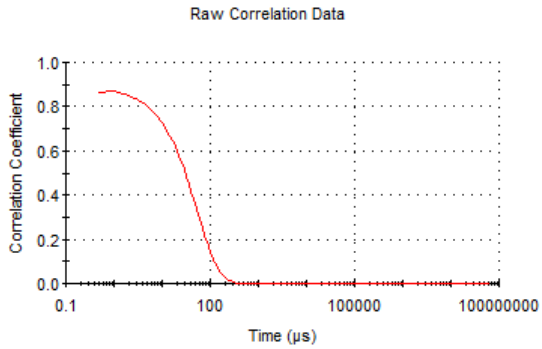

Figure 7.43 Autocorrelation function recorded from "liquid" sample, in the first minutes of the experiment.

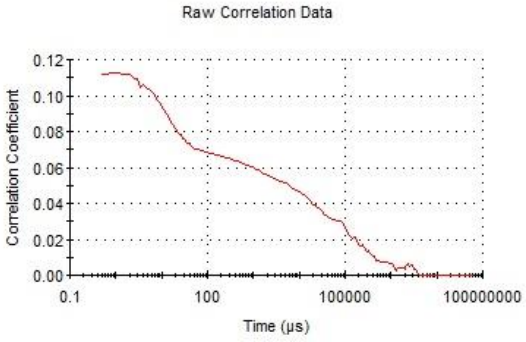

Figure 7.44 Autocorrelation function recorded from gel sample at the end of the experiment.

These results show how the crosslinking becomes faster at higher polymer concentration at constant temperature. These experiments were carried out at 15°C, i.e. below the temperature at which physical gelation occurs at this polymer concentration, and it is low enough to slow down Michael-type addition reaction. In this way, we have enough time to appreciate gel transitions in these measurements. Indeed, these tests did not aim to return a precise value of viscosity but were carried out with the intention of provide a qualitative analysis of crosslinking rates. In fact, in these cases, especially for 20% w/v the reaction is very fast, and therefore a precise calculation of the gelation time is not possible.

7.2.8 Swelling measurements

As seen in Chapter 2 the swelling behaviour implies an increase in the polymer matrix volume due to the absorption of a solvent (PBS in this case).

The degree of swelling of F-127 gels obtained by Michael-type addition were measured at different polymer concentrations and temperatures, and results are reported in the Figure 7.45 and Figure 7.46.

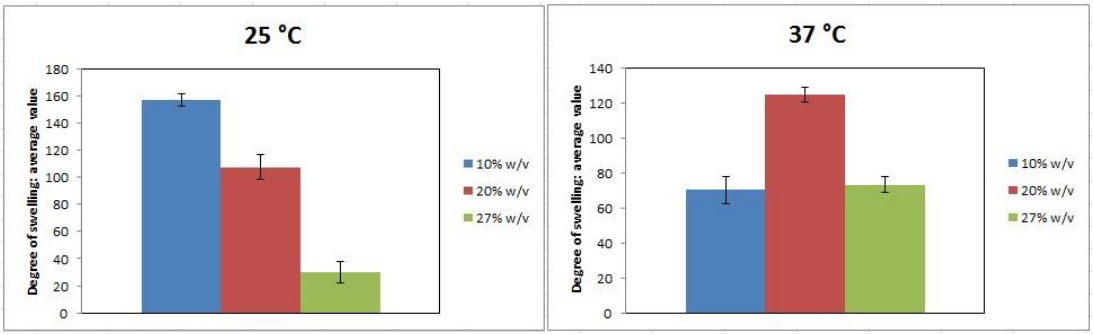

Figure 7.45 Degree of swelling at room temperature (25°C) (left) and at physiological temperature (37°C) (right).

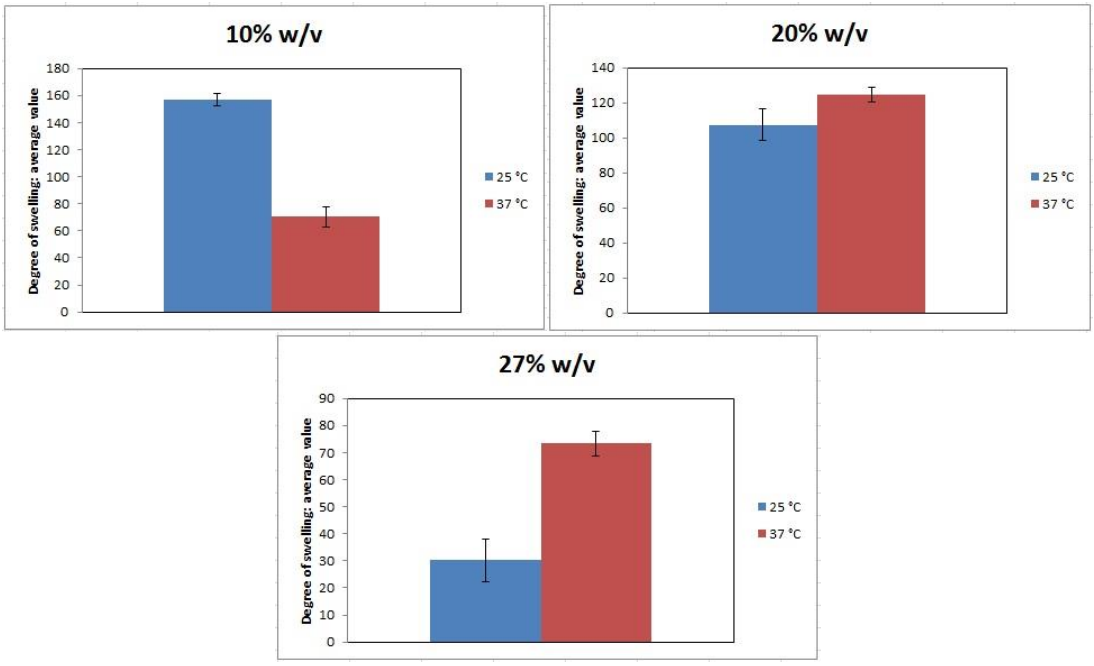

Figure 7.46 Degree of swelling at physiological (37°C) and room temperature (25°C) for 10% w/v gel concentration (top, left) 20% w/v gel concentration (top, right) and 27% w/v gel concentration(bottom).

As expected, the degree of swelling at room temperature (≈25°C) increased as the Pluronic concentration decreased, as an effect of the lower crosslinking density (Figure 7.45). In fact, as the polymer concentration decreases, the number of crosslinking points decrease too, according to the design of the gel network proposed: this leads to a more mobility of the polymer chains that constitute the hydrogel network favouring an expansion that allows water molecules to penetrate. Higher gel concentrations present reduced swelling due to the strictly crosslinked network that results in a less extended solvent uptake.

At physiological temperature an unexpected trend was obtained. Due to the LCST of Pluronic, the increase of temperature led to an increase of hydrophobic interactions between polymer chains, and indeed the 10% w/v Pluronic gel decreased its swelling at 37°C (Figure 7.46 (top, left)). However, 20% w/v gels and 27% w/v gels did not show this behaviour; in particular the 27% w/v gels almost doubled its swelling degree from room to physiological temperature (Figure 7.46 (bottom)).

This inverse trend could be ascribed to an effect of hydrolysis (which took place in 24 h) of the ester bonds of the gel crosslinks, which are particularly unstable at 37°C because of the neighbouring sulphides generated by the Michael-type addition [83]. Clearly, this hydrolysis may be favoured by the higher concentrations of esters in the gels, and therefore the effect of a reduction of crosslinking density would be more significant for the 27% w/v samples.

7.2.9 Diffusion tests

The effect of gel network on the diffusion of a standard low molecular weight drug (Ibuprofen) was evaluated by High Resolution Magic-Angle Spinning (HR MAS) NMR spectroscopy.

The ^{1}H NMR spectrum of hydrogels is characterised by broad signals due to the residual solid-state effects related to the dipole-dipole coupling. As a consequence classical NMR techniques, normally applied to liquid phase, cannot be used to calculate the diffusion coefficient of compounds diffusing within the gel. The use of HR MAS allows the application of HR NMR spectroscopy to suspended solid- or gel-like samples [84]. In this technique the sample is rotated at a rate between 8 and 70 kHz at an angle of 54.7°, relative to the external magnetic field. At this so-called 'magic angle' (the diagonal through a cube) dipole-dipole interactions and susceptibility distortions are averaged, reducing the observed line widths to be similar to those observed in solution high resolution NMR spectroscopy [85,86].

All the spectra were recorded on a Bruker Avance spectrometer operating at 500 MHz proton frequency, equipped with a dual 1H/13C HR-MAS probe.

Self diffusion coefficient were measured by Diffusion Ordered Correlation Spectroscopy (DOSY) experiments, based on the pulsed field gradient spin echo (PGSE) approach (combination of the enhanced resolution afforded by HR-MAS with pulse field gradient (PFG) capabilities that allow to diffusion measurements of complex heterogeneous materials).

The duration of the magnetic field pulse gradient (d) and the z direction were optimized for each sample in order to obtain complete dephasing of the signals with the maximum gradient strength. In each DOSY experiment, a series of 32 spectra with 32 k points were collected. For each experiment 24 scans were acquired. The pulse gradients were incremented from 2 to 95% of the maximum gradient strength in a linear ramp. The temperature was set at 305° K (32 °C) and the spinning rate at 4 kHz.

During the analysis it was used a Spin echo pulse program reported in Figure 7.47

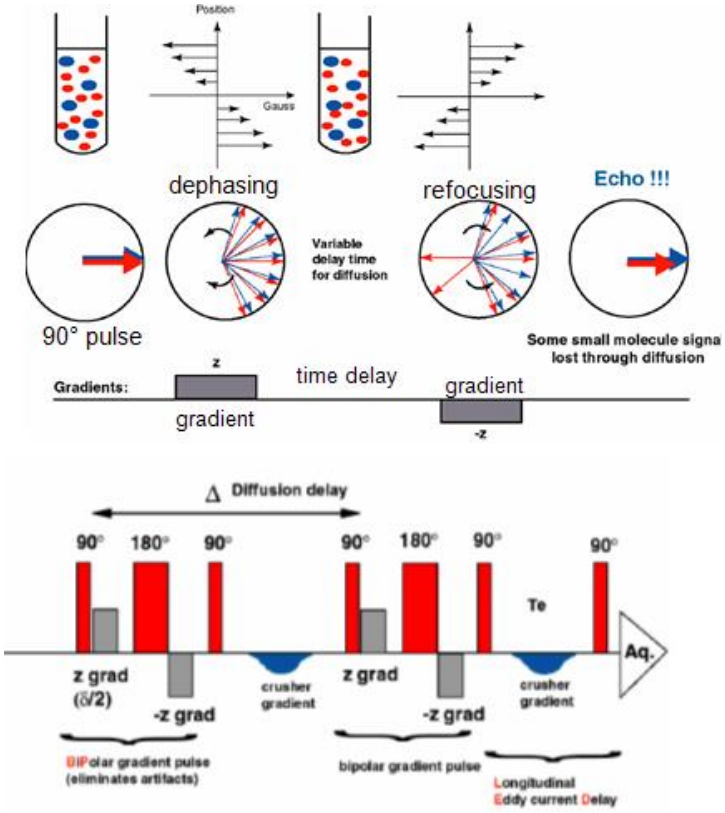

Figure 7.47 Sketch of spin echo pulse sequence.

An impulse of 90° was applied to the sample. A gradient was generated and it was possible to obtain a *spin dephasing*. After a variable time Δ ("big delta") an opposite gradient was applied and thus it was observed the *spin refocus*. If the molecule diffused away from its initial position during the diffusion delay Δ, the local field experienced during the second pulse field gradient would not exactly match that of the first pulse. Only partial refocusing of the signal would therefore occur [87] and the NMR signal decreases over time. This signal decay is exposed in Figure 7.48.

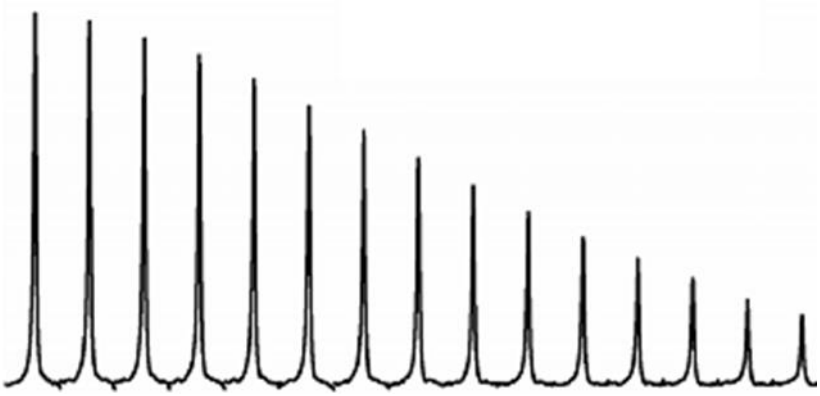

Figure 7.48 Signal decay.

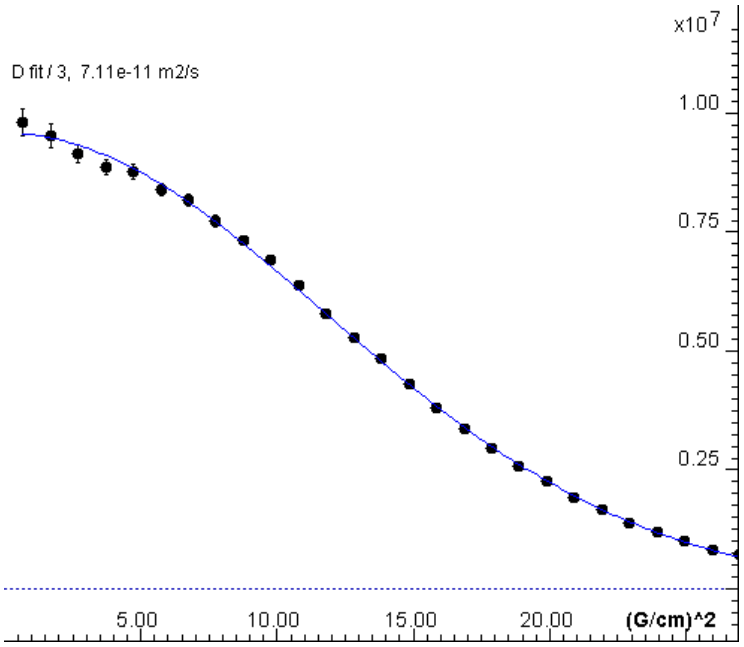

Figure 7.49 Intensity (I_G) against square gradient (G^2).

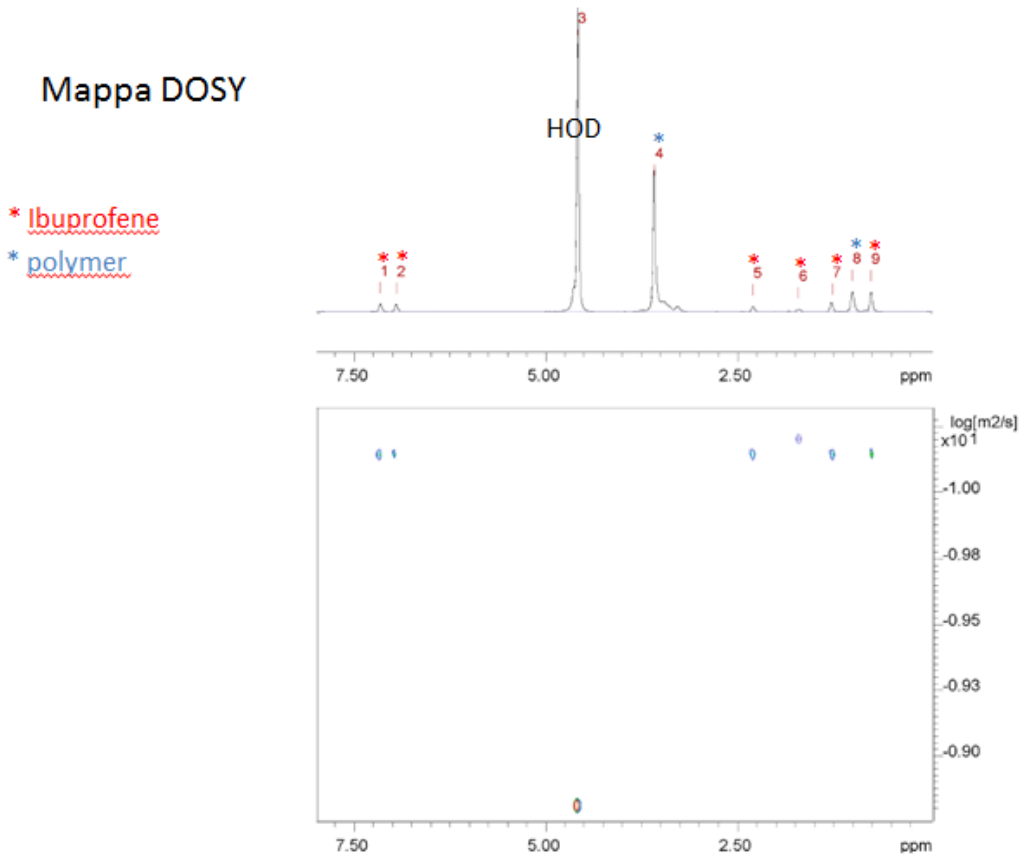

Figure 7.50 Pseudo 2D results representation.

Once the diffusion data set, consisting of a 1D traces, obtained with increasing gradient amplitudes, was collected, it was possible to extract the diffusion coefficient by data fitting (Figure 7.49). Data fitting procedures rely on the measurement of the decay in signal intensity (recorded either as peak height or integrated area) as a function of the applied gradient strength. Diffusion coefficient could be extracted directly from regression fits of the peak intensities versus gradient strength [87]. Diffusion coefficient could be extracted with an appropriate non-linear approach [87]:

$$S = S_0 \exp(-\mathcal{D}\gamma^2\delta^2 g^2 \Delta')$$

Where S is the NMR signal intensity at time t

S_0 is the initial signal intensity value

$\mathcal{D}$ is the diffusion coefficient

γ represents the gyromagnetic ratio (depending on the proton nucleus)

δ is the length of the gradient pulses

g represents a strumental value

Δ is the diffusion period (big delta)

The resulting diffusion coefficient values for the F-127 TA-HA gels are exposed in Table 7.9

Table 7.9 Resultant diffusion coefficient for Ibuprofen in F-127 TA-HA gel.

SAMPLE	D [m^2/s]
D_2O solution	4.20E-10
10% w/v	9.28E-11
20% w/v	1.65E-10
27% w/v	1.31E-10

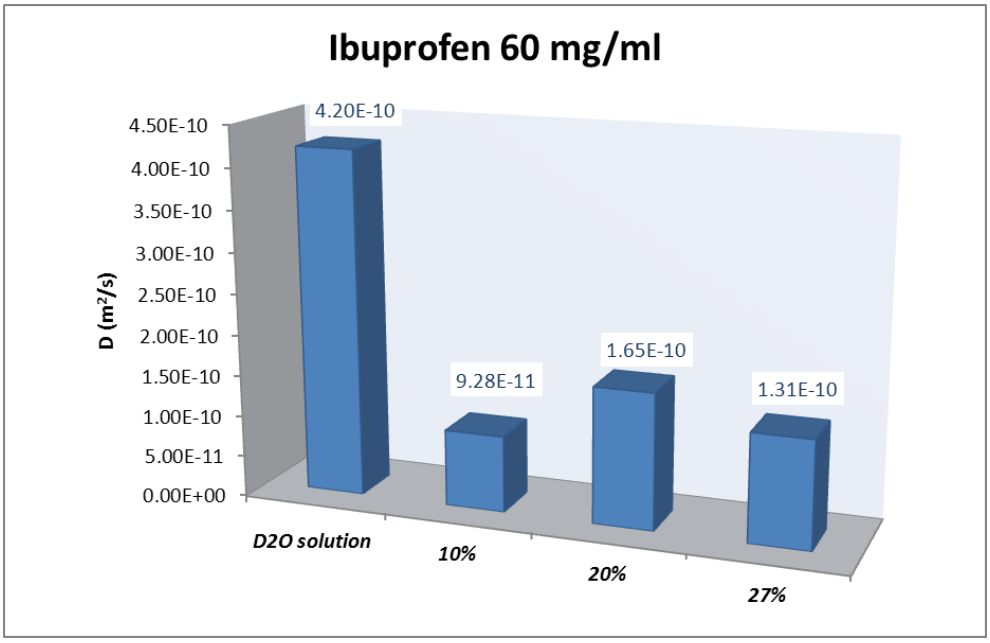

Figure 7.51 Diffusion coefficient for Ibuprofen in F-127 TA-HA gel (histogram).

From the results above it is possible to note that the ibuprofen diffusion coefficient values in the gels are lower respect to the value in pure D_2O solution (without F-127). Moreover, the polymer concentration in the gels does not greatly affect the diffusion coefficient values. Further experiments will be carried out in future to provide statistical relevance to these data and a physical interpretation of the results.

Biological tests

7.2.10 Cell culture

Three sets of experiments, using both fibroblast , endothelial cells and podocytes, were performed.

The first set was performed using non-treated gels (**procedure 1**), i.e. gels with no RGD peptide grafted nor serum proteins entangled with the polymer network, where we expected to have no adhesion due to protein repellent properties of PEG, which is the main constituent of Pluronic F-127.

Then, experiments were carried out with pre-treated gels with culture medium, thus containing serum proteins (**procedure 2**) and with gels functionalized with the cell adhesive RGD peptide (**procedure 3**), in order to assess the effect of gel functionalization over cell adhesion and response. The RGD peptide (sequence GRGDSPC) was easily linked to the hydrogel thanks to the presence of the end –SH group (see Figure 5.3). Thus, a Michael-type addition reaction occurred between –SH group of the peptide and not-crosslinked acrylates groups of F-127 HA. It was chosen to assure the highest possible concentration of RGD peptide in the final gel network, that consists in the bonding of 2/5 mol of RGD for acrylates equivalents. The addition of TCEP was necessary to reduce the RGD disulphide eventually formed.

Three types of cells, such as fibroblasts, endothelial cells and podocytes were tested to investigate their different behaviour, in terms of adhesion and growth.

In fact, the use of cells that respond in different ways to an external environment could represent a good model for the assessment of the biocompatibility of our gels. In particular, we expected that podocytes were the most difficult cells to culture on Pluronic gels. In fact, podocytes need a layer of collagen type IV in order to grow and adhere also in the biological flask, because they do not adhere directly on plastic as fibroblasts or endothelial cells.

7.2.10.1 Fibroblasts cultured on F-127 TA-HA gels

Figure 7.52, Figure 7.53 and Figure 7.54 represent microscope images obtained from fibroblasts cultured on 13% w/v F-127 TA-HA gels according to the **procedure 1**, **procedure 2** and **procedure 3**, as described in Materials and methods section. Pictures are taken after 24 h and 96 h.

Procedure 1.

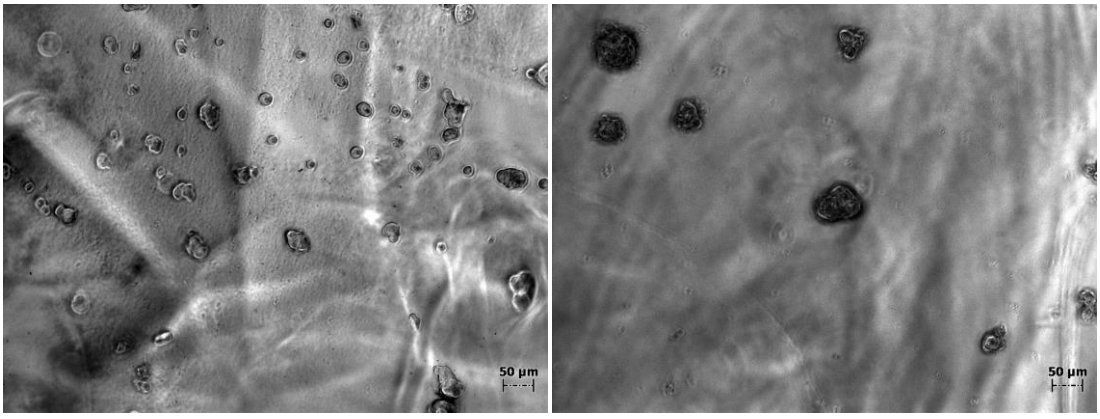

Figure 7.52 Fibroblast culture following procedure 1 after 24 h (left) and after 96 h (right).

Procedure 2.

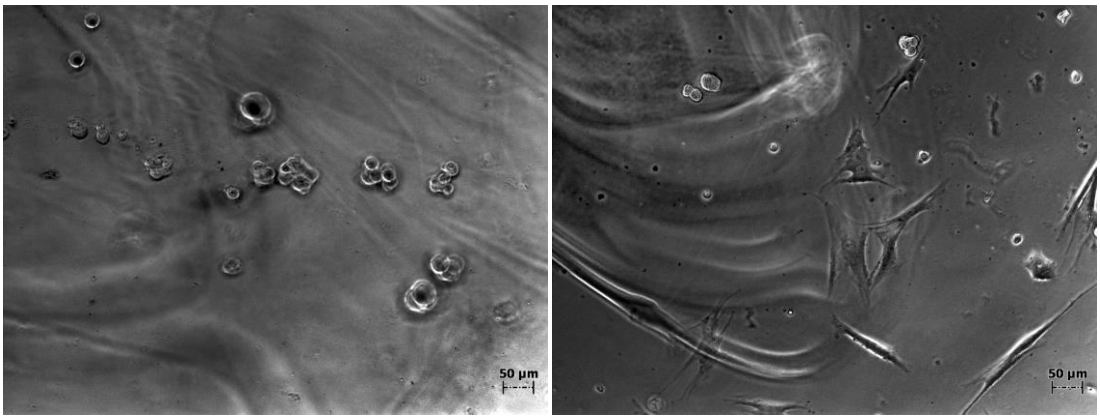

Figure 7.53 Fibroblast culture following procedure 2 after 24 h (left) and after 96 h (right).

Procedure 3.

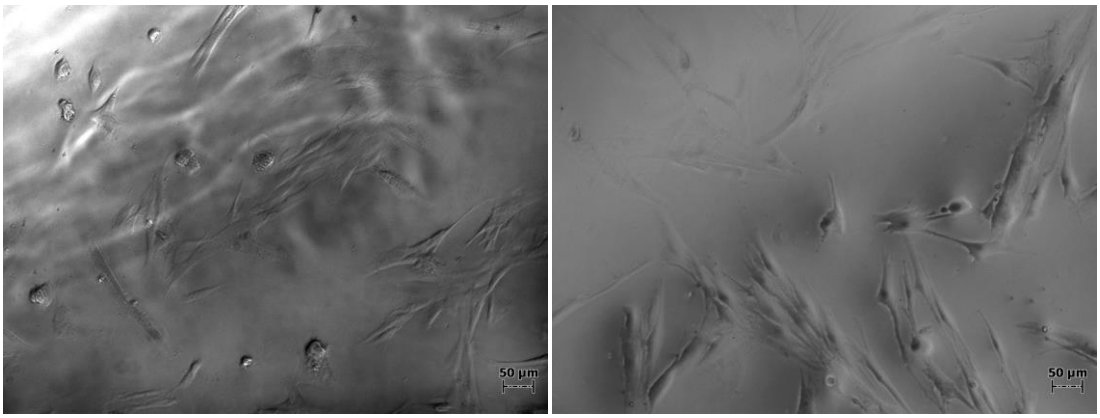

Figure 7.54 Fibroblast culture following procedure 3 after 24 h (left) and after 96 h (right, in this case picture was taken after removing cellular medium).

Figure 7.53 shows the result for procedure 2-gels. Cells presented their typical elongated shape, thus indicating that they adhered on gels. This suggested that serum proteins presented during the crosslinking reaction may have been embedded in the final gel and in some way displaced at the gel surface. Since several serum proteins contain integrin binding domains, this facilitate cell adhesion.

In procedure 3 good cell adhesion results were achieved, as shown in Figure 7.54. As seen in Chapter 5, RGD peptide is widely used to guarantee cell adhesion properties to the gels for tissue engineering applications.
Cell adhesion can be appreciated especially when the results are compared with non-treated gel (Figure 7.52). In fact, in procedure 1 fibroblasts have a completely round shape, thus indicating no adhesion and most likely cell death. These results also confirmed the non adhesive property of Pluronic (i.e. PEG-based) gels when no additional adhesion signals are introduced.

7.2.10.2 Endothelial cells cultured on F-127 TA-HA gels

Microscope pictures for endothelial cells cultured on 13% w/v F-127 TA-HA gels following the **procedure 1**, **procedure 2 and procedure 3** are shown in Figure 7.55, Figure 7.56 and Figure 7.57. Pictures were taken after 24 h and 96 h incubation for procedure 1 and procedure 2 and after 24 h and 48 h for procedure 3.

Procedure 1.

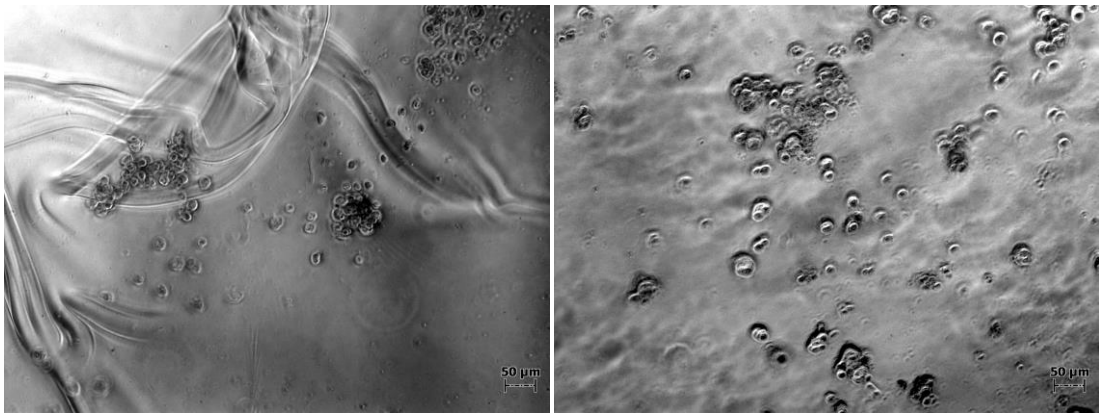

Figure 7.55 Endothelium culture following procedure 1 after 24 h (left) and after 96 h (right).

Procedure 2.

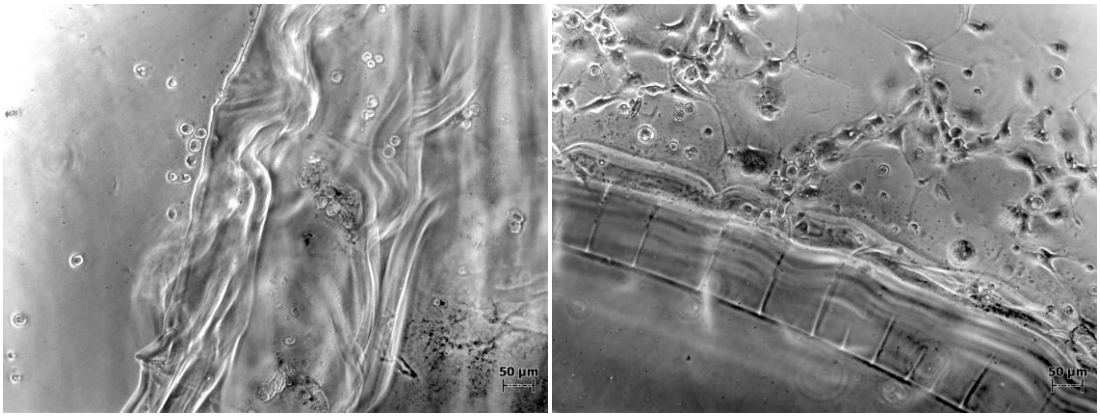

Figure 7.56 Endothelium culture following procedure 2 after 24 h (left) and after 96 h (right).

Procedure 3.

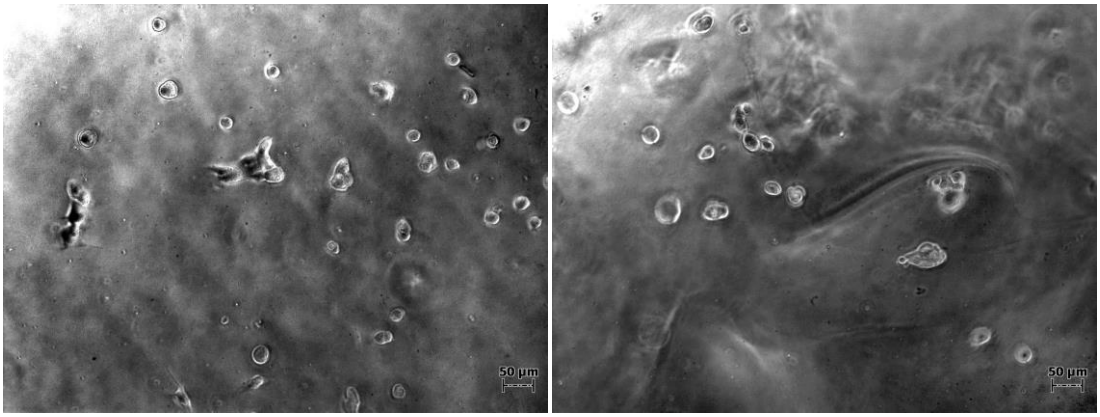

Figure 7.57 Endothelium culture following procedure 3 after 24 h (left) and after 48 h (right).

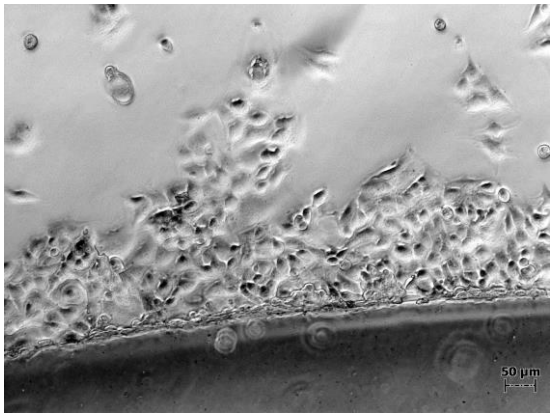

Figure 7.58 Endothelium culture after 24 h following procedure 3 interface between gel spot and well plate.

Both procedure 2 and procedure 3 did not show significant cell adhesion improvement compared with non-treated gels, probably due to less adaption capabilities of endothelium cells than fibroblasts to adhere on these gels, considering the relatively simple adhesion signalling used. Anyway, the action of RGD was clearly visible in Figure 7.58. In this case results showed an unexpected trend: it is worth to note a competitive behaviour between the cell adhesive action guaranteed by RGD chains (outer corona around the gel) and the less cell friendly environment produced by gel (see gel centre, with no cells adhered).

This may be due to possible release of cytotoxic substances from the gels, (i.e. traces of organic solvents, reactants, unreacted polymer chains etc.) which could affect cell viability (although this was not noticed with fibroblasts), or by specific unfavourable Pluronic interactions with endothelial cell surface.

7.2.10.3 Podocytes cultured on F-127 TA-HA gels

In vitro tests on podocytes, summarised in Figure 7.59, Figure 7.60 and Figure 7.61 confirmed the difficulties in culturing this type of cells on Pluronic gels, respect to fibroblasts and also endothelial cells. Pictures were taken after 24 h and 48 h incubation for both the three procedures.

Procedure 1.

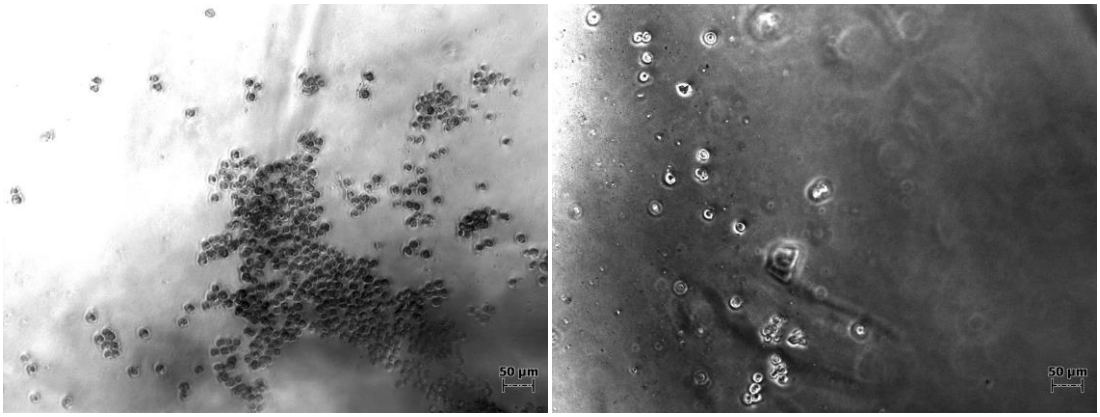

Figure 7.59 Podocyte culture following procedure 1 after 24 h (left) and after 48 h (right).

Procedure 2.

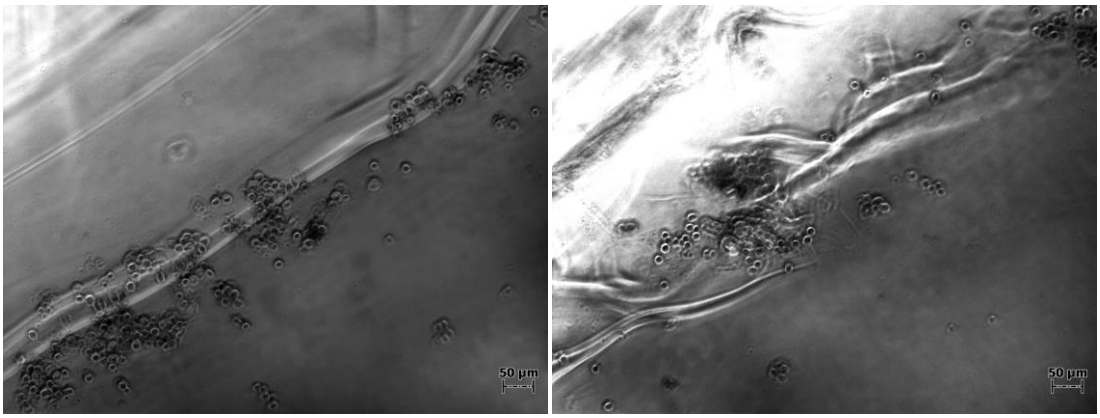

Figure 7.60 Podocyte culture following procedure 2 after 24 h (left) and after 48 h (right).

Procedure 3.

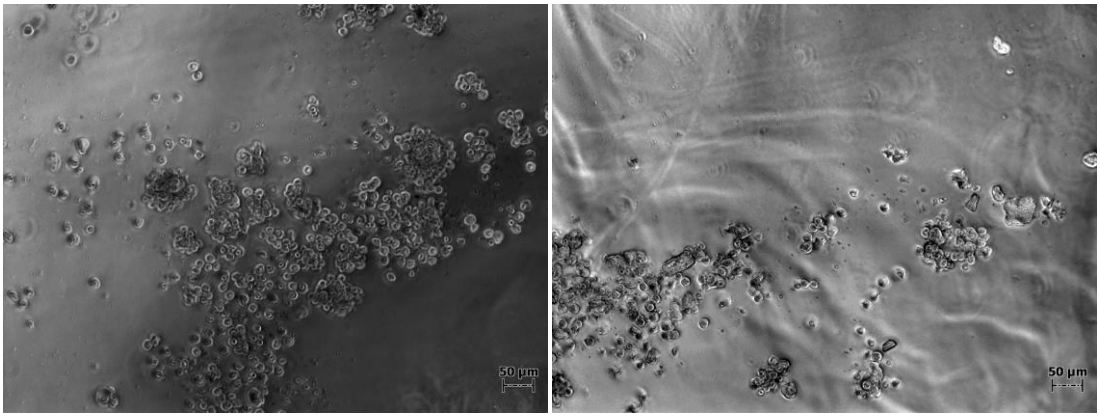

Figure 7.61 Podocyte culture following procedure 3 after 24 h (left) and after 48 h (right).

Podocyte failed to adhere to the gels surfaces for both the three procedures. This is possibly due to the particular extracellular environment that podocytes need for adhesion and proliferation. As previously mentioned, podocytes need a layer of collagen type IV in order to adhere and grow, and this specific component of extracellular matrix was not present in these studies. A more sophisticated design of the Pluronic gel properties may be required to develop specific biomaterials for podocyte culture systems.

7.3 Conclusions

The synthesis of Pluronic F-127 hexaacrylate (F-127 HA) and Pluronic F-127 thioacetate (F-127 TA) allowed to produce Pluronic hydrogels crosslinked through Michael-type addition.

The main outcomes of the synthesized Pluronic-based hydrogels are exposed below:

1. The hydrogels were obtained without using radical initiators or cytotoxic crosslinking agents, therefore a high gel biocompatibility was guaranteed.
2. Due to the well know Pluronic F-127 thermoresponsive properties, this gelation technique can be used for biomedical applications where in situ gelation is required [21,82]. The final hydrogels also present thermoresponsive properties, as suggested by swelling tests.
3. Cell adhesion to these gels was obtained in fibroblast cultures only when the materials were functionalised with RGD peptides or crosslinked in presence of serum proteins.

8 Hydrogel via radical crosslinking: Pluronic F-127 DA

There are some types of monomers that, in presence of a photoinitiator and a source of UV light, can be photopolymerized in vivo and in vitro. Photopolymerization has several advantages over other conventional polymerization techniques: a minimal heat production, fast polymerization rate and, overall, the possibility to obtain hydrogels in situ from aqueous solutions in a non invasive manner (for example using laparoscopic devices [88,89]; catheters [90] or subcutaneous injection with transdermal illumination [91]). The possibility to synthetize hydrogels in situ is very attractive because it allows to produce materials with complex shape that adhere and conform to tissue structure [92] (see Chapter 1).

It is possible to obtain crosslinked hydrogels via radical polymerization not only by photopolimerization but also using an initiator/co-initiator system, e.g. APS/TEMED pair. Acrylate functionalized monomers are common molecules to crosslink via radical polymerization.

In this chapter we report a study on gels prepared by radical polymerization of Pluronic F-127 Diacrylate (DA). The preparation of this monomer is relatively simple and the final product was characterised using NMR and IR, in order to determine monomer conversion and purity.

Radical crosslinking kinetics was determined using Dynamic Light Scattering and swelling tests were performed at various concentrations and temperature.

Finally, cell adhesion tests were carried out, in order to evaluate possible use of the gel for biomedical applications.

8.1.1 Photopolymerization

In the presence of an electron donor such as triethanolamine (TEA), which acts as a co-initiator, EOSIN Y initiates acrylate polymerization under irradiation.

The photoinitiation mechanism, described in Figure 8.1, starts with the irradiation of EOSIN dye: as a consequence EOSIN is excited to the triplet state. Subsequently an electron transfer from TEA to the excited EOSIN takes place and this generates an EOSIN radical anion and a TEA radical cation that, after a rapid proton losing, generates a α-amino radical, which is assumed to initiate free radical polymerization. The proton released from TEA radical cation regenerates the neutral EOSIN molecule [93].

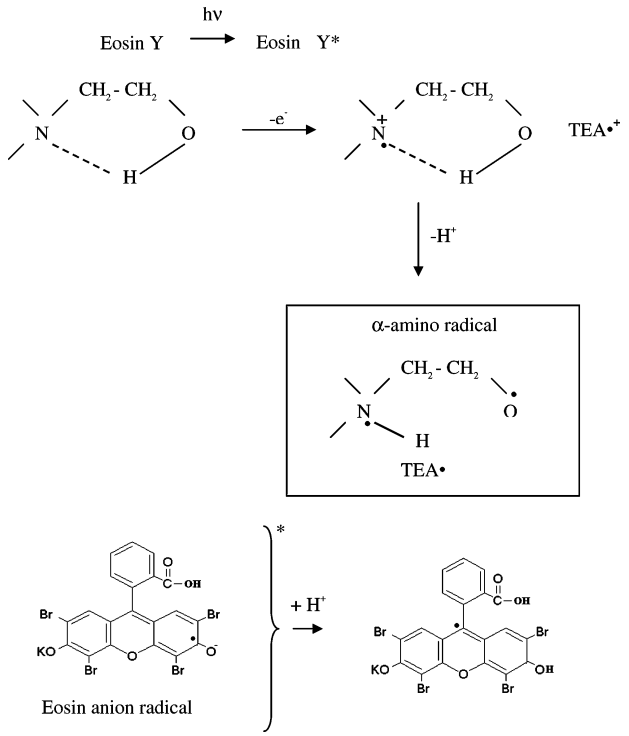

Figure 8.1 EOSIN Y/triethanolamine radical generation [94].

Differently from TEMED/APS pair, EOSIN Y/TEA photoinitiator systems are not a significant source of toxicity [95] but the use of a UV light source is necessary.

8.1.2 Polymerization mechanism via TEMED and APS

Polymerization is initiated by Ammonium Persulfate (APS) while tetramethylethyldiamine (TEMED) accelerates the formation of radicals from APS: the persulfate free radicals convert acrylate monomers in free radicals which react with inactivated monomers to start polymerization chain reaction [96].

TEMED and APS generate radicals via a REDOX pathway, as shown in Figure 8.2.

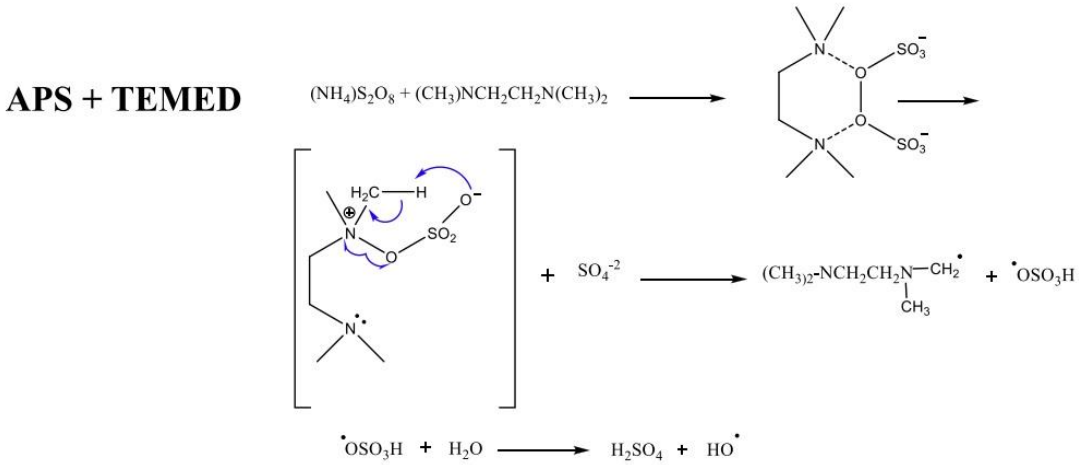

Figure 8.2 Persulfate/TEMED system radical generation [97].

Both TEMED and APS are subjected to rapid oxidation and are very igroscopic. All the compounds that serve as a free radical trap inhibit the reaction: oxygen is such an inhibitor, and it is a good practice to proper degas gel solution prior to start polymerization.

An important limitation in the use of TEMED and APS is their toxicity for cells: gels crosslinked using these compounds need a careful washing prior to depose cells [98]. Anyway gels crosslinked via TEMED and APS are easier to obtain and do not need the use of a UV lamp, with evident practical advantages. Since both photopolymerization and TEMED\APS system are radical polymerizations, they are supposed to polymerize Pluronic acrylate through a free radical mechanism, which ends up with very similar gel properties, particularly in terms of composition and crosslinking density. We therefore focused our investigation on gels prepared via TEMED\APS, taking into account that this approach does not require additional devices such as light sources and optical fibers.

8.2 Experimental Part

Synthesis of the precursor

Pluronic F-127 DA was characterized using an 400 MHz Bruker ^{1}H NMR spectrometer and a Thermo Scientific Nicolet iS50 FT-IR spectrometer in ATR mode. GPC was performed in tetrahydrofuran on a Jasco GPC System at 35°C and $\overline{M_n}$ were obtained using a standard calibration with Polysterene standards. DLS measures were performed on a Malvern Zetasizer Nano ZS.

8.2.1 Synthesis of Pluronic F-127 Diacrylate (F-127 DA)

Materials. Pluronic F-127 (MW=12600, 70% PEG), acryloyl chloride (purity: 97%, contains <210ppm MEHQ as stabilizer), triethylamine (purity ≥99%), sodium chloride, sodium sulphate and toluene were purchased from Sigma-Aldrich (composition for organic compounds confirmed by ^{1}H NMR Spectroscopy) and used as received.

Synthesis. 10 g of Pluronic F-127 (0,793 mmol, 1.587 meq of –OH groups) were dissolved in 150 mL of toluene under nitrogen atmosphere and dried by refluxing toluene through a Soxhlet extractor filled with 4 Å molecular sieves. After 3 h the solution was cooled to room temperature and then immersed in an ice bath. In the reactor 0.66 mL of TEA (4.76 mmol, 2 mol per mol of acryloyl chloride) were introduced using a 1 mL syringe while 0.193 mL of acryloyl chloride (2.38 mmol, 1.5 equiv. per –OH group) diluted in 10 mL of toluene were dropped using a dropping funnel.

The dropping funnel was washed with additional 10 mL of toluene, and the mixture was stirred overnight.

In order to purify F-127 DA the precipitated triethylammonium hydrochloride was filtered away using Buchner filter and the solvent evaporated at the rotary evaporator. The resulting viscous oil was dissolved in 200 mL of DCM and washed two times with 30 mL of water saturated with sodium chloride. The solution was dried with sodium sulphate, filtered, the solvent evaporated and then precipitated two times in cold diethyl ether [54]**.** Conversion = 100% (from ^{1}H NMR data). Yield = 80%.

^{1}H NMR ($CdCl_3$): δ=1.1 (m, 206H,PPG C**H_3**=69 monomeric units), 3.4 (m, 68H, PPG C**H**=68 monomeric units), 3.5 (m, 131H, PPG C**H_2**=66 monomeric units), 3.65 (m, 924H, PEG C**H_2**=231 monomeric units), 4.3 (t, 2H, –CH_2C**H_2**–O–CO–CH=CH_2), 5.8 (dd, 2H, CH_2=C**H**–COO–), 6.15 and 6.4 ppm (both dd, 2H, C**H_2**=CH–COO).
FT-IR (film on ATR plate): 2990–2790 (ν C-H), 1724 (ν C=O), 1467 (δ_s CH_2), 1342, 1279, 1242, 1097 (ν_{as} C-O-C), 962, 841 (ν_s C-O-C) cm^{-1}.

8.2.2 Preparation of Gelling Solutions and gel formation

The appropriate quantity of F-127 DA was dissolved in the adequate volume of PBS 10 mM (PH=7.4) to obtain the desired final concentration (10%-30% w/v) of polymer, and the mixture was left in an ice bath for 30 minutes until complete dissolution. Then 0.94 μL of APS and 0.21 μL of TEMED were added to the cold polymer solution and transferred in a 48-well plate (180 μL for each well). After 30 minutes the gel crosslinking was completed, as monitored by crosslinking kinetics (see Chapter 8.3.4).

Physico-chemical characterisation

8.2.3 Phase diagram

Various concentrations of F-127 DA gelling solutions (15%-40% w/v) were prepared as described above. LCST was evaluated via an "inverted tube test". Temperature was varied by incubating the gel vials in a thermostatically-controlled water bath.

8.2.4 Crosslinking kinetics

10% w/v and 20% w/v F-127 DA solutions were prepared as described above. Then 500 μL of F-127 DA and 500 μL of commercial 40 nm gold nanoparticles (Sigma-Aldrich, stabilized suspension in 0.1 mM PBS, reactant free) were dispersed together and transferred in a DLS cuvette. The kinetics crosslinking was studied evaluating the increase of the dispersion viscosity, by measuring the apparent size variation of the nanoparticles, using the Stokes-Einstein equation as reported in Chapter 7.2.7. For each gelling solution concentration (10% and 20% w/v) a series of size measurements (every 150 s) were performed at 15, 20 and 25 °C (for more details see Results and discussions section)

8.2.5 Swelling measurements

F-127 DA gelling solutions at different concentration (10%, 20% and 30% w/v) were prepared as described above and transferred in the moulds shown in Figure 7.5. Once the gels were crosslinked, they were weighted and transferred in a 6-well plate filled with PBS 10mM (PH=7.4).

The swelling degree was defined as $\%\, degree\ of\ swelling = \frac{\Delta w}{w_0}$, where w_0 is the initial gel weight and $\Delta w = w - w_0$. The $\%\, degree\ of\ swelling$ was measured at fridge temperature (4°C), room temperature (about 25 °C) and physiological temperature (37°C). Three different samples were tested at each temperature to obtain mean values and standard deviations. The weight measurements of the swollen gels were carried out after removing the excess of water, which was often present around the gel surface, with blotting paper.

Biological tests

8.2.6 Cell culture

Materials. RGD (synthetic peptide, sequence GRGDSPC, MW=690.74, purity 96.15% purchased by CASLO), P.S. (antibiotic solution, see Chapter 6.7 for further details).

Procedure 1. 15% w/v gel solution was prepared as described above and transferred in 48-well plate. Cells were deposed using gels with no further treatments.

Procedure 2. 15% w/v gel solution was prepared as described above and transferred in 48-well plate. After crosslinking, 300 μL of medium were added to each well. The well-plate with the medium was left in incubation for 24 h then the medium was removed and each well-plate was washed six times with 300 μL of sterile PBS 10 mM (10 minutes each) in order to remove both TEMED and APS completely. Cells (8000 cells/well) were cultured in this environment.

Procedure 3. 0.108 g of F-127 DA was dissolved in 677 μL of sterile PBS + P.S. and 42.5 μL of 20 mg/mL RGD stock solution were added. The mixture was stirred overnight, after which 1.60 μL of APS and 0.55 μL of TEMED were added and 180 μL of gelling solution were transferred in each well of a 48-well plate. After crosslinking (1 h) wells were washed as described above. Cells (8000 cells/well) were cultured in this environment.

8.3 Results and Discussions

Synthesis of the precursor

8.3.1 Synthesis of Pluronic F-127 Diacrylate (F-127 DA)

The reaction mechanism is the same already seen in the acrylation of Tetronic 701 and it is reassumed in Figure 8.3.

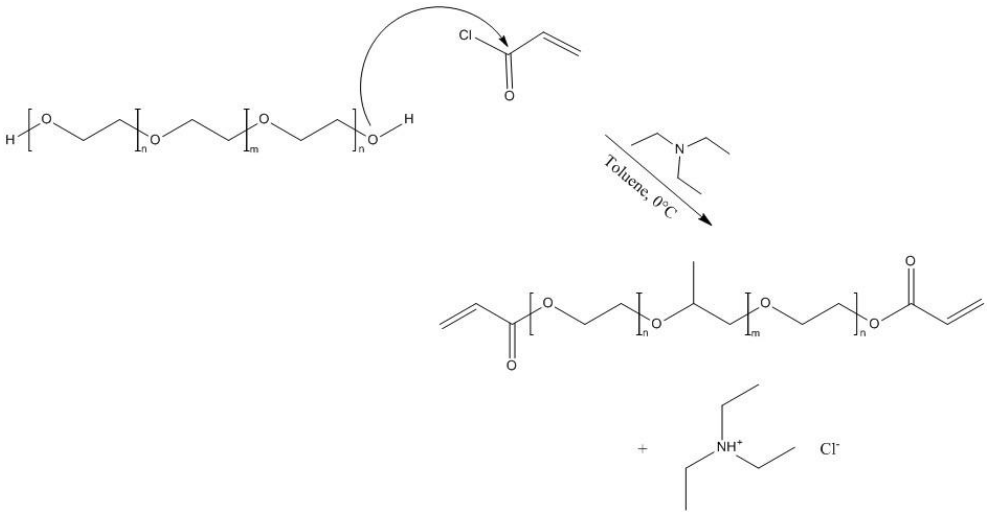

Figure 8.3 Pluronic F-127 DA synthesis.

Briefly, –OH groups in the Pluronic F-127 chains attacks acryloyl chloride leading to F-127 DA and hydrogen chloride. Triethylamine, commonly used as a base in organic synthesis, remove hydrogen chloride, producing salt trietrylamine hydrochloride (or triethylammonium hydrochloride) and allowing reaction to proceed as quantitative.

^{1}H NMR and IR spectra are shown in Figure 8.5, Figure 8.6 and Figure 8.7.

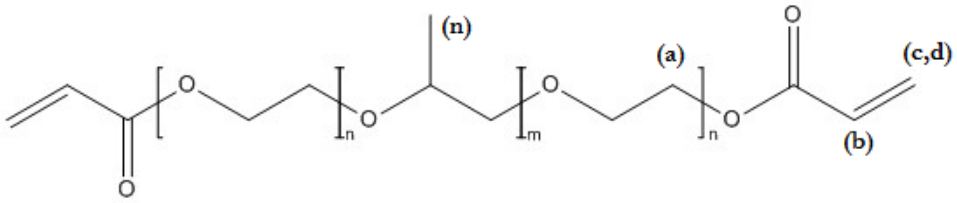

Figure 8.4 F-127 DA structure with ^{1}H NMR peaks identification.

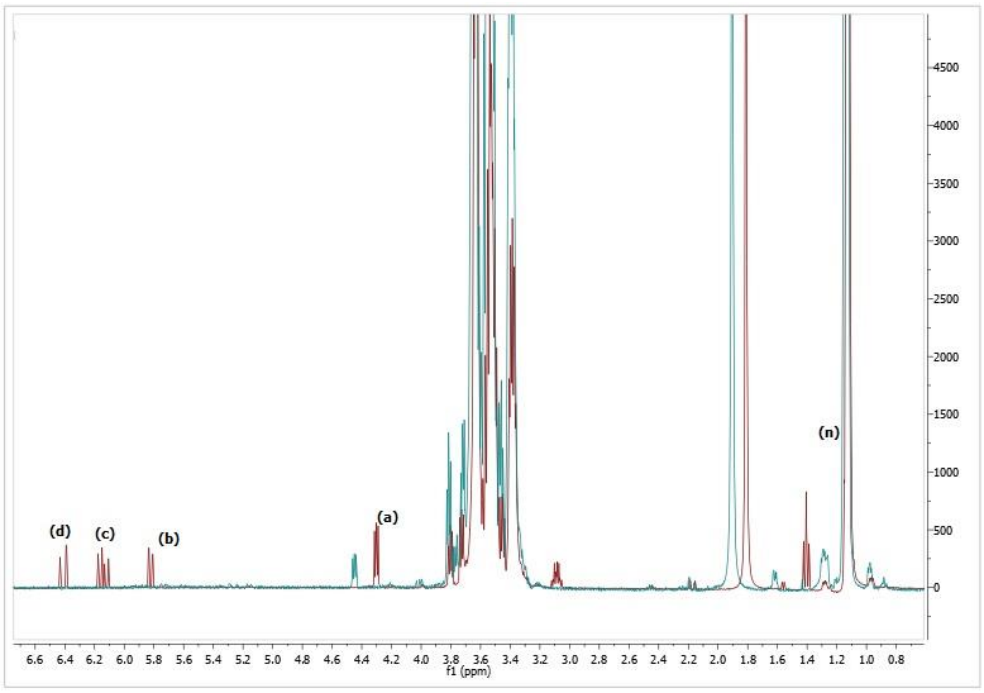

Figure 8.5 F-127 DA (red line) ^{1}H NMR vs. pure F-127 (blue line).

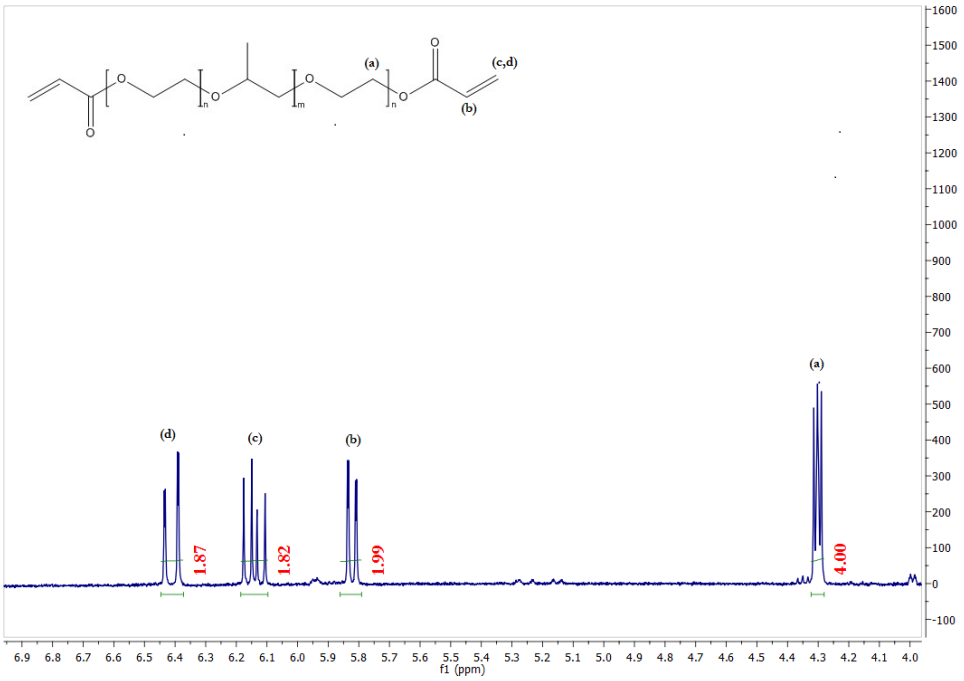

Figure 8.6 F-127 DA ^{1}H NMR; magnified view of the NMR spectrum within the region 4.0<δ<6.9

^{1}H NMR ($CDCl_3$): δ=1.1 (m, 206H, PPG C**H**$_3$=69 monomeric units), 3.4 (m, 68H, PPG C**H**=68 monomeric units), 3.5 (m, 131H, PPG C**H**$_2$=66 monomeric units), 3.65 (m, 924H, PEG C**H**$_2$=231 monomeric units), 4.3 (t, 2H, –CH_2C**H**$_2$–O–CO–CH=CH_2), 5.8 (dd, 2H, CH_2=C**H**–COO–), 6.15 and 6.4 ppm (both dd, 2H, C**H**$_2$=CH–COO).

The peaks integrals were normalised with respect to the first peak at δ=1.1 (m, 206H, PPG C**H**$_3$ = 69 monomeric units).

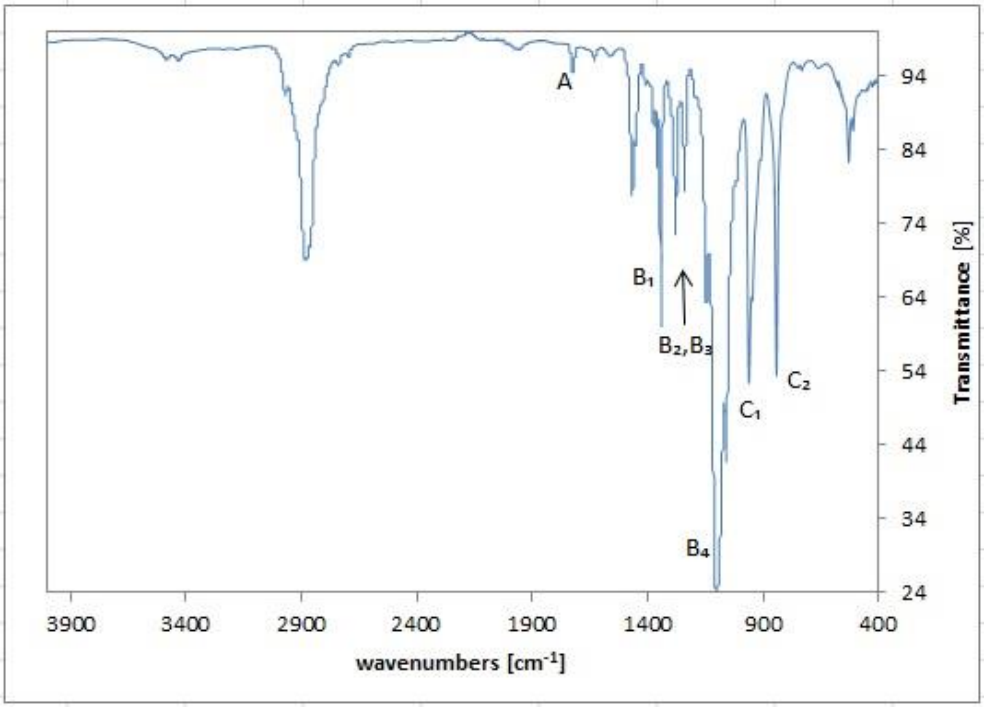

Figure 8.7 F-127 DA FT-IR.

FT-IR (film on ATR plate): 2990-2790 (ν C-H), A: 1724 (ν C=O), 1467 (δ_s CH_2), B_1-B_4: 1342, 1279, 1242, 1097 (ν_{as} C-O-C), C_1-C_2: 962, 841 (ν_s C-O-C) cm^{-1}.

The IR-spectrum reported in Figure 8.7 confirmed the functionalization of F-127 DA in agreement with data reported in literature [54].

8.3.2 Gel Permeation Chromatography (GPC) of F-127 DA

The F-127 DA was analysed by GPC in THF and its chromatogram is shown in Figure 8.8

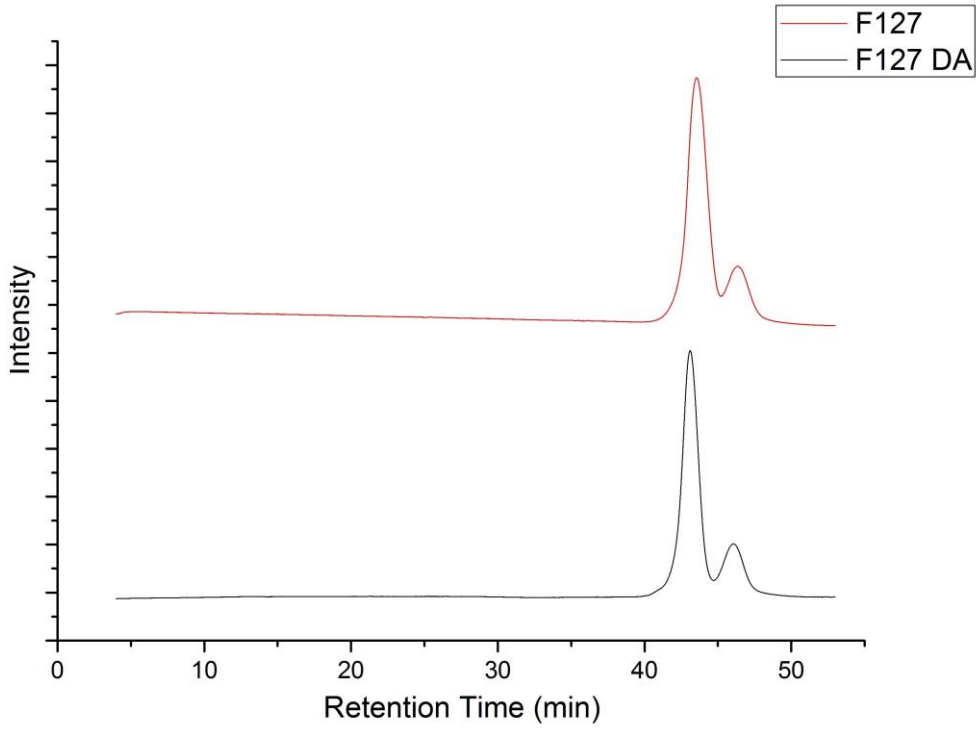

Figure 8.8 F-127 DA (black line) and pure F-127 (red line) GPC chromatograms.

By integrating the whole F-127 DA chromatogram we evaluated the following values for $\overline{M_n}$, $\overline{M_w}$, and the polydispersity index, PDI (Table 8.1)

Table 8.1 $\overline{M_n}$, $\overline{M_w}$, PDI values for F-127 DA.

$\overline{M_n}$	$\overline{M_w}$	PDI
15040	17713	1.18

The Expected F-127 DA $\overline{M_n}$, using 13240 for non-functionalized F-127 (see Chapter 1.1.1) and adding the molecular weight of the acrylate groups is 13421.

In order to explain the difference between the expected and evaluated $\overline{M_n}$ in F-127 DA, we decomposed the peaks in F-127 DA and non-functionalized F-127 chromatograms using the *Multiple Peak Fit* functions in *Origin 9.1* software, following the same procedure reported in 1.1.1.

The used algorithm was a Non-Linear curve fitting, where the fitting curve was assume to be a sum of gaussian curves (one for each peak). The *Gaussian* equation representing a single peak is reported below:

$$y = y_0 + \frac{A}{w \cdot \sqrt{\frac{\pi}{2}}} \cdot e^{-\frac{2(x-x_0)^2}{w^2}}$$

Where: y_0: baseline offset

A: total area under the curve from the baseline

x_0: center of the peak

w: equal to 2 times "sigma", approximately 0.849 the width of the peak at half height

The centre x_0 represents the "mean", while $w/2$ is the standard deviation.

The fitting parameters and resulting curve for F-127 DA are reported, respectively, in Table 8.2 and Figure 8.9 while the results for non-functionalized F-127 are reported in Chapter 1.1.1.

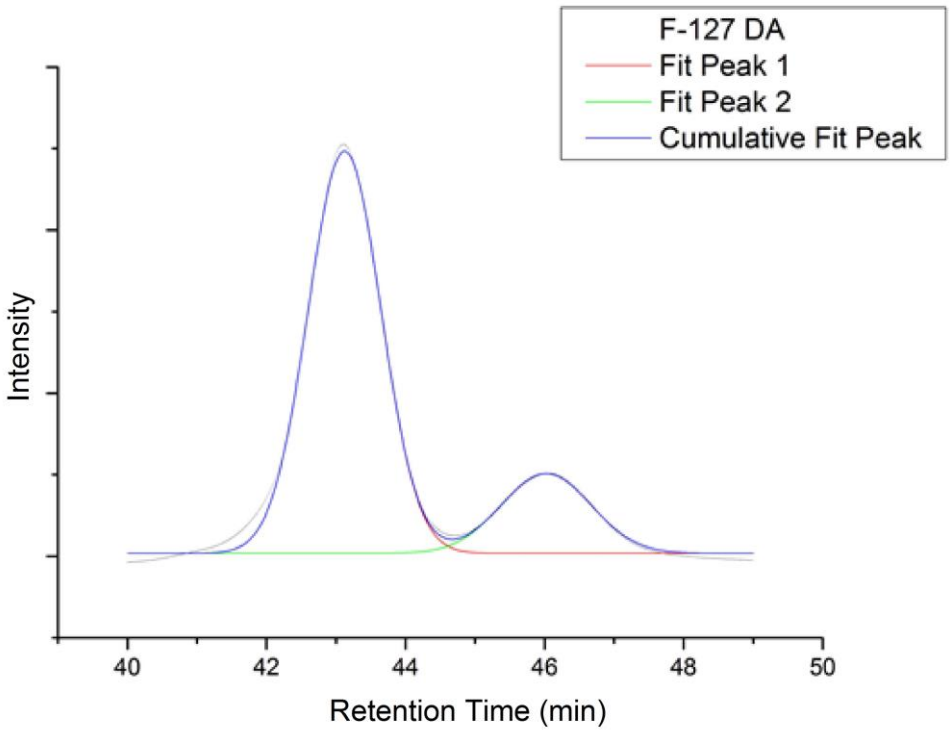

Figure 8.9 Peaks decomposition of F-127 DA GPC chromatogram.

Table 8.2 Evaluated model parameters for peaks decomposition of F-127 DA GPC chromatogram.

	Peak 1		Peak 2	
Model Parameter	*Value*	*Standard Error*	*Value*	*Standard Error*
y_0	241.1	55.6	241.1	55.6
x_0	43.1	0.01	46.2	0.07
A	32226.0	713.5	7728.3	791.4
w	1.2	0.03	1.5	0.17

As evident in Figure 8.9, especially the cumulative fit peak curve, the chromatogram is well fitted by the evaluated peaks.

The average molecular weights and PDI were therefore calculated for each peak after their deconvolution, assuming a *gaussian* distribution with the fitting parameters previously calculated.

The non-functionalized F-127, reported in previous chapter, reveals the presence of an high Mw specie and a low Mw specie, as evident by the $\overline{M_n}$ and $\overline{M_w}$ evaluated for the two peaks (Table 7.4).

Regarding F-127 DA we have identified two different species too as summarised in Table 8.3.

Table 8.3 $\overline{M_n}$, $\overline{M_w}$, **PDI** values for the two peaks of F-127 DA.

	Peak 1	Peak 2
$\overline{M_n}$	19216	7735
$\overline{M_w}$	19831	8281
PDI	1.03	1.07

The difference between results and expected values for the individual peaks is probably due to discrepancies with the GPC calibration, due to the recent replacement of the Jasco GPC system in our lab.

Physico-chemical characterisation

8.3.3 Phase Diagram

In the following figure, phase diagrams for both F-127 and F-127 DA are reported.

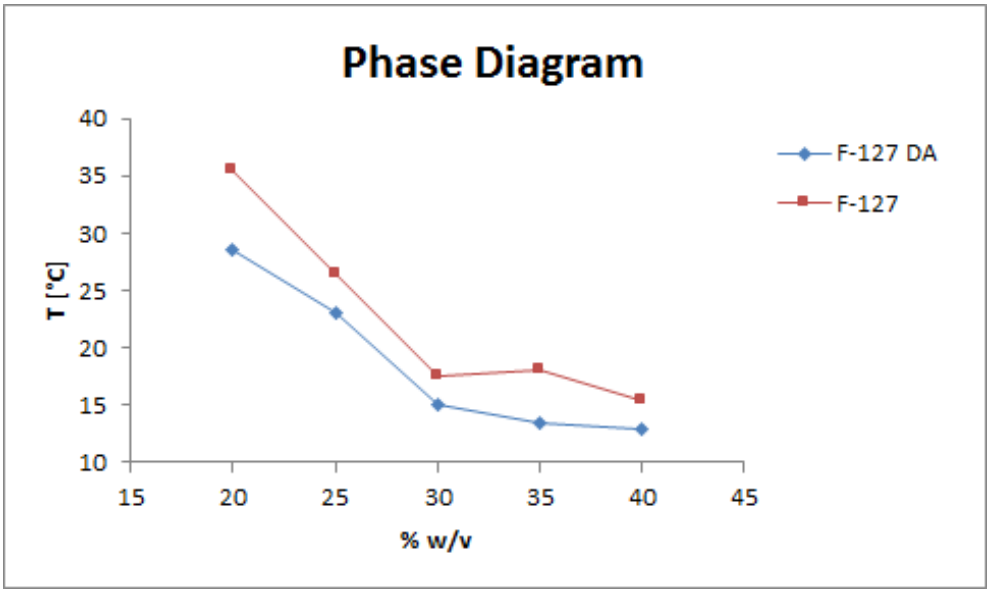

Figure 8.10 Phase diagrams for F-127 (red line) and F-127 DA (blue line).

Comparing the two graphs it is worth to note that the functionalization of F-127 does not significantly change the LCST.

8.3.4 Crosslinking kinetics

The kinetics of radical crosslinking was studied with Dynamic Light Scattering, as seen in Chapter 7.2.7, evaluating the increase in apparent viscosity due to crosslinking by measuring the size variation of commercial 40 nm gold nanoparticles using the Stokes-Einstein equation.

Results are shown in Figure 8.11 and Figure 8.12:

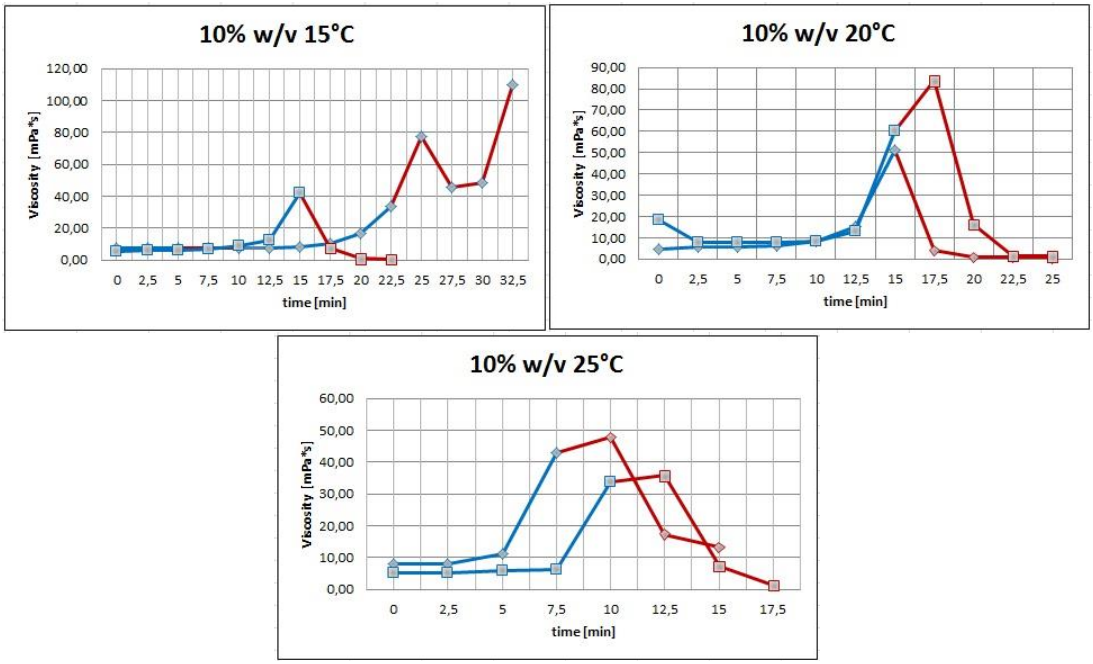

Figure 8.11 Recorded viscosity vs. reaction time for 10% w/v gelling solution at 15°C (top, left), 20°C (top, right) and 25°C (bottom, centre).

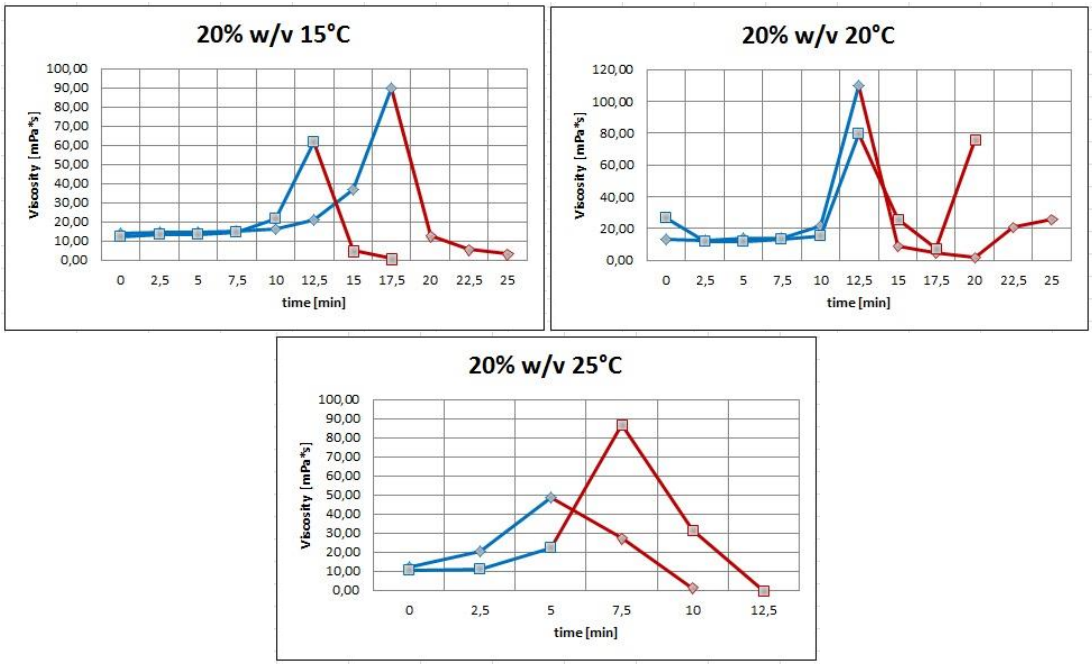

Figure 8.12 Recorded viscosity vs. reaction time for 20% w/v gelling solution at 15°C (top, left), 20°C (top, right) and 25°C (bottom, centre).

In the graphs above the two lines represent the two different measures performed on the same formulation and experimental conditions: blue segments represent reasonable viscosity values beside red segments represent viscosity values calculated by the Zetasizer software from poor quality autocorrelation function as an effect of the sol-gel transition around the gel point, which makes the calculations of the apparent NP size in viscoelastic material unfeasible as reported in Figure 7.43 and Figure 7.44 in previous chapter.

In order to attempt a numerical evaluation of the time needed to reach a gel point, we extrapolated a gel time, $t_{gel,}$ defined as the average value of the crossing point between the line passing through the last two viscosity values of each measure (taking into account the blue segments only), and the baseline passing from the first measured viscosity value as reported in Figure 8.13

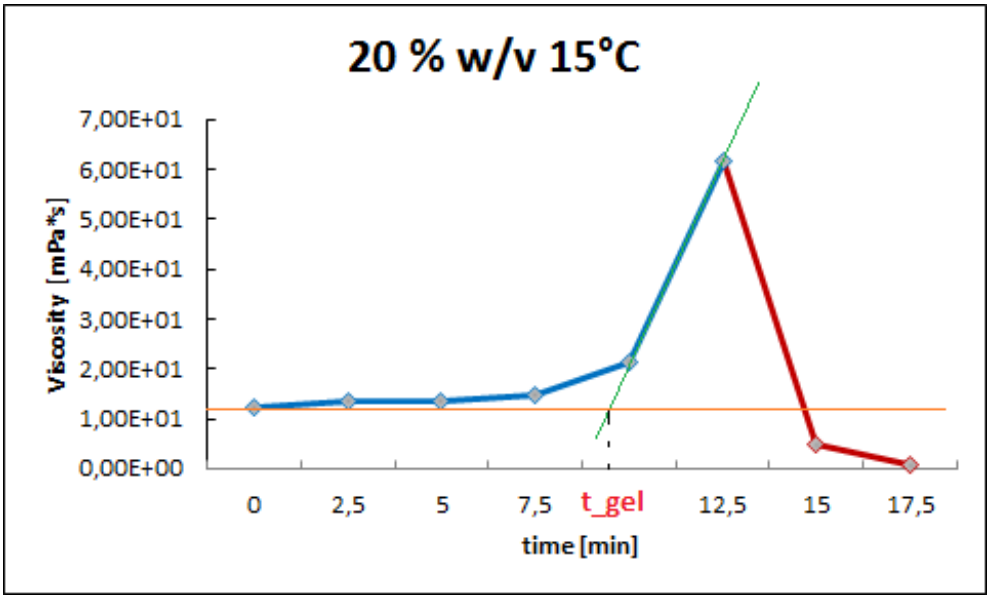

Figure 8.13 Calculation of t_{gel}.

The $t_{gel,}$ points obtained for crosslinking reactions at 25°C were relatively uncertain, due to the faster kinetics which made the t_{gel} extrapolation unfeasible. In this case it was chosen to define the t_{gel} as the average value between the last two experimental points of the blue line (corresponding to the reasonable viscosity values).

The evaluated t_{gel} are reported in the following table:

Table 8.4 t_{gel} for F-127 DA 10% w/v.

T [°C]	t_{gel} [min]
15°C	15
20°C	12
25°C	7.5

Table 8.5 t_{gel} for F-127 DA 10% w/v.

T [°C]	t_{gel} [min]
15°C	12
20°C	10
25°C	5

It is worth to note that crosslinking became faster with temperature and that reproducibility of measures decrease at low temperature, along with viscosity values.

8.3.5 Swelling measurements

Results of swelling measures are summarised in Figure 8.14 and Figure 8.15 as reported hereafter:

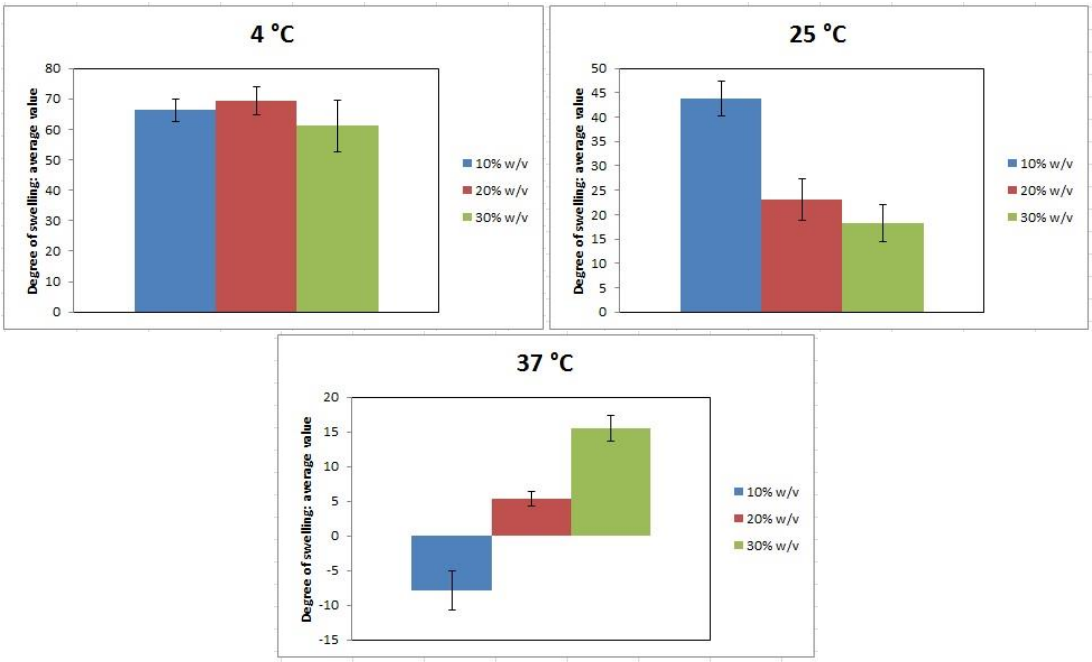

Figure 8.14 Degree of swelling for 10, 20, 30% w/v gel concentration at 4°C (top, left), 25°C (top, right) and 37°C (bottom, centre).

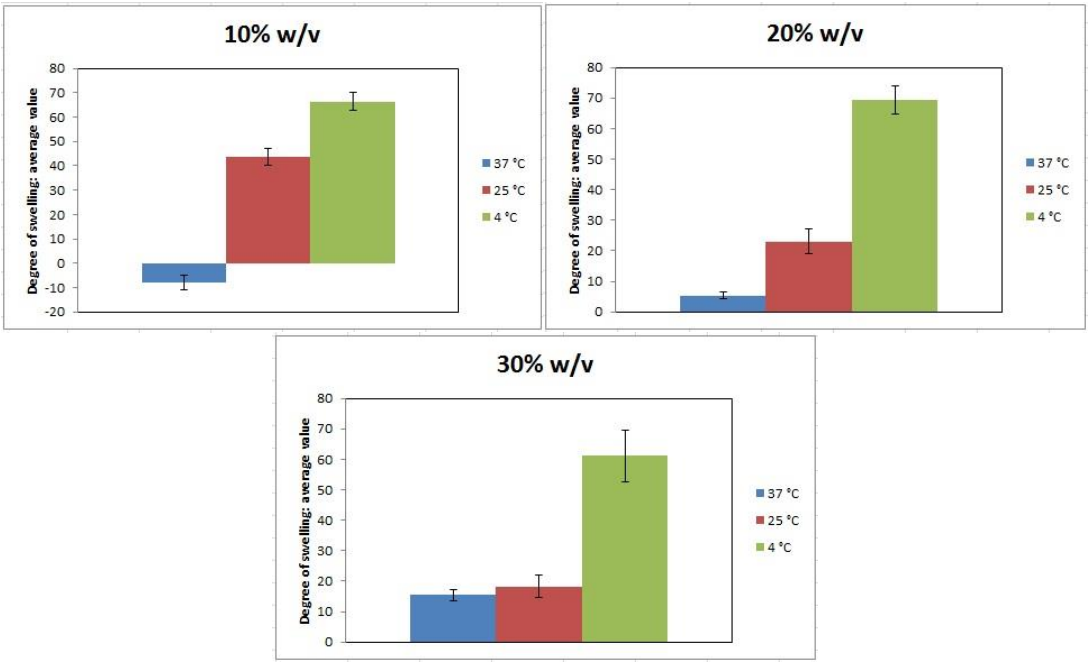

Figure 8.15 Degree of swelling at 4, 25, 30 °C for 10% w/v gel concentration (top, left), 20% w/v gel concentration (top, right) and 30% w/v gel concentration (bottom, centre).

In Figure 8.14 (top, left), we can observe that the swelling degree was almost the same for the three different concentrations: at this temperature we do not have the effects of LCST but it is hard to predict the effect of crosslinking density on Pluronic gels at different concentrations. In fact by increasing concentration we do not only increase crosslinking but, probably, termination reactions too. The trend may reflect this competitive behaviour.

Figure 8.14 (top, right) shows the effects of LCST: we can observe that swelling degree decreased with concentration due to the increase of hydrophobic interactions.

In Figure 8.14 (bottom) it is interesting to note the shrinkage of the 10% w/v sample at temperatures above LCST.

As shown in Figure 8.15 this shrinkage is less pronounced for higher polymer concentrations, and this behaviour is probably due to a concurrent effect of the increase of osmotic pressure at higher polymer concentrations, which tends to increase swelling.

Biological tests

8.3.6 Cell culture

The first set was performed using non-treated gels (**procedure 1**), i.e. gels with no RGD peptide grafted nor serum proteins entangled with the polymer network, where we expected to have no adhesion due to protein repellent properties of PEG, which is the main constituent of Pluronic F-127. Then, experiments were carried out with pre-treated gels with culture medium, thus containing serum proteins (**procedure 2**) and with gels functionalized with the cell adhesive RGD peptide (**procedure 3**), in order to assess the effect of gel functionalization over cell adhesion and response. The RGD peptide (sequence GRGDSPC) was easily linked to the hydrogel thanks to the presence of the end –SH group (Figure 5.3). Thus, a Michael-type addition reaction occurred between –SH group of the peptide and free acrylate groups of F-127 DA. It was chosen to assure an RGD molar concentration corresponding to the 10% of the molar concentration of acrylate groups, that is, the same already used for F-127 TA-HA gel.

Two types of cells, i.e. fibroblasts and endothelial cells were tested to investigate their different behaviour, in terms of adhesion and growth. In fact, the use of cells that respond in different ways to an external environment could represent a good model for the assessment of the biocompatibility of our gels. Differently from F-127 TA-HA reported in the previous chapter it was chosen to not test podocyte cells, considering the difficulty already encountered in the culture of endothelial cells.

8.3.6.1 Fibroblast cultured on F-127 DA gels

Figure 8.16**,** Figure 8.17 and Figure 8.18 represent microscope pictures of 3T3 fibroblasts cultured according to the **procedure 1**, **procedure 2** and **procedure 3** described in Materials and methods section. Pictures were taken after 24 h and 96 h of incubation.

Procedure 1.

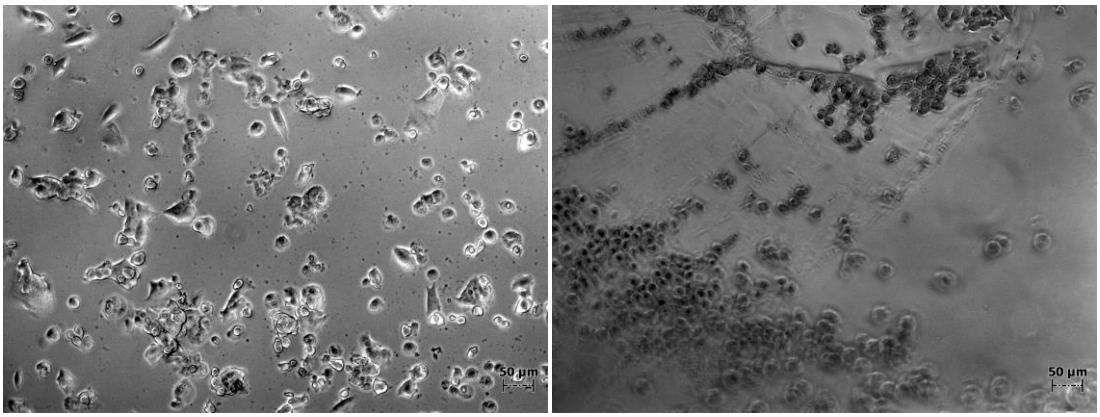

Figure 8.16 Fibroblast culture following procedure 1 after 24 h (left) and after 96 h (right).

Procedure 2.

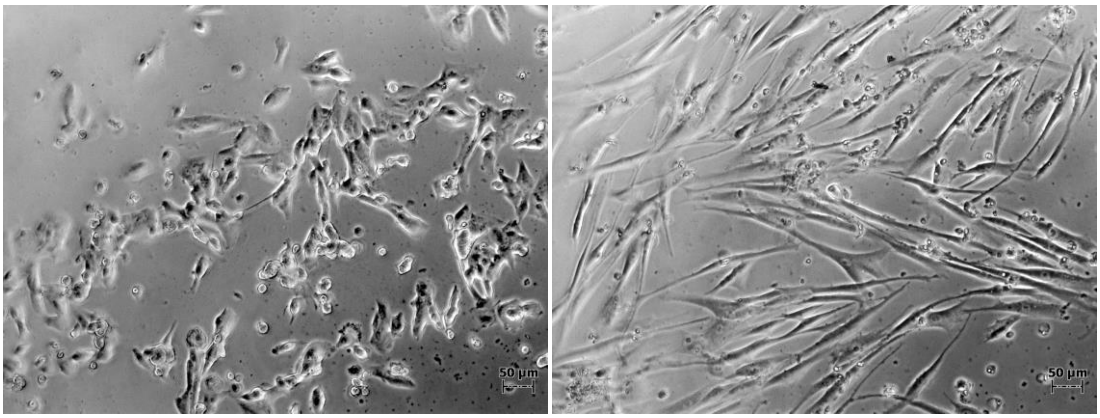

Figure 8.17 Fibroblast culture following procedure 2 after 24 h (left) and after 96 h(right).

Procedure 3.

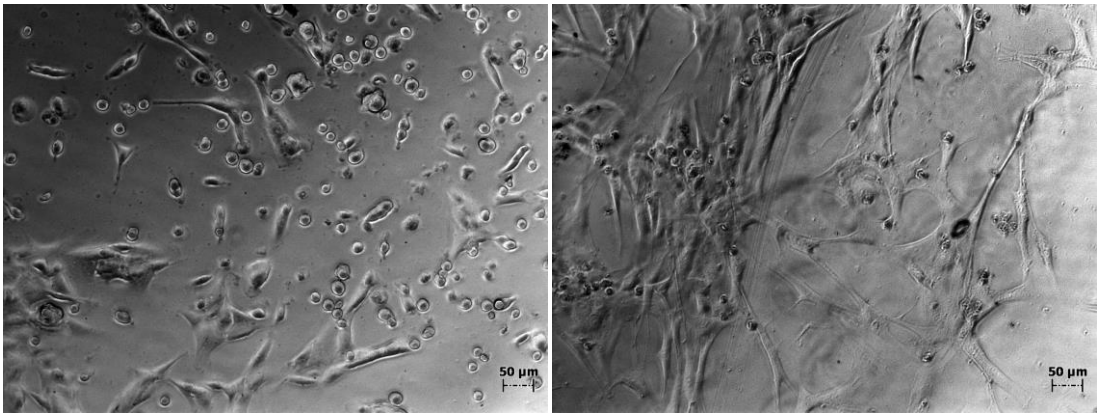

Figure 8.18 Fibroblast culture following procedure 3 after 24 h (left)and after 96 h (right).

We can observe that in both procedure 2 and procedure 3 good cell adhesion results are achieved, while partial adhesion was observed in procedure 1 after 24 h (not confirmed after 96 h).

Results reported for procedure 2 suggested that serum proteins presented during the crosslinking reaction may have been embedded in the final gel and in some way displaced at the gel surface. Since several serum proteins contain integrin binding domains, this facilitate cell adhesion.

The good results obtained following the procedure 3 confirm the adhesive action of RGD-functionalized gels. Differently from F-127 TA-HA, the F-127 DA was functionalized with the RGD peptide before the gels crosslinking.

Cell adhesion can be appreciated especially when the results are compared with non-treated gel (procedure 1) where only a partial adhesion was observed.

8.3.6.2 Endothelium cultured on F-127 DA gels

Differently from the results obtained with fibroblast, gels treated both with RGD or culture medium did not show a significant improvement in the adhesive capabilities, as shown in the following Figure 8.19 and Figure 8.20:

Procedure 1.

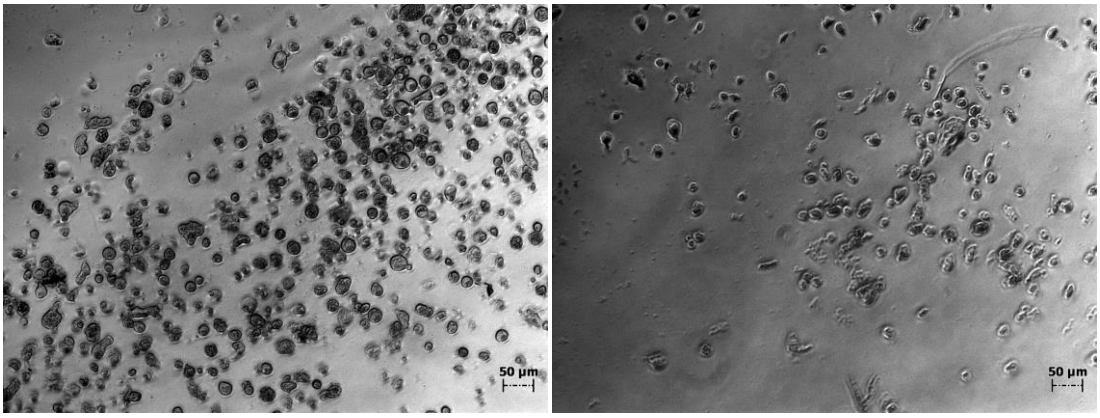

Figure 8.19 Endothelium culture following procedure 1 after 24 h (left) and 96 h (right).

Procedure 2.

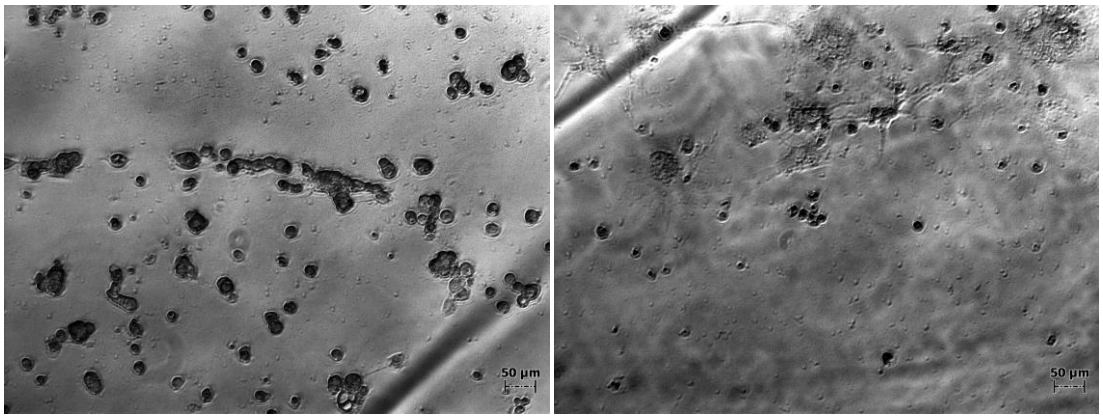

Figure 8.20 Endothelium culture following procedure 2 after 24 h (left) and 96 h (right).

Due to the limited availability of The RGD peptide, the adhesion of endothelial cells on RGD-functionalized gels were not carried out in this case. Future work has been scheduled to evaluate the behavior of endothelial cells with this specific type of gel.

8.4 Conclusions

Several applications in tissue engineering require thermosensitive hydrogels with high biocompatibility, particularly when in situ gelation is required. Pluronic F-127 with acrylate functional end groups has shown to retain its LCST behaviour and to crosslink by radical polymerization. It was also demonstrated a good biological behaviour with high adaptable cells, i.e. fibroblast. The main advantages of this Pluronic-based hydrogels over other polymeric biomaterials are summarized here:

1. Easy and rapid synthesis of the functional polymeric precursor.
2. Presence of only one monomer precursor; no additional crosslinking molecules are needed.
3. Gels are crosslinked rapidly and in an easy manner by free radical polymerisation This is considered an advantage since materials obtained by photopolymerization are usually accepted for in vivo tests and in clinic.
4. A relatively low gel swelling degree, which is due to the thermosensitive properties of the gels, guarantee a minimal stress for cells in vitro and in vivo. Pluronic gels are *protein repellent* and this material is useful when cell adhesion and/or protein adsorption is unwanted.

Conclusions and Future Work

Pluronic F-127-based hydrogels were synthetized via both radical and Michael-type addition crosslinking. Gels were physically and chemically characterised and cell-adhesive properties were investigated. The results discussed in the previous chapters has shown advantages and disadvantages for both formulations in terms of preparation of the polymeric precursors, gel formation, physical properties and cellular adhesion. The biological tests revealed good cell adhesion for high adaptable cells (i.e. fibroblasts), while a limited or null adhesion was recorded for endothelial cells and podocytes.

These results could be explained considering, together with the less adaptability of endothelial cells and fibroblasts, the high concentration of the polymer in the gels and the presence of a hydrophobic PPG block in F-127 which could strongly interact with the lipid bilayer of the cell membrane and interfere with cellular activity.

In order to reduce Pluronic concentration in these gels it was thought to design a new colloidal gel constituted of a network of gelatin nanoparticles, coated with functional Pluronic F-127. In this way the total F-127 concentration in the gel would be dramatically reduced, while gelatin acts as highly biocompatible *spacer* among crosslinks.

Gelatin is a natural occurring polymer, with low antigenicity, obtained by the hydrolysis of collagen. Two kinds of gelatin with different isoelectric points, called gelatin type A and B, (IEP) are produced, respectively, via acid or basic hydrolysis. Gelatin is particularly rich in three amino acids: glycine, proline and alanine [99].

Gelatin NPs can be easily prepared both by desolvation and nanoprecipitation methods [100].

The crosslinking between NPs and F-127 could be assured exploiting the amine groups on the protein that build up gelatin: for example by conjugating these amine groups with

a functionalized F-127 Aldehyde (F-127 ALD) [101] that can be synthesized using a Dess-Martin reagent [102].

In order to prove the availability of this strategy, gelatin NPs were synthetized via a two-step desolvation method and characterised with DLS measurements.The following results (size distribution and Zeta potential) were obtained:

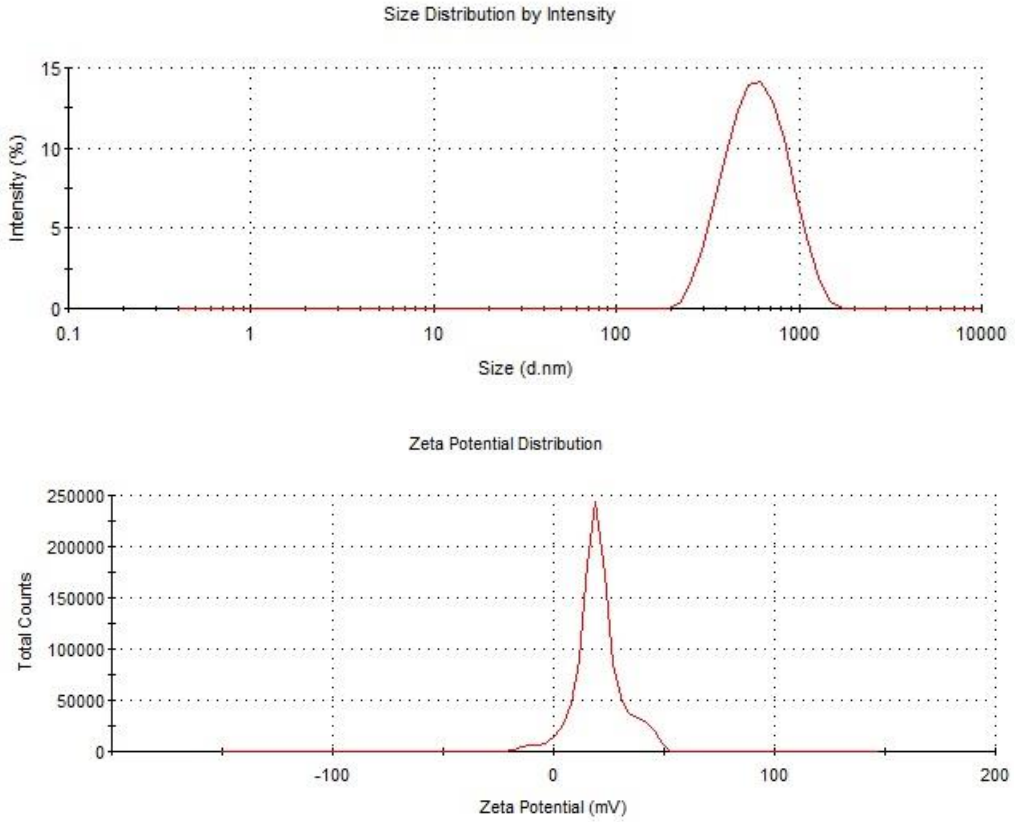

Figure 1 Size distribution (top) and Zeta potential distribution(bottom) of gelatin nanoparticles (Type A) obtained by Dynamic Light Scattering (Z-sizer).

The next step of this work will focus on the synthesis of F-127 ALD and the study of the physico-chemical behaviour of the Pluronic in the NPs suspension.

In order to enhance biocompatibility and, above all, biodegradability of the gel, we also speculated about the possibility of substituting the PPG block in the polymeric precursors with biocompatible polyesters, i.e. using PEG-polyester-PEG block copolymers rather than Pluronics.

For example the family of block copolymers comprising poly(ethylene glycol)-poly(lactic acid)-poly(ethylene glycole) (PEG-PLA-PEG) is widely used: PLA, compared to PPG , is non-toxic, biodegradable and biocompatible [103]. Another possibility is to use a PEG-PCL-PEG sequence, where poly(ε-caprolactone) (PCL) is another biocompatible polymer already approved for clinical use [104].

Bibliography

[1] I. Armentano, M. Dottori, E. Fortunati, S. Mattioli, and J. M. Kenny, "Biodegradable polymer matrix nanocomposites for tissue engineering: A review," Polym. Degrad. Stab., vol. 95, no. 11, pp. 2126–2146, Nov. 2010.

[2] J. Jagur-Grodzinski, "Polymers for tissue engineering, medical devices, and regenerative medicine. Concise general review of recent studies," Polym. Adv. Technol., vol. 17, no. 6, pp. 395–418, Jun. 2006.

[3] T. Billiet, M. Vandenhaute, J. Schelfhout, S. Van Vlierberghe, and P. Dubruel, "A review of trends and limitations in hydrogel-rapid prototyping for tissue engineering," Biomaterials, vol. 33, no. 26, pp. 6020–6041, Sep. 2012.

[4] Q. Chen, S. Liang, and G. A. Thouas, "Elastomeric biomaterials for tissue engineering," Prog. Polym. Sci., vol. 38, no. 3–4, pp. 584–671, Mar. 2013.

[5] C. Vacanti, "The history of tissue engineering," J. Cell. Mol. Med., vol. 1, no. 3, pp. 569–576, Sep. 2006.

[6] R. P. Lanza, R. S. Langer, and J. Vacanti, Principles of tissue engineering. San Diego, CA: Academic Press, 2000.

[7] E. A. Phelps and A. J. García, "Engineering more than a cell: vascularization strategies in tissue engineering," Curr. Opin. Biotechnol., vol. 21, no. 5, pp. 704–709, Oct. 2010.

[8] W. Mahfouz, S. Elsalmy, J. Corcos, and A. S. Fayed, "Fundamentals of bladder tissue engineering," Afr. J. Urol., vol. 19, no. 2, pp. 51–57, Jun. 2013.

[9] M. Okamoto and B. John, "Synthetic biopolymer nanocomposites for tissue engineering scaffolds," Prog. Polym. Sci., vol. 38, no. 10–11, pp. 1487–1503, Oct. 2013.

[10] B. Jiang, B. Akar, T. M. Waller, J. C. Larson, A. A. Appel, and E. M. Brey, "Design of a composite biomaterial system for tissue engineering applications," Acta Biomater., vol. 10, no. 3, pp. 1177–1186, Mar. 2014.

[11] M. P. Lutolf and J. A. Hubbell, "Synthetic biomaterials as instructive extracellular microenvironments for morphogenesis in tissue engineering," Nat. Biotechnol., vol. 23, no. 1, pp. 47–55, Jan. 2005.

[12] A. Vats, N. S. Tolley, J. M. Polak, and J. E. Gough, "Scaffolds and biomaterials for tissue engineering: a review of clinical applications," Clin. Otolaryngol. Allied Sci., vol. 28, no. 3, pp. 165–172, 2003.

[13] Sigma-Aldrich, "Product Information: Collagen from human placenta Bornstein Traub Type IV." .

[14] Glanvillc, Robert W., Structure and function of collagen types, 2012th ed. .

[15] J. L. Drury and D. J. Mooney, "Hydrogels for tissue engineering: scaffold design variables and applications," Biomaterials, vol. 24, no. 24, pp. 4337–4351, Nov. 2003.

[16] J. Radhakrishnan, U. M. Krishnan, and S. Sethuraman, "Hydrogel based injectable scaffolds for cardiac tissue regeneration," Biotechnol. Adv., vol. 32, no. 2, pp. 449–461, Mar. 2014.

[17] H. Otsuka, Y. Nagasaki, and K. Kataoka, "Self-assembly of poly(ethylene glycol)-based block copolymers for biomedical applications," Curr. Opin. Colloid Interface Sci., vol. 6, no. 1, pp. 3–10, Feb. 2001.

[18] S. Vijayasekaran, T. V. Chirila, T. A. Robertson, X. Lou, J. H. Fitton, C. R. Hicks, and I. J. Constable, "Calcification of poly(2-hydroxyethyl methacrylate) hydrogel sponges implanted in the rabbit cornea: a 3-month study," J. Biomater. Sci. Polym. Ed., vol. 11, no. 6, pp. 599–615, 2000.

[19] R. Rai, M. Tallawi, A. Grigore, and A. R. Boccaccini, "Synthesis, properties and biomedical applications of poly(glycerol sebacate) (PGS): A review," Prog. Polym. Sci., vol. 37, no. 8, pp. 1051–1078, Aug. 2012.

[20] R. R. Rao and J. P. Stegemann, "Cell-based approaches to the engineering of vascularized bone tissue," Cytotherapy, vol. 15, no. 11, pp. 1309–1322, Nov. 2013.

[21] F. Cellesi, "Thermoresponsive hydrogels for cellular delivery," Ther. Deliv., vol. 3, no. 12, pp. 1395–1407, Dec. 2012.

[22] T. A. Prokhorova, L. M. Harkness, U. Frandsen, N. Ditzel, H. D. Schrøder, J. S. Burns, and M. Kassem, "Teratoma formation by human embryonic stem cells is site dependent and enhanced by the presence of Matrigel," Stem Cells Dev., vol. 18, no. 1, pp. 47–54, Feb. 2009.

[23] T. Schroeder, "Hematopoietic Stem Cell Heterogeneity: Subtypes, Not Unpredictable Behavior," Cell Stem Cell, vol. 6, no. 3, pp. 203–207, Mar. 2010.

[24] T. C. Grikscheit and J. P. Vacanti, "The history and current status of tissue engineering: The future of pediatric surgery," J. Pediatr. Surg., vol. 37, no. 3, pp. 277–288, Mar. 2002.

[25] D. H. Kim, S.-J. Heo, J.-W. Shin, C. W. Mun, K. M. Park, K. D. Park, and K. S. Jee, "Preparation of thermosensitive gelatin-pluronic copolymer for cartilage tissue engineering," Macromol. Res., vol. 18, no. 4, pp. 387–391, Apr. 2010.

[26] C. T. Brighton and R. M. Hunt, "Early histologic and ultrastructural changes in microvessels of periosteal callus," J. Orthop. Trauma, vol. 11, no. 4, pp. 244–253, May 1997.

[27] K. Deligkaris, T. S. Tadele, W. Olthuis, and A. van den Berg, "Hydrogel-based devices for biomedical applications," Sens. Actuators B Chem., vol. 147, no. 2, pp. 765–774, Jun. 2010.

[28] M. Hamidi, A. Azadi, and P. Rafiei, "Hydrogel nanoparticles in drug delivery," Adv. Drug Deliv. Rev., vol. 60, no. 15, pp. 1638–1649, Dec. 2008.
[29] A. C. Jen, M. C. Wake, and A. G. Mikos, "Review: Hydrogels for cell immobilization," Biotechnol. Bioeng., vol. 50, no. 4, pp. 357–364, May 1996.
[30] P. M. Kharkar, K. L. Kiick, and A. M. Kloxin, "Designing degradable hydrogels for orthogonal control of cell microenvironments," Chem. Soc. Rev., vol. 42, no. 17, p. 7335, 2013.
[31] T. R. Hoare and D. S. Kohane, "Hydrogels in drug delivery: Progress and challenges," Polymer, vol. 49, no. 8, pp. 1993–2007, Apr. 2008.
[32] F. Ganji, S. Vasheghani-Farahani, and E. Vasheghani-Farahani, "Theoretical description of hydrogel swelling: a review," Iran Polym J, vol. 19, no. 5, pp. 375–398, 2010.
[33] D. Mawad, R. Odell, and L. A. Poole-Warren, "Network structure and macromolecular drug release from poly(vinyl alcohol) hydrogels fabricated via two crosslinking strategies," Int. J. Pharm., vol. 366, no. 1–2, pp. 31–37, Jan. 2009.
[34] M. A. Azagarsamy, D. D. McKinnon, D. L. Alge, and K. S. Anseth, "Coumarin-Based Photodegradable Hydrogel: Design, Synthesis, Gelation, and Degradation Kinetics," ACS Macro Lett., vol. 3, no. 6, pp. 515–519, Jun. 2014.
[35] A. S. Hoffman, "Hydrogels for biomedical applications," Adv. Drug Deliv. Rev., vol. 54, no. 1, pp. 3–12, Jan. 2002.
[36] N. A. Peppas, "7 Kinetics of Smart Hydrogels," Reflexive Polym. Hydrogels Underst. Des. Fast Responsive Polym. Syst., p. 99, 2004.
[37] E. M. Ahmed, "Hydrogel: Preparation, characterization, and applications," J. Adv. Res., Jul. 2013.
[38] M. Verhulsel, M. Vignes, S. Descroix, L. Malaquin, D. M. Vignjevic, and J.-L. Viovy, "A review of microfabrication and hydrogel engineering for micro-organs on chips," Biomaterials, vol. 35, no. 6, pp. 1816–1832, Feb. 2014.
[39] L. Yu and J. Ding, "Injectable hydrogels as unique biomedical materials," Chem. Soc. Rev., vol. 37, no. 8, p. 1473, 2008.
[40] M. R. Matanović, J. Kristl, and P. A. Grabnar, "Thermoresponsive polymers: Insights into decisive hydrogel characteristics, mechanisms of gelation, and promising biomedical applications," Int. J. Pharm., vol. 472, no. 1–2, pp. 262–275, Sep. 2014.
[41] B. Vernon, Ed., Injectable biomaterials: science and applications. Oxford ; Philadelphia: Woodhead Pub, 2011.
[42] J. J. Escobar-Chávez, M. López-Cervantes, A. Naik, Y. Kalia, D. Quintanar-Guerrero, and A. Ganem-Quintanar, "Applications of thermo-reversible pluronic F-127 gels in pharmaceutical formulations," J. Pharm. Pharm. Sci., vol. 9, no. 3, pp. 339–58, 2006.

[43] M. Guzálin, M. R. Aberturas, F. Garcia, and J. Molpeceres, "Gelatine Gels and Polyoxyethylene-Polyoxypropylene Gels: Comparative Study of Their Properties," Drug Dev. Ind. Pharm., vol. 20, no. 12, pp. 2041–2048, Jan. 1994.

[44] G. Riess, "Micellization of block copolymers," Prog. Polym. Sci., vol. 28, no. 7, pp. 1107–1170, Jul. 2003.

[45] Z. Zhou, Y.-W. Yang, C. Booth, and B. Chu, "Association of a triblock ethylene oxide (E) and butylene oxide (B) copolymer (B12E260B12) in aqueous solution," Macromolecules, vol. 29, no. 26, pp. 8357–8361, 1996.

[46] I. W. Hamley, The Physics of Block Copolymers. Oxford ; New York: Oxford University Press, 1999.

[47] Z. Zhou and B. Chu, "Phase behavior and association properties of poly (oxypropylene)-poly (oxyethylene)-poly (oxypropylene) triblock copolymer in aqueous solution," Macromolecules, vol. 27, no. 8, pp. 2025–2033, 1994.

[48] S. Lapanje, "Hydrophobic interactions," Biochem. Educ., vol. 8, no. 4, p. 124, Oct. 1980.

[49] I. R. Schmolka, "Artificial skin I. Preparation and properties of pluronic F-127 gels for treatment of burns," J. Biomed. Mater. Res., vol. 6, no. 6, pp. 571–582, 1972.

[50] S. Miyazaki, S. Takeuchi, C. Yokouchi, and M. Takada, "Pluronic F-127 gels as a vehicle for topical administration of anticancer agents," Chem. Pharm. Bull. (Tokyo), vol. 32, no. 10, pp. 4205–4208, Oct. 1984.

[51] S.-C. Chi, KR, H.-K. Tan, KR, and H.-W. Chun, "United States Patent: 5527832 - Antiinflammatory and analgesic transdermal gel," 5527832, 18-Jun-1996.

[52] Y.-Y. Wang, C.-T. Hong, W.-T. Chiu, and J.-Y. Fang, "In vitro and in vivo evaluations of topically applied capsaicin and nonivamide from hydrogels," Int. J. Pharm., vol. 224, no. 1, pp. 89–104, 2001.

[53] F. Cellesi, N. Tirelli, and J. A. Hubbell, "Towards a fully-synthetic substitute of alginate: development of a new process using thermal gelation and chemical cross-linking," Biomaterials, vol. 25, no. 21, pp. 5115–5124, Sep. 2004.

[54] F. Cellesi, N. Tirelli, and J. A. Hubbell, "Materials for cell encapsulation via a new tandem approach combining reverse thermal gelation and covalent crosslinking," Macromol. Chem. Phys., vol. 203, no. 10–11, pp. 1466–1472, 2002.

[55] N. K. Singha and H. Schlaad, "Thiol-ene Based Functionalization of Polymers," in Functional Polymers by Post-Polymerization Modification, P. Theato and H.-A. Klok, Eds. Weinheim, Germany: Wiley-VCH Verlag GmbH & Co. KGaA, 2013, pp. 65–86.

[56] H. Tan and K. G. Marra, "Injectable, Biodegradable Hydrogels for Tissue Engineering Applications," Materials, vol. 3, no. 3, pp. 1746–1767, Mar. 2010.

[57] H. C. Kolb, M. G. Finn, and K. B. Sharpless, "Click Chemistry: Diverse Chemical Function from a Few Good Reactions," Angew. Chem. Int. Ed Engl., vol. 40, no. 11, pp. 2004–2021, Jun. 2001.

[58] G. D. Nicodemus and S. J. Bryant, "Cell Encapsulation in Biodegradable Hydrogels for Tissue Engineering Applications," Tissue Eng. Part B Rev., vol. 14, no. 2, pp. 149–165, Jun. 2008.

[59] G.-Z. Li, R. K. Randev, A. H. Soeriyadi, G. Rees, C. Boyer, Z. Tong, T. P. Davis, C. R. Becer, and D. M. Haddleton, "Investigation into thiol-(meth)acrylate Michael addition reactions using amine and phosphine catalysts," Polym. Chem., vol. 1, no. 8, p. 1196, 2010.

[60] L. Liang and D. Astruc, "The copper(I)-catalyzed alkyne-azide cycloaddition (CuAAC) 'click' reaction and its applications. An overview," Coord. Chem. Rev., vol. 255, no. 23–24, pp. 2933–2945, Dec. 2011.

[61] J. A. Burns, M. I. Gibson, and C. R. Becer, "Glycopolymers via Post-Polymerization Modification Techniques," in Functional Polymers by Post-Polymerization Modification, P. Theato and H.-A. Klok, Eds. Weinheim, Germany: Wiley-VCH Verlag GmbH & Co. KGaA, 2013, pp. 237–265.

[62] D. C. Kennedy, C. S. McKay, M. C. B. Legault, D. C. Danielson, J. A. Blake, A. F. Pegoraro, A. Stolow, Z. Mester, and J. P. Pezacki, "Cellular Consequences of Copper Complexes Used To Catalyze Bioorthogonal Click Reactions," J. Am. Chem. Soc., vol. 133, no. 44, pp. 17993–18001, Nov. 2011.

[63] G. N. Grover, J. Lam, T. H. Nguyen, T. Segura, and H. D. Maynard, "Biocompatible Hydrogels by Oxime Click Chemistry," Biomacromolecules, vol. 13, no. 10, pp. 3013–3017, Oct. 2012.

[64] L. Perlin, S. MacNeil, and S. Rimmer, "Production and performance of biomaterials containing RGD peptides," Soft Matter, vol. 4, no. 12, p. 2331, 2008.

[65] E. Ruoslahti and M. D. Pierschbacher, "Arg-Gly-Asp: a versatile cell recognition signal," Cell, vol. 44, no. 4, pp. 517–518, 1986.

[66] "RGD Peptides - Molecular Glue? A Cell Adhesion Motif." Peptide International.

[67] C. B. Pattillo, F. Sari-Sarraf, R. Nallamothu, B. M. Moore, G. C. Wood, and M. F. Kiani, "Targeting of the Antivascular Drug Combretastatin to Irradiated Tumors Results in Tumor Growth Delay," Pharm. Res., vol. 22, no. 7, pp. 1117–1120, Jul. 2005.

[68] R. M. Schiffelers, G. A. Koning, T. L. M. ten Hagen, M. H. A. M. Fens, A. J. Schraa, A. P. C. A. Janssen, R. J. Kok, G. Molema, and G. Storm, "Anti-tumor efficacy of tumor vasculature-targeted liposomal doxorubicin," J. Controlled Release, vol. 91, no. 1–2, pp. 115–122, Aug. 2003.

[69] S. Ouasti, R. Donno, F. Cellesi, M. J. Sherratt, G. Terenghi, and N. Tirelli, "Network connectivity, mechanical properties and cell adhesion for hyaluronic acid/PEG hydrogels," Biomaterials, vol. 32, no. 27, pp. 6456–6470, Sep. 2011.

[70] T. Wong, J. A. McGrath, and H. Navsaria, "The role of fibroblasts in tissue engineering and regeneration," Br. J. Dermatol., vol. 156, no. 6, pp. 1149–1155, 2007.

[71] CLS Cell Lines Service GmbH, "3T3-Swiss Albino, Murine embryonal fibroblast cell line product information." .

[72] J. Obeso, J. Weber, and R. Auerbach, "A hemangioendothelioma-derived cell line: its use as a model for the study of endothelial cell biology," Lab. Investig. J. Tech. Methods Pathol., vol. 63, no. 2, pp. 259–269, Aug. 1990.

[73] S. C. Satchell and F. Braet, "Glomerular endothelial cell fenestrations: an integral component of the glomerular filtration barrier," AJP Ren. Physiol., vol. 296, no. 5, pp. F947–F956, May 2009.

[74] S. Armelloni, M. Li, P. Messa, and M. P. Rastaldi, "Podocytes: A new player for glutamate signaling," Int. J. Biochem. Cell Biol., vol. 44, no. 12, pp. 2272–2277, Dec. 2012.

[75] P. Mundel and W. Kriz, "Structure and function of podocytes: an update," Anat. Embryol. (Berl.), vol. 192, no. 5, pp. 385–397, Nov. 1995.

[76] CLS Cell Lines Service GmbH, "SVI, Murine Kidney Podocyte cell line product information." .

[77] INTERNATIONAL SERUM and INDUSTRY ASSOCIATION, "Frequently Asked Questions - Bovine Serum." .

[78] T. S. Lange, K. Kirchberg, A. K. Bielinsky, A. Leuker, I. Bank, T. Ruzicka, and K. Scharffetter-Kochanek, "Divalent cations (Mg2+, Ca2+) differentially influence the β1 integrin-mediated migration of human fibroblasts and keratinocytes to different extracellular matrix proteins," Exp. Dermatol., vol. 4, no. 3, pp. 130–137, 1995.

[79] L. Weiss, "Studies on cellular adhesion in tissue-culture," Exp. Cell Res., vol. 30, no. 3, pp. 509–520, May 1963.

[80] B. D. Mather, K. Viswanathan, K. M. Miller, and T. E. Long, "Michael addition reactions in macromolecular design for emerging technologies," Prog. Polym. Sci., vol. 31, no. 5, pp. 487–531, May 2006.

[81] F. Cellesi and N. Tirelli, "A new process for cell microencapsulation and other biomaterial applications: Thermal gelation and chemical cross-linking in 'tandem,'" J. Mater. Sci. Mater. Med., vol. 16, no. 6, pp. 559–565, 2005.

[82] F. Cellesi, N. Tirelli, and J. A. Hubbell, "Towards a fully-synthetic substitute of alginate: development of a new process using thermal gelation and chemical cross-linking," Biomaterials, vol. 25, no. 21, pp. 5115–5124, Sep. 2004.

[83] H. Shih and C.-C. Lin, "Cross-Linking and Degradation of Step-Growth Hydrogels Formed by Thiol–Ene Photoclick Chemistry," Biomacromolecules, vol. 13, no. 7, pp. 2003–2012, Jul. 2012.

[84] H. Händel, E. Gesele, K. Gottschall, and K. Albert, "Application of HRMAS 1H NMR spectroscopy to investigate interactions between ligands and synthetic receptors," Angew. Chem. Int. Ed Engl., vol. 42, no. 4, pp. 438–442, Jan. 2003.

[85] T. M. and J. E., "HR-MAS NMR Spectroscopy in Material Science," in Advanced Aspects of Spectroscopy, M. Akhyar Farrukh, Ed. InTech, 2012.

[86] M. Santoro, P. Marchetti, F. Rossi, G. Perale, F. Castiglione, A. Mele, and M. Masi, "Smart Approach To Evaluate Drug Diffusivity in Injectable Agar−Carbomer Hydrogels for Drug Delivery," J. Phys. Chem. B, vol. 115, no. 11, pp. 2503–2510, Mar. 2011.

[87] T. D. W. Claridge, High-resolution NMR techniques in organic chemistry. Amsterdam; London: Elsevier, 2009.

[88] J. L. Hill-West, S. M. Chowdhury, A. S. Sawhney, C. P. Pathak, R. C. Dunn, and J. A. Hubbell, "Prevention of postoperative adhesions in the rat by in situ photopolymerization of bioresorbable hydrogel barriers," Obstet. Gynecol., vol. 83, no. 1, pp. 59–64, Jan. 1994.

[89] J. L. Hill-West, S. M. Chowdhury, R. C. Dunn, and J. A. Hubbell, "Efficacy of a resorbable hydrogel barrier, oxidized regenerated cellulose, and hyaluronic acid in the prevention of ovarian adhesions in a rabbit model," Fertil. Steril., vol. 62, no. 3, pp. 630–634, Sep. 1994.

[90] J. L. Hill-West, S. M. Chowdhury, M. J. Slepian, and J. A. Hubbell, "Inhibition of thrombosis and intimal thickening by in situ photopolymerization of thin hydrogel barriers," Proc. Natl. Acad. Sci. U. S. A., vol. 91, no. 13, pp. 5967–5971, Jun. 1994.

[91] J. Elisseeff, K. Anseth, D. Sims, W. McIntosh, M. Randolph, and R. Langer, "Transdermal photopolymerization for minimally invasive implantation," Proc. Natl. Acad. Sci. U. S. A., vol. 96, no. 6, pp. 3104–3107, Mar. 1999.

[92] K. T. Nguyen and J. L. West, "Photopolymerizable hydrogels for tissue engineering applications," Biomaterials, vol. 23, no. 22, pp. 4307–4314, Nov. 2002.

[93] O. Valdes-Aguilera, C. P. Pathak, J. Shi, D. Watson, and D. C. Neckers, "Photopolymerization studies using visible light photoinitiators," Macromolecules, vol. 25, no. 2, pp. 541–547, 1992.

[94] S. Kızılel, V. H. Pérez-Luna, and F. Teymour, "Photopolymerization of Poly(Ethylene Glycol) Diacrylate on Eosin-Functionalized Surfaces," Langmuir, vol. 20, no. 20, pp. 8652–8658, Sep. 2004.

[95] C. S. Bahney, T. J. Lujan, C. W. Hsu, M. Bottlang, J. L. West, and B. Johnstone, "Visible light photoinitiation of mesenchymal stem cell-laden bioresponsive hydrogels," Eur. Cell. Mater., vol. 22, pp. 43–55; discussion 55, 2011.

[96] X. D. Feng, X. Q. Guo, and K. Y. Qiu, "Study of the initiation mechanism of the vinyl polymerization with the system persulfate/N,N,N',N'-tetramethylethylenediamine," Makromol. Chem., vol. 189, no. 1, pp. 77–83, Jan. 1988.

[97] I. Mironi-Harpaz, D. Y. Wang, S. Venkatraman, and D. Seliktar, "Photopolymerization of cell-encapsulating hydrogels: Crosslinking efficiency versus cytotoxicity," Acta Biomater., vol. 8, no. 5, pp. 1838–1848, May 2012.

[98] E. S. Desai, M. Y. Tang, A. E. Ross, and R. A. Gemeinhart, "Critical factors affecting cell encapsulation in superporous hydrogels," Biomed. Mater., vol. 7, no. 2, p. 024108, Apr. 2012.

[99] S. Azarmi, Y. Huang, H. Chen, S. McQuarrie, D. Abrams, W. Roa, W. H. Finlay, G. G. Miller, and R. Löbenberg, "Optimization of a two-step desolvation method for preparing gelatin nanoparticles and cell uptake studies in 143B osteosarcoma cancer cells," J Pharm Pharm Sci, vol. 9, no. 1, pp. 124–132, 2006.

[100] H. Wang, O. C. Boerman, K. Sariibrahimoglu, Y. Li, J. A. Jansen, and S. C. G. Leeuwenburgh, "Comparison of micro- vs. nanostructured colloidal gelatin gels for sustained delivery of osteogenic proteins: Bone morphogenetic protein-2 and alkaline phosphatase," Biomaterials, vol. 33, no. 33, pp. 8695–8703, Nov. 2012.

[101] A. O. Elzoghby, "Gelatin-based nanoparticles as drug and gene delivery systems: Reviewing three decades of research," J. Controlled Release, vol. 172, no. 3, pp. 1075–1091, Dec. 2013.

[102] J. Zhu, Y. Zhang, D. Lu, R. N. Zare, J. Ge, and Z. Liu, "Temperature-responsive enzyme–polymer nanoconjugates with enhanced catalytic activities in organic media," Chem. Commun., vol. 49, no. 54, p. 6090, 2013.

[103] N. Kumar, M. N. Ravikumar, and A. J. Domb, "Biodegradable block copolymers," Adv. Drug Deliv. Rev., vol. 53, no. 1, pp. 23–44, 2001.

[104] M. J. Hwang, J. M. Suh, Y. H. Bae, S. W. Kim, and B. Jeong, "Caprolactonic Poloxamer Analog: PEG-PCL-PEG," Biomacromolecules, vol. 6, no. 2, pp. 885–890, Mar. 2005.